

Quench dynamics of noninteracting fermions with a delta impurity

Gabriel Gouraud¹, Pierre Le Doussal¹, and Grégory Schehr²

¹Laboratoire de Physique de l'École Normale Supérieure, ENS, Université PSL, CNRS, Sorbonne Université, Université de Paris, 75005 Paris, France

²Sorbonne Université, Laboratoire de Physique Théorique et Hautes Energies, CNRS UMR 7589, 4 Place Jussieu, 75252 Paris Cedex 05, France

Abstract

We study the out-of-equilibrium dynamics of noninteracting fermions in one dimension and in continuum space, in the presence of a delta impurity potential at the origin whose strength g is varied at time $t = 0$. The system is prepared in its ground state with $g = g_0 = +\infty$, with two different densities and Fermi wave-vectors k_L and k_R on the two half-spaces $x > 0$ and $x < 0$ respectively. It then evolves for $t > 0$ as an isolated system, with a finite impurity strength g . We compute exactly the time dependent density and current. For a fixed position x and in the large time limit $t \rightarrow \infty$, the system reaches a non-equilibrium stationary state (NESS). We obtain analytically the correlation kernel, density, particle current, and energy current in the NESS, and characterize their relaxation, which is algebraic in time. In particular, in the NESS, we show that, away from the impurity, the particle density displays oscillations which are the non-equilibrium analog of the Friedel oscillations. In the regime of “rays”, $x/t = \xi$ fixed with $x, t \rightarrow \infty$, we compute the same quantities and observe the emergence of two light cones, associated to the Fermi velocities k_L and k_R in the initial state. Interestingly, we find non trivial quantum correlations between two opposite rays with velocities ξ and $-\xi$ which we compute explicitly. We extend to a continuum setting and to a correlated initial state the analytical methods developed in a recent work of Ljubotina, Sotiriadis and Prosen, in the context of a discrete fermionic chain with an impurity. We also generalize our results to an initial state at finite temperature, recovering, via explicit calculations, some predictions of conformal field theory in the low energy limit.

Contents

1	Introduction	4
2	Model, quench protocol and observables	6
2.1	Model	6
2.2	Initial state	6
2.3	Dynamical evolution and observables	7
3	Main results	8
3.1	Non equilibrium stationary state (NESS)	8
3.1.1	The case of a repulsive impurity ($g > 0$)	9
3.1.2	The case of an attractive impurity ($g < 0$)	12
3.1.3	Relaxation to the NESS for $g > 0$	13
3.2	Large time regime with $\xi = x/t$ fixed (ray regime)	14
3.3	Finite temperature generalisation	16
3.4	Energy current	17
4	Exact calculation at finite time and finite size	19
4.1	Eigenbasis of \hat{H}_g	19
4.2	Time dependent kernel	20
5	Thermodynamic limit $\ell \rightarrow +\infty$	22
6	Large time limit: stationary state at fixed position x	25
7	Large time limit with $\xi = x/t, \xi' = x'/t$ fixed	27
8	Wigner function and semi-classical approach	31
9	Conclusion	35
Appendix A: Large ℓ limit, term B		36
A.1	The off-diagonal part	36
A.2	The diagonal part	37
Appendix B: Convergence to the NESS at large time ($x, x' = O(1)$)		38
B.1	Time decay of the term C	38
B.2	Time decay of the term B	40
B.3	Summary	41
Appendix C: Details for $g < 0$		42
Appendix D: Details for finite temperature		44
D.1	Large ℓ limit	44
D.2	Large time limit: regime of the NESS	47
D.3	Large time limit: ray regime at fixed $\xi = \frac{x}{t}$	48
Appendix E: Energy current		49

Appendix F: Low temperature expansions	51
F.1 Energy current	51
F.2 Particle current	51
Appendix G: Remarks on NESS and GGE	52
Bibliography	53

1 Introduction

There is a recent revived interest in noninteracting fermions in continuum inhomogeneous settings as analytically tractable models for studying equilibrium and out-of-equilibrium quantum correlations. For one-dimensional fermions at equilibrium in an external potential, there are interesting connections to random matrix theory (for a review see [1]). These relations allow to compute the density, the full counting statistics and the entanglement entropy in a variety of potentials [2, 3] using the tools of determinantal point processes [4, 5] in agreement with other approaches using inhomogeneous bosonization [6]. In particular, the correlation functions can be expressed as determinants built from a central object called the kernel [7, 8]. In the limit of a large number of fermions the kernel in the bulk of the Fermi gas becomes universal at the scale of the inter-particle distance k_F^{-1} , where k_F is the local Fermi wave-vector. It is given, at zero temperature, by the celebrated sine kernel [7]. This universal behavior holds for smooth potentials [1] but breaks down for more singular potentials which vary over a region \mathcal{D} of size $O(k_F^{-1})$. In this case, the kernel differs from the sine kernel and has been calculated, for instance, for the hard wall [9, 10, 11, 12], the step potential [13], as well as for static impurities modeled by a delta potential [14]. Far from the singular region \mathcal{D} the kernel exhibits Friedel type oscillations [15, 16, 17], which have been characterized using reflection and transmission coefficients through \mathcal{D} [13, 18].

It was shown that the bulk universality for smooth potentials can be extended to equilibrium dynamics [19] (in terms of the so-called extended sine kernel [20]). It is natural to ask similar questions in the case of non-equilibrium dynamics. In the case of fermions trapped in a confining potential it was found for some time-dependent potentials (such as the harmonic oscillator or the $1/x^2$ potential) and some initial conditions, that the kernel keeps its equilibrium form up to time dependent factors [21, 22, 23, 24]. For more general potentials and initial conditions the situation is more complicated [24, 25, 26]. The large time limit of the kernel can be obtained from the so-called diagonal ensemble and coincides with the prediction from the generalized Gibbs ensemble (GGE) [27]. However the large time limit of the multi-point correlations exhibits a more complicated behavior [24].

One can also consider the out of equilibrium dynamics in the absence of a confining potential. A seminal example is the Landauer-Büttiker theory for transport between two reservoirs [28, 29]. Another important question, much studied in the context of Luttinger liquids, is to characterize the transport that takes place when two $1d$ systems are connected via a contact [30, 31, 32, 33, 34, 35]. This problem has attracted a renewed interest in the context of quantum quenches where the system is translationally invariant but the initial condition is inhomogeneous. Important questions concern the large time behavior of the system, in particular the local convergence to a non equilibrium steady state (NESS), characterized by stationary currents, density profiles and counting statistics. Another question concerns non-stationary fluctuations and moving fronts. These questions have been addressed using conformal field theory (CFT) [36, 37, 38], generalized hydrodynamics [39, 40], as well as exact solutions of free fermions either on a lattice [41, 42, 43, 44, 45, 46, 47, 48] or in the continuum [49, 50].

It is natural to ask how these results for noninteracting fermions will be modified in the presence of a (non-confining) external potential. The simplest example is the delta function impurity model in the continuum which was solved at equilibrium in [14, 15, 16, 17]. In this paper we explore the out-of-equilibrium counterpart of this model, starting from an inhomogeneous initial condition. It is inspired by a recent work of Ljubotina, Sotiriadis and Prosen [51] where a similar model with an impurity was studied for a discrete fermionic chain. In that work the initial state was chosen fully decorrelated. On the other hand it is known that fermionic correlations can affect the transport, see e. g. [52]. In the present work, we consider an initial

state that consists in two independent Fermi gases on semi-infinite lines \mathbb{R}^\pm separated by an infinite wall which are each in their ground state, and hence both exhibit the sine kernel bulk correlations with different Fermi wavevectors $k_R > k_L$. They are joined at $t = 0$ and evolve freely in the presence of a delta impurity at the origin. We find that the system reaches a NESS at large time. We calculate exactly the asymptotic kernel in the NESS, from which we obtain the asymptotic particle and energy current as well as the density profile. These quantities depend only on k_R, k_L and g the strength of the impurity. In the case where $k_L = k_R$ and when the impurity is repulsive $g > 0$, one finds that the NESS coincides with the ground state of the system on the infinite line, although the initial state is far from equilibrium. In this case one thus recovers the equilibrium kernel obtained in [14]. This can be understood since all the excitations move to infinity. On the contrary when $g < 0$, the Hamiltonian possesses a bound state and one finds that the NESS always differs from the ground state (even when $k_L = k_R$). In this case, the mean occupation number of the bound state does not converge to unity at large time. Our methods also allow us to study the relaxation towards the NESS, which we find to be algebraic in time. We also compute the kernel in the vicinity of space-time “rays” in the (x, t) plane with fixed velocities $\xi = x/t$. It exhibits a change of behaviors on the two light cones $\xi = k_R$ and $\xi = k_L$. Interestingly we find nontrivial correlations between points belonging to rays with opposite velocities $\pm\xi$, an effect not discussed in [51], although we expect this effect to be also present in the discrete setting. An important difference with Ref. [51] is the existence of two light cones which is due to the presence of local correlations in the initial state which are different on both sides of the impurity. Outside these light cones one recovers the sine kernel, but inside the light cones (including in the NESS for $\xi = 0$) the asymptotic currents are non zero and the kernel is different from the sine kernel.

Our results are then extended to an initial condition with two different nonzero temperatures T_L and T_R . In the low temperature and weak impurity strength limit and equal Fermi wavevectors $k_L = k_R$, we recover, via explicit computations, the result for the energy current in the NESS obtained from CFT given in [32]. Finally we show that the asymptotic kernel, hence the correlations, along rays at fixed velocity $\xi = x/t$ can be recovered by a semi-classical argument. However this is not the case for correlations between points belonging to rays with opposite velocities $\pm\xi$. Also, the semi-classical method does not allow to recover the kernel inside the NESS. Finally our main results are checked versus numerical evaluation of the exact starting formulas.

Note that other recent works have addressed different effects of an impurity on the dynamics. In particular, full counting statistics and entanglement growth in fermionic chains [53, 54, 55, 56], interactions localized at a contact [57], dynamics starting from a homogeneous state [58] and moving and time dependent defects [59, 60, 61, 62] have been studied.

The paper is organized as follows. In Section 2 we define the model, the initial conditions and the observables that we study here. In Section 3 we give a detailed and pedagogical presentation of our main results. In Section 4 we derive the expression of the time dependent kernel in a hard box of finite size $[-\ell/2, \ell/2]$. In Section 5 we obtain the finite time kernel in the limit $\ell \rightarrow +\infty$. To this aim we have adapted a trick based on contour integrals used in [51] (see also [63, 64]). As we show in that section, the study of the limit $\ell \rightarrow +\infty$ turns out to be more involved in the present continuum setting with a correlated initial condition. In Section 6 we obtain the large time limit of the kernel in the regime $x = O(1)$ which characterizes the NESS. From it we compute the density and currents. In Section 7 we study the large time limit of the kernel along rays. In Section 8 we apply a semi-classical method which allows us to recover some of the above exact results in the regime of rays. Finally, we conclude in Section 9. The appendices contain many of the technical details of the calculations.

2 Model, quench protocol and observables

2.1 Model

We consider N noninteracting fermions in one dimension and in the presence of a delta impurity at the origin described by the single particle Hamiltonian \hat{H}_g

$$\hat{H}_g = -\frac{1}{2}\partial_x^2 + g\delta(x) . \quad (1)$$

We work here in units where the fermion mass is unity and $\hbar = 1$. In these units, g denotes the strength of the impurity, which can be repulsive ($g > 0$) or attractive ($g < 0$). To fully specify the model we define it on the interval $[-\ell/2, \ell/2]$ with a hard wall boundary condition (i.e., vanishing wave-function at $x = \pm\ell/2$). We will be eventually interested in the problem on the full line obtained by taking the limit $\ell \rightarrow +\infty$, with fixed fermion densities.

2.2 Initial state

The system is prepared at $t = 0$ in the ground state of the many body Hamiltonian with $g = +\infty$, associated to the single particle Hamiltonian \hat{H}_∞ . This corresponds to imposing a hard-wall at $x = 0$, so that the system is cut into two independent halves $x > 0$ and $x < 0$ at $t = 0$. We will denote by N_L and N_R respectively the number of fermions in the left ($x < 0$) and right ($x > 0$) halves. Let us introduce $\phi_n^L(x)$ and $\phi_n^R(x)$, with $n = 1, 2, \dots$, the normalized eigenfunctions of the single particle Hamiltonian \hat{H}_∞

$$\phi_n^L(x) = \Theta(-x)\sqrt{\frac{4}{\ell}}\sin(k_n x) \quad , \quad \phi_n^R(x) = \Theta(x)\sqrt{\frac{4}{\ell}}\sin(k_n x) , \quad (2)$$

where $\Theta(x)$ denotes the Heaviside theta function and

$$k_n = \frac{2\pi n}{\ell} . \quad (3)$$

The corresponding energy levels are $\epsilon_n = \frac{1}{2}k_n^2 = \frac{2\pi^2 n^2}{\ell^2}$ which are doubly degenerate (L, R).

The ground state many-body wave function is a Slater determinant built from the eigenstates $\phi_n^L(x)$ and $\phi_{n'}^R(x)$ with $1 \leq n \leq N_L$ and $1 \leq n' \leq N_R$. The m -point correlation function (see below for a precise definition) can be expressed as a $m \times m$ determinant built from the so-called correlation kernel

$$K_0(x, x') = K_L(x, x') + K_R(x, x') , \quad (4)$$

where

$$K_L(x, x') = \Theta(-x)\Theta(-x') \sum_{n=1}^{N_L} \frac{4}{\ell} \sin\left(\frac{2\pi n x}{\ell}\right) \sin\left(\frac{2\pi n x'}{\ell}\right) , \quad (5)$$

$$K_R(x, x') = \Theta(x)\Theta(x') \sum_{n'=1}^{N_R} \frac{4}{\ell} \sin\left(\frac{2\pi n' x}{\ell}\right) \sin\left(\frac{2\pi n' x'}{\ell}\right) . \quad (6)$$

In particular, the mean fermion density is given by $\rho(x, t = 0) = K_0(x, x) = \rho_L(x) + \rho_R(x)$ with $\rho_{L/R}(x) = K_{L/R}(x, x)$, where $\rho_L(x)$ and $\rho_R(x)$ denote respectively the average fermion density to the left and to the right of the origin. We also define the Fermi momenta of the left and right half-spaces associated to the initial condition

$$k_L = k_{N_L} = \frac{2\pi N_L}{\ell} \quad , \quad k_R = k_{N_R} = \frac{2\pi N_R}{\ell} \quad (7)$$

and the corresponding Fermi energies

$$\mu_L = \frac{k_L^2}{2} \quad , \quad \mu_R = \frac{k_R^2}{2} \quad , \quad (8)$$

which will be useful in the following.

2.3 Dynamical evolution and observables

We now consider the time evolution for $t > 0$ described by the single particle Hamiltonian \hat{H}_g (1) with a finite strength g of the impurity at $x = 0$. We denote $\psi_n^L(x, t)$ the solution of the Schrödinger equation $i\partial_t\psi_n^L(x, t) = \hat{H}_g\psi_n^L(x, t)$ with initial condition $\psi_n^L(x, t=0) = \phi_n^L(x)$, and similarly $\psi_n^R(x, t)$ with $\psi_n^R(x, t=0) = \phi_n^R(x)$ where $\phi_n^{L/R}(x)$ are given in Eq. (2). Under this evolution, the time dependent many-body wave function for the $N = N_R + N_L$ fermions, $\Psi(x_1, \dots, x_N; t)$, remains a Slater determinant at all times, built from the time-dependent wave-functions $\psi_n^L(x, t)$ and $\psi_{n'}^R(x, t)$ with $1 \leq n \leq N_L$ and $1 \leq n' \leq N_R$. The observables of interest are the time dependent m -point correlations defined as

$$R_m(x_1, \dots, x_m; t) = \frac{N!}{(N-m)!} \int dx_{m+1} \dots dx_N |\Psi(x_1, \dots, x_N; t)|^2 . \quad (9)$$

Using standard manipulations, $R_m(x_1, \dots, x_m, t)$ can be written as (see e.g. [24])

$$R_m(x_1, \dots, x_m; t) = \det_{1 \leq i, j \leq m} K(x_i, x_j, t) , \quad (10)$$

where $K(x_i, x_j; t)$ is the time dependent correlation kernel. In the present case it reads

$$K(x, x', t) = K_L(x, x', t) + K_R(x, x', t) \quad (11)$$

where

$$K_L(x, x', t) = \sum_{n=1}^{N_L} \psi_n^{L*}(x, t) \psi_n^L(x', t) \quad , \quad K_R(x, x', t) = \sum_{n=1}^{N_R} \psi_n^{R*}(x, t) \psi_n^R(x', t) . \quad (12)$$

Of particular interest is the time-dependent density $\rho(x, t)$ given by

$$\rho(x, t) = K(x, x, t) . \quad (13)$$

Another important observable is the total particle current defined as

$$\begin{aligned} J(x, t) &= J_L(x, t) + J_R(x, t) \\ J_{L/R}(x, t) &= \frac{1}{2i} \sum_{n=1}^{N_{L/R}} (\psi_n^{L/R*}(x, t) \partial_x \psi_n^{L/R}(x, t) - \psi_n^{L/R}(x, t) \partial_x \psi_n^{L/R*}(x, t)) , \end{aligned} \quad (14)$$

which can be rewritten in terms of the kernel as

$$J(x, t) = \frac{1}{2i} (\partial_{x'} - \partial_x) K(x, x'; t)|_{x'=x} = \text{Im} K_{01}(x, x; t) , \quad (15)$$

where $K_{01}(x, y, t) = \partial_y K(x, y, t)$. From the Schrödinger equation, the current $J(x, t)$ satisfies the fermion number conservation equation

$$\partial_t \rho(x, t) + \partial_x J(x, t) = 0 . \quad (16)$$

In this paper we compute the time evolution of the density $\rho(x, t)$, of the kernel $K(x, x', t)$ and of the current $J(x, t)$. Since we are interested in the large time behavior of the bulk of the system, we will take the limit $\ell \rightarrow +\infty$ before taking $t \rightarrow +\infty$. More precisely we will take the limit $\ell \rightarrow +\infty$, $N_{L/R} \rightarrow +\infty$ with fixed k_L and k_R , i.e. with fixed mean densities

$$\rho_L = \frac{2N_L}{\ell} = \frac{k_L}{\pi} \quad , \quad \rho_R = \frac{2N_R}{\ell} = \frac{k_R}{\pi} \quad (17)$$

or equivalently with fixed Fermi energies μ_L, μ_R (see Eq. (8)).

3 Main results

In this section we present our main results. The first one is the expression for the kernel $K(x, x', t)$ in the thermodynamic limit $\ell \rightarrow +\infty$ at any fixed time t . It is a lengthy although fully explicit expression which is given in (81) as a sum of terms which are given respectively in (82), (85), (89), (90) and (92). From this expression one can read the time dependent density from (13) and the current from (15).

The subsequent results concern the large time behavior obtained from the kernel, once the thermodynamic limit is taken. We have found that there are actually two different scaling regimes. The first one is the NESS where $x, x' = O(1)$ and the second one is the regime of rays where both $x, x' = O(t)$. Since the analytical computations of the asymptotic behaviors are quite tricky, we have carefully checked numerically our main predictions, which are shown in Figs. 1, 2 and 4 below.

Finally, we extend our study to an initial state at finite temperature, with two different temperatures T_L and T_R to the left and to the right of the origin. We also obtain the heat current as a function of these two temperatures.

As we will see below some of these results (but not all) can also be obtained from a heuristic semi-classical method which relies on the momentum dependent transmission and reflection coefficients $T(k)$ and $R(k)$, which for a delta function impurity are given by

$$T(k) = \frac{k^2}{k^2 + g^2} \quad , \quad R(k) = 1 - T(k) = \frac{g^2}{k^2 + g^2} \quad (18)$$

The results presented here are derived from first principles, starting from an exact expansion over the eigenfunctions of many-body system.

3.1 Non equilibrium stationary state (NESS)

The first regime corresponds to fixed spatial positions x, x' with $t \rightarrow +\infty$. In this case the kernel, the density and the particle current reach a stationary limit which we compute explicitly, namely

$$\rho(x, t) \rightarrow \rho_\infty(x) \quad , \quad J(x, t) \rightarrow J_\infty \quad , \quad K(x, x'; t) \rightarrow K_\infty(x, x') \quad (19)$$

Note that from the fermion number conservation in Eq. (16) the current is constant in space in the large time limit. From the symmetry of the problem under the change $x \rightarrow -x$, these observables satisfy the following relations

$$K_\infty(x, x')|_{k_L, k_R} = K_\infty(-x, -x')|_{k_R, k_L} \quad , \quad \rho_\infty(x)|_{k_L, k_R} = \rho_\infty(-x)|_{k_R, k_L} \quad , \quad J_\infty|_{k_R, k_L} = -J_\infty|_{k_L, k_R} \quad (20)$$

3.1.1 The case of a repulsive impurity ($g > 0$)

We first give the results in the case of a repulsive impurity $g > 0$, and consider the case $g < 0$ in the next section.

Density. For the density we find, for $x > 0$

$$\begin{aligned}\rho_\infty(x > 0) &= \frac{k_R}{\pi} - \int_{k_L}^{k_R} \frac{dk}{2\pi} \frac{k^2}{g^2 + k^2} + \frac{g}{\pi} \int_0^{k_R} dk \frac{k \sin(2k|x|) - g \cos(2kx)}{g^2 + k^2} \\ &= \frac{k_R}{\pi} - \int_{k_L}^{k_R} \frac{dk}{2\pi} \frac{k^2}{g^2 + k^2} + \frac{g}{\pi} e^{2g|x|} \text{Im} E_1(2(g + ik_R)|x|). \end{aligned} \quad (21)$$

Note that $\rho_\infty(x < 0)$ is obtained from this expression Eq. (21) together with the symmetry relation (20). In the second line of Eq. (21), Im denotes the imaginary part and $E_1(z) = \int_z^{+\infty} e^{-t} dt/t$ denotes the exponential integral (see [14] for details on obtaining the second line from the first one). The function $E_1(z)$ is also denoted $\Gamma(0, z)$ in Mathematica, the incomplete gamma function of index 0, and the contour of integration defining it should not cross the negative real axis. This result for $\rho_\infty(x)$ is shown in Fig. (1) and compared with a numerical evaluation of the exact formula for $\rho(x, t)$ (from (80) with $x = x'$) at a relatively large time. It is also plotted in Fig. 3 for smaller values of the time. As one can see on these figures, the convergence to our prediction within the NESS is rather fast.

Let us now discuss a few salient features of this result. Far from the impurity, which is located at $x = 0$, the stationary density profile approaches constant which is different on both sides and given by

$$\begin{aligned}\lim_{x \rightarrow \pm\infty} \rho_\infty(x) &= \frac{\rho_L + \rho_R}{2} \pm \int_{k_L}^{k_R} \frac{dk}{2\pi} \frac{g^2}{g^2 + k^2} \\ &= \frac{\rho_L + \rho_R}{2} \pm \frac{g}{2\pi} \left(\arctan\left(\frac{\pi\rho_R}{g}\right) - \arctan\left(\frac{\pi\rho_L}{g}\right) \right). \end{aligned} \quad (22)$$

These asymptotic values can also be predicted by the semi classical method (see Section 8) and written in the equivalent form

$$\rho_\infty(+\infty) = \frac{k_R}{\pi} - \int_{k_L}^{k_R} \frac{dk}{2\pi} T(k) \quad , \quad \rho_\infty(-\infty) = \frac{k_L}{\pi} + \int_{k_L}^{k_R} \frac{dk}{2\pi} T(k) \quad , \quad (23)$$

in terms of the transmission coefficient $T(k)$ given in Eq. (18). The mean density is continuous at $x = 0$ but exhibits a cusp, with different left and right derivatives given by

$$\rho'_\infty(0^+) = \int_0^{k_R} \frac{dk}{\pi} \frac{2k^2 g}{k^2 + g^2} \quad , \quad \rho'_\infty(0^-) = - \int_0^{k_L} \frac{dk}{\pi} \frac{2k^2 g}{k^2 + g^2}. \quad (24)$$

At variance with the equilibrium case (see below), this cusp is asymmetric.

Finally, the result for $\rho_\infty(x)$ can be compared to the result obtained in [14] for the mean density $\rho_{\text{eq}}(x)$ of the equilibrium problem, i.e. in the ground state with Fermi energy $\mu = \frac{k_F^2}{2}$ in the presence of a repulsive delta impurity of strength $g > 0$ (see formula (60) and (138) there with $\lambda = g$)

$$\begin{aligned}\rho_{\text{eq}}(x) &= \frac{k_F}{\pi} + \frac{g}{\pi} \int_0^{k_F} dk \frac{k \sin(2k|x|) - g \cos(2kx)}{k^2 + g^2} \\ &= \frac{k_F}{\pi} + \frac{g}{\pi} e^{2g|x|} \text{Im} E_1(2(g + ik_F)|x|). \end{aligned} \quad (25)$$

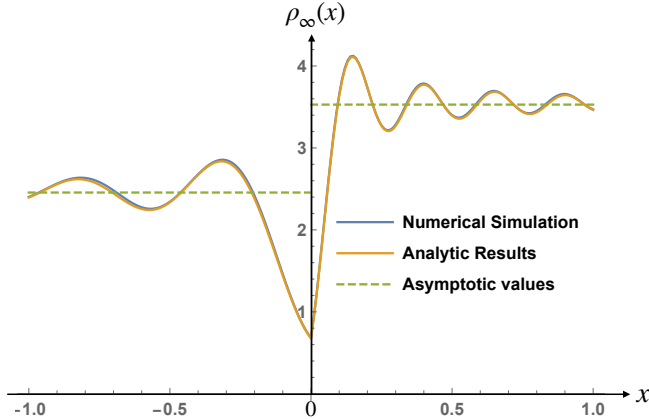


Figure 1: Plot of the mean fermion density $\rho_\infty(x)$ (in orange) as a function of x in the presence of a repulsive impurity ($g > 0$) in the non equilibrium stationary state (NESS) given by Eq. (21) for $\rho_R = 4$, $\rho_L = 2$ and $g = 10$. The oscillating behavior of $\rho_\infty(x)$ is the non-equilibrium analog of the Friedel oscillations. The asymptotic values for $\rho_\infty(\pm\infty)$ given by (23) are indicated as horizontal dashed lines. These analytical results are compared with a numerical evaluation (blue) of $\rho(x, t)$ evaluated from the exact formula in (80) with $x = x'$ for large time $t = \frac{\ell}{4\pi\rho_R}$ and system size $\ell = 50$. The agreement is excellent. Although large, this time has to be small enough so that the fastest fermions traveling at speed k_R have not been reflected by the boundaries at $x = \pm\frac{\ell}{2}$. This is achieved if $k_R t < \frac{\ell}{2}$, i.e., if $t < t_\ell = \frac{\ell}{2\pi\rho_R}$.

We see that for $k_L = k_R = k_F$ the NESS density coincides with the equilibrium (ground state) density (as discussed below this holds only for $g \geq 0$). This is quite interesting since the initial state in the present work is far from the ground state of the system in the presence of the impurity. An explanation for this property is that the components of the initial state on the excited states correspond to fermionic waves (quasi particles) propagating towards the edges of the system. If the observation time is smaller than $t_\ell = \frac{\ell}{2\pi\rho_R}$, such that the fastest fermions traveling at speed k_R have not been reflected yet, i.e. $k_R t < \frac{\ell}{2}$, we expect relaxation to the equilibrium state for $k_L = k_R$ (and to the NESS for $k_L \neq k_R$). This will always occur if the limit $\ell \rightarrow +\infty$ is taken first. For a finite size system, oscillations will take place on larger time scales.

Current. In addition, in the NESS, we show that there is a non zero particle current given by

$$J_\infty = - \int_{k_L}^{k_R} \frac{dk}{2\pi} \frac{k^3}{k^2 + g^2} = \frac{1}{2\pi} \left(\mu_L - \mu_R + \frac{g^2}{2} \ln \left(\frac{g^2 + 2\mu_R}{g^2 + 2\mu_L} \right) \right), \quad (26)$$

which can alternatively be expressed, using the transmission coefficient $T(k)$ given in Eq. (18), as

$$J_\infty = - \int_{k_L}^{k_R} \frac{dk}{2\pi} k T(k). \quad (27)$$

This result can also be obtained by a semi-classical method, see Section 8. The current is shown in Fig. 2 for $\rho_R = 4$, $\rho_L = 2$ (note that it is negative in that case). Its maximal (absolute) value is reached for $g = 0$ when there is no defect. In that case one finds $J_\infty = \frac{1}{2\pi}(\mu_L - \mu_R)$ which corresponds to a unit conductance e^2/h . In the limit $g \rightarrow +\infty$ it vanishes as

$$J_\infty = \frac{1}{2\pi g^2}(\mu_L^2 - \mu_R^2) + O\left(\frac{1}{g^4}\right), \quad (28)$$

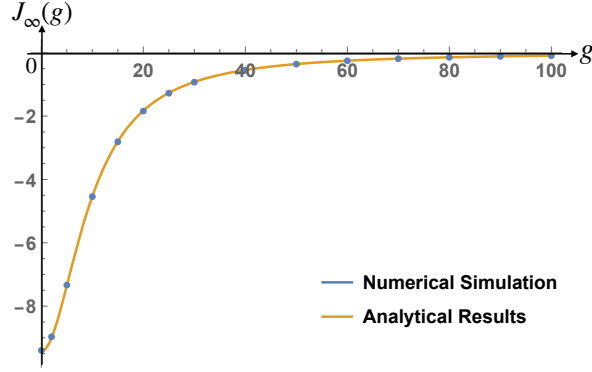


Figure 2: Plot of the current J_∞ (orange solid line) in the NESS as a function of g , the strength of the delta impurity, as given by formula Eq. (26), with $\rho_R = 4$, $\rho_L = 2$. It is compared with a numerical evaluation (blue dots) of the exact expression of $J(x = 0, t)$, obtained from Eq. (80) together with (15), for large time $t = \frac{\ell^2}{8\pi N_R} = t_\ell/2$ and system size $\ell = 50$ for several values of g .

which shows, as expected, that for a very strong defect the system is effectively cut into two almost independent halves.

Kernel. Finally we also obtain the kernel in the NESS which reads explicitly for $x, x' > 0$

$$K_\infty(x > 0, x' > 0) = \int_0^{k_R} \frac{dk}{\pi} \cos(k(x - x')) - \int_{k_L}^{k_R} \frac{dk}{2\pi} \frac{k^2}{k^2 + g^2} e^{-ik(x-x')} \quad (29)$$

$$+ \int_0^{k_R} \frac{dk}{\pi} \frac{gk \sin(k(x + x')) - g^2 \cos(k(x + x'))}{k^2 + g^2},$$

while for $x > 0, x' < 0$ it reads

$$K_\infty(x > 0, x' < 0) = \left(\int_0^{k_R} + \int_0^{k_L} \right) \frac{dk}{2\pi} \frac{k}{k^2 + g^2} (k \cos(k(x - x')) + g \sin(k(x - x'))) \quad (30)$$

$$+ i \int_{k_L}^{k_R} \frac{dk}{2\pi} \frac{k}{k^2 + g^2} \left(k \sin k(x - x') - g \cos k(x - x') + g e^{-ik(x+x')} \right),$$

the other cases being obtained by symmetry (see (20)). For $g > 0$ equivalent expressions are given in (111). The kernel simplifies in the limit where the points $x, x' \rightarrow \infty$. In this limit, keeping $x - x' = O(1)$ one finds the asymptotic behavior

$$K_\infty(x, x') \simeq \int_0^{k_R} \frac{dk}{\pi} \cos(k(x - x')) - \int_{k_L}^{k_R} \frac{dk}{2\pi} \frac{k^2}{k^2 + g^2} e^{-ik(x-x')}. \quad (31)$$

On the other hand, if $x \rightarrow +\infty$ and $x' \rightarrow -\infty$ with $x + x' = O(1)$ one finds

$$K_\infty(x, x') \simeq i \int_{k_L}^{k_R} \frac{dk}{2\pi} \frac{kg}{k^2 + g^2} e^{-ik(x+x')}, \quad (32)$$

while the asymptotic kernel, for $x, x' \rightarrow \infty$, vanishes for generic value of x'/x different from ± 1 .

It is interesting to note that although the semi-classical method cannot obtain the full expressions in Eqs. (29), (30), it does predict the asymptotic form in (31), see Section 8. However, we will see that the result (32) cannot be predicted by this semi-classical method.

Comparison with the GGE. It is interesting to compare our result for the kernel $K_\infty(x, x')$ in the NESS to the prediction $K_{\text{GGE}}(x, x')$ from the GGE. This is done in details in the Appendix G. The main result is that the kernel $K_{\text{GGE}}(x, x')$ contains only "diagonal" terms (which are time independent already at finite ℓ) and does not lead to any current. However we show that there are non-diagonal terms (called C below) which carry current and contribute to the NESS if the limit $\ell \rightarrow \infty$ is carried first.

3.1.2 The case of an attractive impurity ($g < 0$)

If g is negative there is an additional eigenstate of \hat{H}_g , denoted $\phi_g(x) \underset{\ell \rightarrow \infty}{\simeq} \sqrt{|g|} e^{g|x|}$ with eigenenergy $E = -\frac{g^2}{2}$, which is a bound state. All other eigenstates have positive energies and hence propagate over the whole system. One finds that the kernel K_∞ for $g < 0$ has the same expression as above [see Eqs. (29) and (30)], up to an additive term denoted δK_∞ which takes the form

$$\delta K_\infty(x, x') = 2g^2 e^{g(|x|+|x'|)} \left(\int_0^{k_R} + \int_0^{k_L} \right) \frac{dk}{\pi} \frac{k^2}{(g^2 + k^2)^2} \quad (33)$$

Because of the exponential factor $e^{g(|x|+|x'|)} = e^{-|g|(|x|+|x'|)}$, this additional contribution δK_∞ in the kernel is localised around $x = 0$.

From the result for the kernel one obtains that for $g < 0$ the density in the NESS is given for $x > 0$

$$\begin{aligned} \rho_\infty(x > 0) &= \frac{k_R}{\pi} - \int_{k_L}^{k_R} \frac{dk}{2\pi} \frac{k^2}{g^2 + k^2} + \frac{g}{\pi} \int_0^{k_R} dk \frac{k \sin(2k|x|) - g \cos(2kx)}{g^2 + k^2} \\ &\quad + 2g^2 e^{2g|x|} \left(\int_0^{k_R} + \int_0^{k_L} \right) \frac{dk}{\pi} \frac{k^2}{(g^2 + k^2)^2} \\ &= \frac{k_R}{\pi} - \int_{k_L}^{k_R} \frac{dk}{2\pi} \frac{k^2}{g^2 + k^2} + \frac{g}{\pi} e^{2g|x|} \text{Im} E_1(2(g + ik_R)|x|) \\ &\quad - \frac{2g^2}{\pi} e^{2g|x|} \left(\int_{k_R}^\infty + \int_{k_L}^\infty \right) dk \frac{k^2}{(k^2 + g^2)^2}. \end{aligned} \quad (34)$$

For $x < 0$ the formula for $\rho_\infty(x < 0)$ is again obtained from (34) simply by permuting k_L and k_R . Finally the current in the NESS is still given by formula (26), which is invariant under the change $g \rightarrow -g$, and is thus not affected by the bound state.

In the case $k_L = k_R = k_F$ one can compare with the equilibrium result for $g < 0$ obtained in [14]. For the density it was found there that at equilibrium for $g < 0$

$$\begin{aligned} \rho_{\text{eq}}(x) &= \frac{k_F}{\pi} + \frac{g}{\pi} \int_0^{k_F} dk \frac{k \sin(2k|x|) - g \cos(2kx)}{k^2 + g^2} + \frac{g}{\pi} e^{2g|x|} \\ &= \frac{k_F}{\pi} + \frac{g}{\pi} e^{2g|x|} \text{Im} E_1(2(g + ik_F)|x|), \end{aligned} \quad (35)$$

which is compatible with (25) because the function $E_1(z)$ has a branch cut on the negative real axis. Hence, by comparing Eq. (34) and (35), we see that, at variance with the case $g > 0$, the NESS for $g < 0$ differs from the equilibrium ground state. This is because the mean occupation

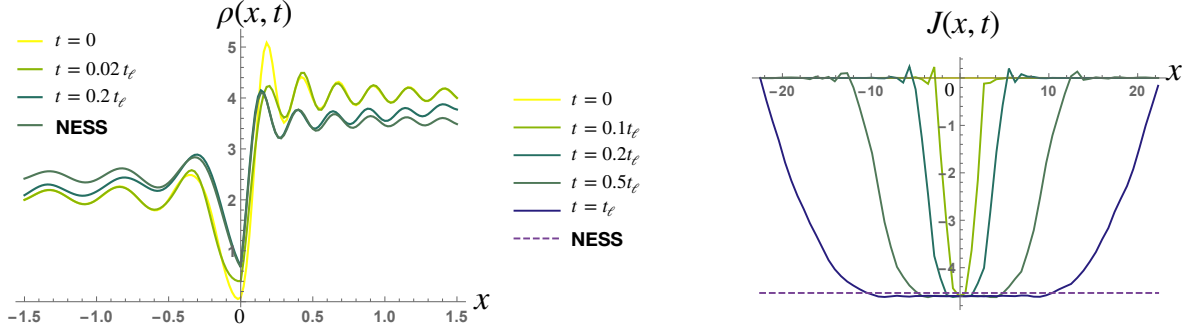


Figure 3: Plots showing the relaxation towards the non-equilibrium steady state (NESS). Left panel: plot of $\rho(x, t)$ (obtained from Eq. (80 for $x = x'$) vs x for various times t compared to $t_\ell = \frac{\ell}{2\pi\rho_R}$, the time at which the fastest fermions reach the boundaries at $x = \pm\frac{\ell}{2}$ with $\ell = 15$. The density in the steady state $\rho_\infty(x)$ is given in Eq. (21) and is also plotted in Fig. 1. The parameter used are $\rho_R = 4$, $\rho_L = 2$, $g = 10$. We can see waves propagating away until the steady state value is reached. Right panel: plot of $J(x, t)$ obtained from Eq. (80) together with Eq. (15) vs x for $\ell = 45$. The dashed line indicates the exact value of J_∞ in the NESS, given in Eq. (26).

number n_g of the bound state which is unity in the ground state, and which is defined in the NESS from $\delta K_\infty(x, x') = n_g \phi_g(x) \phi_g(x')$ is given from 33 as

$$n_g = \left(\int_0^{k_R} + \int_0^{k_L} \right) \frac{dk}{\pi} \frac{2|g|k^2}{(g^2 + k^2)^2} = \frac{1}{2} \left(F\left(\frac{k_R}{|g|}\right) + F\left(\frac{k_L}{|g|}\right) \right) \quad (36)$$

$$F(u) = \frac{2}{\pi} \left(\arctan(u) - \frac{u}{1+u^2} \right), \quad (37)$$

is strictly smaller than unity (including in the case $k_L = k_R$). Hence the last term in the last line of Eq. (34) is proportional to $1 - n_g$. Therefore the post-quench bound state is always partially empty in the NESS, see [65] for a related effect in a similar model based on a GGE calculation.

Note that in the present model there is a single bound state. In the case of multiple bound states it has been found in related models that the NESS can present persistent oscillations in time [51, 55, 65]. To obtain such an effect in the present model would require to consider two delta impurities.

3.1.3 Relaxation to the NESS for $g > 0$

We have also obtained the large time decay of the kernel $K(x, x', t)$ towards its value in the NESS for $g > 0$. The result for $\Delta K(x, x', t) = K(x, x', t) - K_\infty(x, x')$ is given in (B22). From it one extract the density and the current. The decay of the density is found to be of the schematic form

$$\rho(x, t) - \rho_\infty(x) = - \left(\frac{1}{k_L} + \frac{1}{k_R} \right) \frac{(1 + g|x|)^2}{\pi^2 g^4 t^3} \quad (38)$$

$$+ \frac{1}{g^4 t^{5/2}} \left(\chi_R \left(\frac{g}{k_R}, k_R x \right) \cos \left(\frac{k_R^2 t}{2} - \frac{\pi}{4} \right) + \chi_L \left(\frac{g}{k_L}, k_L x \right) \cos \left(\frac{k_L^2 t}{2} - \frac{\pi}{4} \right) \right) + o \left(\frac{1}{t^{5/2}} \right)$$

where the functions $\chi_{L/R}(z)$ can be read off from Eq. (B23) in the Appendix B. Hence the leading decay is $t^{-5/2}$ modulated by oscillations, together with a $1/t^3$ term which is non oscillating. We also find that the current has also a leading algebraic decay as $t^{-5/2}$ modulated by

oscillations. Note that power law decays with oscillations have been obtained in other systems of noninteracting fermions [25, 43].

3.2 Large time regime with $\xi = x/t$ fixed (ray regime)

The second regime corresponds to both $x, t \rightarrow \infty$ with a fixed ratio $\xi = x/t$, i.e. along rays. In this case the density and the current reach finite limits, which are only functions of the scaling variable ξ

$$\rho(x, t) \rightarrow \tilde{\rho}(\xi) \quad , \quad J(x, t) \rightarrow \tilde{J}(\xi) . \quad (39)$$

Note that the fermion number conservation Eq. (16) implies that these two functions must be related via

$$\partial_\xi \tilde{J}(\xi) = \xi \partial_\xi \tilde{\rho}(\xi) . \quad (40)$$

All the results below in that regime hold for any g (positive or negative) since the bound state (that exists for $g < 0$) does not contribute in that limit.

Density. We find through explicit calculation of the large time limit, that the scaling function for the density reads

$$\tilde{\rho}(\xi) = \frac{k_L + k_R}{2\pi} + \text{sgn}(\xi) \left(\int_{k_L}^{k_R} \frac{dk}{2\pi} R(k) + \int_{k_L}^{k_R} \frac{dk}{2\pi} T(k) \Theta(|\xi| - k) \right) . \quad (41)$$

This gives, using the explicit formulae for $R(k)$ and $T(k)$ in (18), for $k_R > k_L$,

$$\tilde{\rho}(\xi) = \begin{cases} \rho_L & \text{if } \xi < -k_R \\ \rho_L + \frac{\rho_R + \xi/\pi}{2} + \frac{g}{2\pi} (\arctan(-\frac{\xi}{g}) - \arctan(\frac{\pi\rho_R}{g})) & \text{if } -k_R < \xi < -k_L \\ \frac{\rho_L + \rho_R}{2} - \frac{g}{2\pi} (\arctan(\frac{\pi\rho_R}{g}) - \arctan(\frac{\pi\rho_L}{g})) & \text{if } -k_L < \xi < 0 \\ \frac{\rho_L + \rho_R}{2} + \frac{g}{2\pi} (\arctan(\frac{\pi\rho_R}{g}) - \arctan(\frac{\pi\rho_L}{g})) & \text{if } 0 < \xi < k_L \\ \frac{\rho_R + \xi/\pi}{2} + \frac{g}{2\pi} (\arctan(\frac{\pi\rho_R}{g}) - \arctan(\frac{\xi}{g})) & \text{if } k_L < \xi < k_R \\ \rho_R & \text{if } \xi > k_R \end{cases} . \quad (42)$$

A plot of $\tilde{\rho}(\xi)$ is shown in the right panel of Fig. 4, together with an exact evaluation at finite time illustrating the convergence. Note that $\tilde{\rho}(\xi)$ is a continuous function of ξ except at $\xi = 0$ where it has a jump discontinuity. The values on each side of the jumps at $\xi = 0^\pm$ are found to agree with the large distance limit of the density obtained the NESS regime, i.e.

$$\tilde{\rho}(0^\pm) = \lim_{x \rightarrow \pm\infty} \rho_\infty(x) . \quad (43)$$

This matching shows that there is no additional intermediate regime between the NESS $x = O(1)$, and the regime of rays $x = O(t)$.

Current. For the scaling function of the current we obtain, again through explicit calculation of the large time limit

$$\tilde{J}(\xi) = - \int_{k_L}^{k_R} \frac{dk}{2\pi} k T(k) \Theta(k - |\xi|) , \quad (44)$$

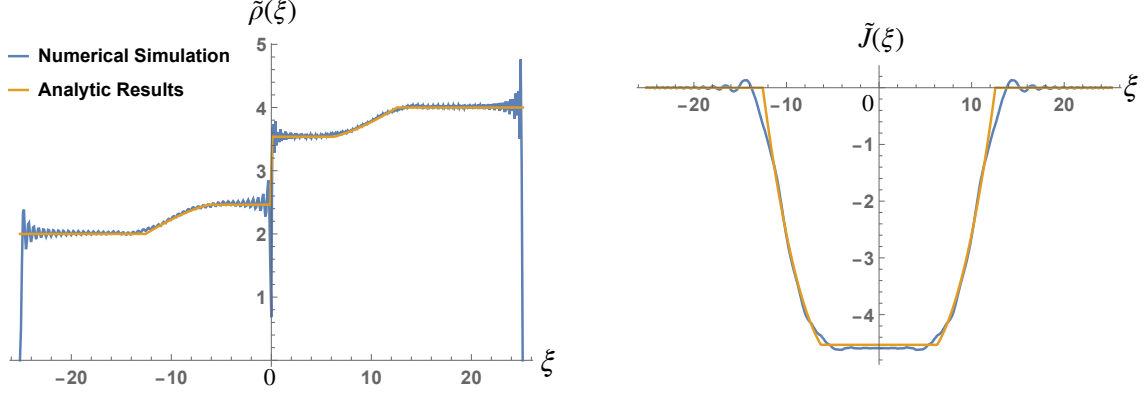


Figure 4: Asymptotic density (left panel) and current (right panel) at large time in the regime of rays $\xi = x/t$ fixed. (Orange) Plots of $\tilde{\rho}(\xi)$ and $\tilde{J}(\xi)$ as a function of $\xi = x/t$ as given in Eqs. 42 and 45 for $\rho_R = 4$, $\rho_L = 2$ and $g = 10$. (Blue) For comparison, $\rho(x, t)$ and $J(x, t)$ are plotted versus $\xi = x/t$ for $t = \frac{\ell}{4\pi\rho_R} = t_\ell/2$ and $\ell = 50$. In this problem there are 2 pairs of light cones at $|\xi| = k_R = 4\pi$ and $|\xi| = k_L = 2\pi$. On this scale the density exhibits a jump at $\xi = 0$, which is rounded on a scale $x = O(1)$ in the NESS (see Fig. 1) with a perfect matching as $\xi \rightarrow 0^\pm$, see Eq. (44) (the oscillations visible here for $\xi \approx 0$ are actually part of the NESS regime).

where $T(k)$ is given in (18). More explicitly, for $k_R > k_L$ it gives

$$\tilde{J}(\xi) = \begin{cases} 0 & \text{if } \xi < -k_R \\ \frac{1}{2\pi} \left(\frac{\xi^2}{2} - \mu_R + \frac{g^2}{2} \ln \left(\frac{g^2 + 2\mu_R}{g^2 + \xi^2} \right) \right) & \text{if } -k_R < \xi < -k_L \\ \frac{1}{2\pi} \left(\mu_L - \mu_R + \frac{g^2}{2} \ln \left(\frac{g^2 + 2\mu_R}{g^2 + 2\mu_L} \right) \right) & \text{if } -k_L < \xi < k_L \\ \frac{1}{2\pi} \left(\frac{\xi^2}{2} - \mu_R + \frac{g^2}{2} \ln \left(\frac{g^2 + 2\mu_R}{g^2 + \xi^2} \right) \right) & \text{if } k_L < \xi < k_R \\ 0 & \text{if } \xi > k_R \end{cases}, \quad (45)$$

where we recall that the Fermi energies are $\mu_{L/R} = \frac{k_{L/R}^2}{2} = \frac{\pi^2}{2} \rho_{L/R}^2$. A plot of $\tilde{J}(\xi)$ is shown in the right panel of Fig. 4, together with an exact evaluation at finite time illustrating the convergence. The function $\tilde{J}(\xi)$ is a continuous function of ξ everywhere. One can check that the conservation equation Eq. (40) is obeyed, including at the point $\xi = 0$ (the delta function in $\partial_\xi \tilde{\rho}(\xi)$ is cancelled by the factor ξ in Eq. (40)). Note that in this model there are two pairs of light cones at $\xi = \pm k_L$ and $\xi = \pm k_R$ respectively. Outside these two light cones ($|\xi| > \max(k_R, k_L)$) the current vanishes at large time. Inside these two light cones ($|\xi| < \min(k_R, k_L)$) the current is constant and equal to its value in the NESS (and so is the density).

Kernel. We have found by explicit calculation that in this ray regime the kernel $K(x = \xi t, x' = \xi' t, t)$ vanishes unless $\xi = \xi'$ or $\xi = -\xi'$. More precisely one obtains the limiting scaling forms for $y, y' = O(1)$

$$\lim_{t \rightarrow +\infty} K(\xi t + y, \pm \xi t + y') = K_\xi^\pm(y, y'). \quad (46)$$

The expression for $K_\xi^+(y, y')$ is obtained as

$$\begin{aligned} K_\xi^+(y, y') &= \int_0^{k_R} \frac{dk}{\pi} \cos(k(y - y')) \Theta(\xi) + \int_0^{k_L} \frac{dk}{\pi} \cos(k(y - y')) \Theta(-\xi) \\ &- \text{sign}(\xi) \int_{k_L}^{k_R} \frac{dk}{2\pi} T(k) e^{-i \text{sign}(\xi) k(y - y')} \Theta(k - |\xi|) \end{aligned} \quad (47)$$

where we recall that $T(k) = k^2/(k^2 + g^2)$. Note that $K_\xi^+(y, y')$ is a function of $y - y'$ only. From this expression (47) in the limit of coinciding points one recovers the density $\tilde{\rho}(\xi)$ in Eq. (41) (using $R(k) = 1 - T(k)$) and the current $J(\xi)$ in Eq. (44) using (15). It is important to note that the kernel (47) matches exactly in the limit $\xi \rightarrow 0^+$ with the result (31) for the kernel $K_\infty(x, x')$ of the NESS in the large distance limit $x, x' > 0$.

The expression for $K_\xi^-(y, y')$ is given by

$$K_\xi^-(y, y') = i \operatorname{sign}(\xi) \int_{k_L}^{k_R} \frac{dk}{2\pi} \frac{gk}{g^2 + k^2} e^{-i \operatorname{sign}(\xi) k(y+y')} \Theta(k - |\xi|). \quad (48)$$

This measures the quantum correlation between opposite rays. Once again the kernel (48) matches exactly in the limit $\xi \rightarrow 0^+$ with the result (32) for the kernel $K_\infty(x, x')$ of the NESS in the limit of very separated points $x > 0, x' < 0$.

It is important to remark that the results for the density (41), the current (44) and the kernel at coinciding rays (47) can be also obtained using the semi-classical method as we will see in Section 8. However the result for $K_\xi^-(y, y')$ for opposite rays in Eq. (48) cannot be obtained from this semi-classical method. Indeed, it contains additional information about correlations at a finite distance from the two opposite rays which correspond to fermion wave-functions which are split between reflected and transmitted waves by the defect.

3.3 Finite temperature generalisation

The previous result can be generalised to an initial state with non zero temperature $T_{L/R}$ different on both sides of the impurity and with associated chemical potential $\mu_{L/R}$. This amounts to take as an initial kernel at $t = 0$

$$K_L(x, x') = \Theta(-x)\Theta(-x') \sum_{n=1}^{\infty} \frac{4}{\ell} f_L \left(\frac{2\pi n}{\ell} \right) \sin \left(\frac{2\pi n x}{\ell} \right) \sin \left(\frac{2\pi n x'}{\ell} \right) \quad (49)$$

$$K_R(x, x') = \Theta(x)\Theta(x') \sum_{n'=1}^{\infty} \frac{4}{\ell} f_R \left(\frac{2\pi n'}{\ell} \right) \sin \left(\frac{2\pi n' x}{\ell} \right) \sin \left(\frac{2\pi n' x'}{\ell} \right), \quad (50)$$

where

$$f_{L/R}(k) = \frac{1}{\exp(\beta_{L/R}(\frac{k^2}{2} - \mu_{L/R})) + 1}, \quad (51)$$

is the Fermi factor with $\beta_{L/R} = 1/T_{L/R}$. The density of fermions in the initial state is now related to the chemical potentials via

$$\rho_{L/R} = \int_0^{+\infty} \frac{dk}{\pi} f_{L/R}(k). \quad (52)$$

The calculation proceeds in the same way as for $T_{L/R} = 0$ with a few additional details which are given in Appendix D. We present here only the result for $g > 0$.

In the NESS regime $x = O(1)$ the full kernel is presented in (D11) and from it we find the asymptotic density at finite temperature, for $x > 0$:

$$\rho_\infty(x > 0) = \int_0^\infty \frac{dk}{\pi} \left(f_R(k) - \frac{(f_R(k) - f_L(k))}{2} T(k) + g f_R(k) \frac{k \sin(2kx) - g \cos(2kx)}{g^2 + k^2} \right), \quad (53)$$

and the expression for $x < 0$ can be obtained from the symmetry (20) with here $\mu_L \leftrightarrow \mu_R$ and $T_L \leftrightarrow T_R$. Note that the density retains a cusp at $x = 0$ even at finite temperature. The current in the NESS at finite temperature is obtained as

$$J_\infty = - \int_0^\infty dk \frac{f_R(k) - f_L(k)}{2\pi} k T(k) . \quad (54)$$

Its low temperature expansion is performed in Appendix F and we display it here in the case $\mu_L = \mu_R = \frac{k_F^2}{2}$

$$J_\infty = \frac{\pi}{6} (T_L^2 - T_R^2) \frac{g^2}{(g^2 + k_F^2)^2} + \frac{7\pi^3}{15} \frac{g^2}{(g^2 + k_F^2)^4} (T_L^4 - T_R^4) . + O(T_R^6, T_L^6) \quad (55)$$

Note that in the absence of impurity, for $g = 0$, one has instead (for any $\mu_{L/R}$)

$$J_\infty|_{g=0} = \frac{\mu_L - \mu_R}{2\pi} + \frac{1}{2\pi} (T_L e^{-\mu_L/T_L} - T_R e^{-\mu_L/T_R}) \quad (56)$$

which generalizes the standard zero temperature result. Note that the $g = 0$ case has been studied for the same model in a high temperature limit $k_R^2/T_R \sim k_L^2/T_L \ll 1$ where interesting equilibration properties were found [50]. In our case ($g \neq 0$), one can show that the current is proportional to $T_R \sim T_L$ at high temperature.

In the ray regime $\xi = x/t = O(1)$ we find the density

$$\tilde{\rho}(\xi) = \int_0^\infty \frac{dk}{2\pi} \left(f_R(k) + f_L(k) + \text{sgn}(\xi) (f_R(k) - f_L(k)) (R(k) + T(k) \Theta(|\xi| - k)) \right) , \quad (57)$$

and the current

$$\tilde{J}(\xi) = - \int_0^\infty dk \frac{f_R(k) - f_L(k)}{2\pi} k T(k) \Theta(k - |\xi|) \quad (58)$$

These results are plotted in Fig. 5.

3.4 Energy current

Let us recall the definition of the heat current in quantum mechanics for a single particle with a Hamiltonian $\hat{H} = -\frac{1}{2}\partial_x^2 + V(x)$ and described by the wavefunction $\psi(x, t)$, see e.g. [66]. The local energy $q(x, t)$ and heat current $j_q(x, t)$ are given by

$$q(x, t) = \frac{1}{2} (\partial_x \psi(x, t)^*) (\partial_x \psi(x, t)) + \psi(x, t)^* V(x) \psi(x, t) , \quad (59)$$

$$j_q(x, t) = -\frac{1}{2} \text{Re} \left(i (\hat{H} \psi)(x, t)^* \partial_x \psi(x, t) \right) . \quad (60)$$

The total averaged energy is recovered from $\int dx q(x, t) = \langle \psi | \hat{H} | \psi \rangle$ while $q(x, t)$ and $j_q(x, t)$ obey the conservation equation (from the Schrödinger equation)

$$\partial_t q(x, t) + \partial_x j_q(x, t) = 0 . \quad (61)$$

For noninteracting fermions with the initial condition considered here (see Section 2.3), each state $\psi_{L/R}^n(x, t)$ evolves independently, hence the total local energy $Q(x, t)$ and energy current

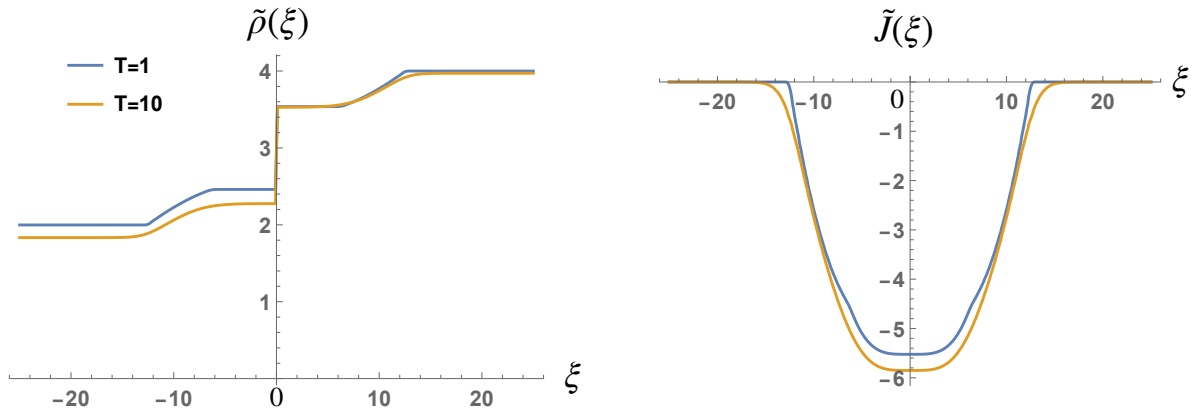


Figure 5: Plot of the asymptotic density $\tilde{\rho}(\xi)$ and current $\tilde{J}(\xi)$ in the ray regime as a function of $\xi = x/t$ for non zero temperature as given by Eqs. 57 and 58 for $\rho_R = 4$, $\rho_L = 2$ and $g = 10$. The temperatures are identical on both sides with $T_L = T_R$ equal to 1 (orange curve) and 10 (blue curve). We notice that the singularities at the light cones $\xi = \pm k_{R/L}$ are rounded compared to the zero temperature case shown in Fig. 4.

$J_Q(x, t)$ are given by the corresponding sums of the one-body contributions weighted by the Fermi factors. The time dependent energy current is thus given by

$$J_Q^{L/R}(x, t) = \sum_{n=1}^{\infty} f_{L/R}(k_n) \text{Im} \left((\hat{H}_g \psi_{L/R}^n(x, t))^* \partial_x \psi_{L/R}^n(x, t) \right), \quad (62)$$

where $k_n = \frac{2\pi n}{\ell}$ and \hat{H}_g is the single-particle Hamiltonian with a delta-impurity in Eq. (1).

The explicit calculation is performed using methods which are similar the ones used for the density and the particle current. They are summarized in Appendix E. One finds that in the large time limit the energy current $J_Q(x, t)$ converges to an asymptotic constant value $J_{Q,\infty}$ which reads

$$J_{Q,\infty} = - \int_0^{\infty} \frac{dk}{2\pi} (f_R(k) - f_L(k)) k E(k) T(k), \quad E(k) = \frac{k^2}{2}. \quad (63)$$

In the low temperature limit and in the case $\mu_L = \mu_R = \frac{k_F^2}{2}$ the current has the following expansion (see Appendix F)

$$J_{Q,\infty} = \frac{\pi}{12} \frac{k_F^2 (2g^2 + k_F^2)}{(g^2 + k_F^2)^2} (T_L^2 - T_R^2) - \frac{7\pi^3}{30} \frac{g^4}{(g^2 + k_F^2)^4} (T_L^4 - T_R^4) + O(T_R^6, T_L^6). \quad (64)$$

It is interesting to compare the first term in this low-temperature expansion with a result for the energy current obtained in [32]

$$J_{Q,\infty}^{\text{CFT}} = c \frac{\pi}{12} \cos^2 \alpha (T_L^2 - T_R^2), \quad (65)$$

where c is the central charge. A simple derivation of this result was given in [32] for free Majorana fermions (corresponding to $c = 1/2$). In that work $\cos^2 \alpha$ is the transmission coefficient of the defect, i.e. the analog of $T(k_F)$ here. However the coefficient of $T_L^2 - T_R^2$ that we obtain here in (64) is not equal to $\frac{\pi}{12} T(k_F)$ as would be predicted by the model of [32] taking into account that here $c = 1$. The discrepancy can be understood as follows. From similar methods as in

Appendix F one can show that for a general dispersion relation $E(k)$ our formula (64) becomes to leading order for small T_L and T_R

$$J_{Q,\infty} \simeq \frac{\pi}{12} \frac{1}{k_F} (\partial_k(E(k)T(k)))|_{k=k_F} (T_L^2 - T_R^2). \quad (66)$$

Performing the derivative with respect to k in (66) we obtain two terms. The first one is $\propto E'(k_F)T(k_F)/k_F = T(k_F)$ and coincides with the result of [32]. The additional term $\propto E(k_F)T'(k_F)/k_F$ is non zero when the transmission coefficient depends on the momentum k , as it is the case here. This additional term is negligible compared to the first one only when the impurity strength is small, i.e., $g \ll k_F$.

Note that in the absence of the impurity, i.e. for $g = 0$, the low-temperature expansion of $J_{Q,\infty}$ reads for arbitrary $\mu_{L/R}$

$$J_{Q,\infty}|_{g=0} = \frac{\mu_L^2 - \mu_R^2}{4\pi} + \frac{\pi}{12} (T_L^2 - T_R^2) - \frac{1}{2\pi} (T_L^2 e^{-\mu_L/T_L} - T_R^2 e^{-\mu_R/T_R}) + O(e^{-2\mu_L/T_L}, e^{-2\mu_R/T_R}) \quad (67)$$

The expansion formula for $g \neq 0$ and $\mu_L \neq \mu_R$ are given in the Appendix F.

4 Exact calculation at finite time and finite size

In this section we derive an exact formula for the kernel at any time t in a system with of size ℓ . This will be the starting point for the asymptotic analysis for $\ell \rightarrow +\infty$ and subsequently for the computation of the large time limit performed in the following sections.

4.1 Eigenbasis of \hat{H}_g

We first consider here $g > 0$, and a finite interval $x \in [-\ell/2, \ell/2]$ and specify further \hat{H}_g by imposing the vanishing of the wavefunctions at $x = \pm\ell/2$. The eigenfunctions of \hat{H}_g are either even or odd in x , respectively labelled by a subscript '+' or '-'. The odd eigenfunctions do not feel the delta impurity (since they vanish at the location of the impurity) hence they read

$$\phi_{-,q}(x) = \sqrt{\frac{2}{\ell}} \sin(qx) \quad , \quad q \in \Lambda_- = \left\{ \frac{2\pi n}{\ell}, n \in \mathbb{N}^* \right\} \quad , \quad (68)$$

where we denote Λ_- the lattice of possible values for the wavevector q .

The even eigenfunctions are also plane waves, and denoted by $\phi_{+,q}(x)$, but with a different quantization condition on q . They read

$$\phi_{+,q}(x) = \frac{1}{\sqrt{(g^2 + q^2)\frac{\ell}{2} + g}} (q \cos(qx) + g \sin(q|x|)) \quad , \quad (69)$$

with the quantification condition (see Fig. (6))

$$q \cos\left(\frac{q\ell}{2}\right) + g \sin\left(\frac{q\ell}{2}\right) = 0 \quad \Leftrightarrow \quad e^{-iq\ell} = -\frac{q - ig}{q + ig} \quad , \quad (70)$$

i.e., $q\ell = -2\text{atan}(q/g) + m\pi$, which defines the lattice of possible wavevectors $q \in \Lambda_+$

$$\Lambda_+ = \left\{ q, q \cos\left(\frac{q\ell}{2}\right) + g \sin\left(\frac{q\ell}{2}\right) = 0 \cap q > 0 \right\} \quad . \quad (71)$$

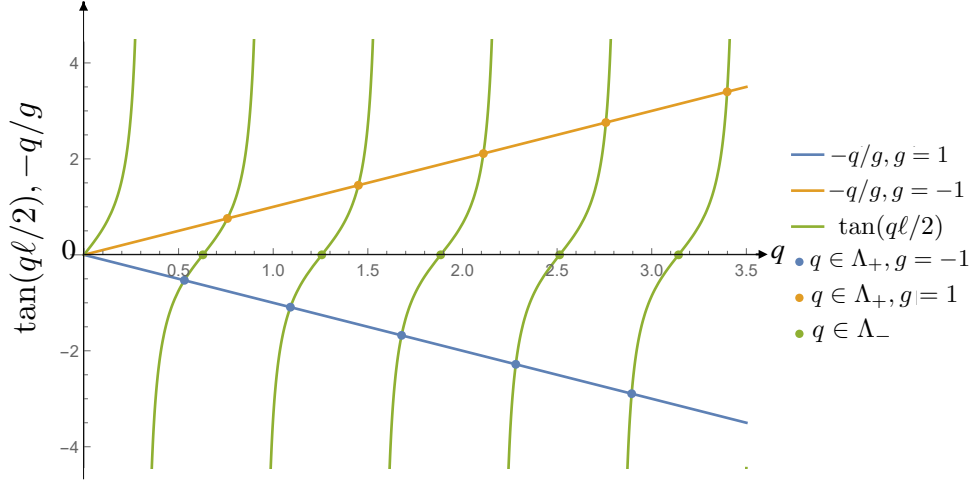


Figure 6: Graphical representation of the quantization condition in Eq. (70). It is plotted here for $g = \pm 1$ and $\ell = 10$. The intersection points $-\frac{q}{g} = \tan(\frac{q\ell}{2})$ generate the lattice $q \in \Lambda_+$ (71). The lattice Λ_- corresponds to the roots of the equation $0 = \tan(\frac{q\ell}{2}) = \sin(\frac{q\ell}{2})$ (see Eq. (68)). Therefore the two lattices Λ_+ and Λ_- are intertwined. For $g < 0$ the situation is almost the same but now $-\frac{q}{g}$ has a positive slope. Note that for $g < 0$, there is an additional bound state which cannot be shown on this figure.

Note that q and $-q$ correspond to the same state, hence the condition $q > 0$. Equivalently the states can be labeled by the strictly positive integers $m \in \mathbb{N}^*$ (see Fig. (6)).

Finally, both the odd and even eigenstates $\phi_{\pm, q}(x)$ are associated to the eigenenergy

$$E(q) = \frac{q^2}{2}. \quad (72)$$

4.2 Time dependent kernel

As discussed above, see Eq. (11), the time dependent kernel splits into two parts

$$K(x, x'; t) = K_L(x, x'; t) + K_R(x, x'; t) \quad (73)$$

where each component evolves independently

$$K_L(x, x'; t) = \sum_{n=1}^{N_L} \psi_n^{L*}(x, t) \psi_n^L(x', t) \quad , \quad K_R(x, x'; t) = \sum_{n=1}^{N_R} \psi_n^{R*}(x, t) \psi_n^R(x', t). \quad (74)$$

Since the $\psi_n^{L/R}$'s evolve according to the Schrödinger equation with Hamiltonian \hat{H}_g in Eq. (1) these components can be rewritten using the real time Green's function

$$G(x, y, t) = \langle x | e^{-i\hat{H}_g t} | y \rangle = \sum_{\sigma=\pm, q \in \Lambda_\sigma} \phi_{\sigma, q}(x) \phi_{\sigma, q}^*(y) e^{-iE(q)t}, \quad (75)$$

where the eigenfunctions $\phi_{\sigma, q}(x)$ of \hat{H}_g are given in (68) and (69). This leads to

$$K_L(x, x'; t) = \sum_{n=1}^{N_L} \psi_n^{L*}(x, t) \psi_n^L(x', t) = \int_{-\ell/2}^0 dy dy' G^*(x, y, t) G(x', y', t) K_L(y, y'), \quad (76)$$

$$K_R(x, x'; t) = \sum_{n=1}^{N_R} \psi_n^{R*}(x, t) \psi_n^R(x', t) = \int_0^{\ell/2} dy dy' G^*(x, y, t) G(x', y', t) K_R(y, y'). \quad (77)$$

The time evolution of the total kernel is thus obtained as the sum as in (73).

Let us first study $K_R(x, x'; t)$ in Eq. (77). Inserting the decomposition (75) of the Green's function together with the explicit expression of $K_R(y, y')$ in Eq. (6) we obtain

$$\begin{aligned}
K_R(x, x', t) &= \int_0^{\ell/2} dy dy' \sum_{\sigma_a=\pm, k_a \in \Lambda_{\sigma_a}} \phi_{\sigma_a, k_a}^*(x) \phi_{\sigma_a, k_a}(y) e^{iE(k_a)t} \\
&\quad \sum_{\sigma_b=\pm, k_b \in \Lambda_{\sigma_b}} \phi_{\sigma_b, k_b}(x') \phi_{\sigma_b, k_b}^*(y') e^{-iE(k_b)t} \sum_{k \in \Lambda_-, k \leq k_R} \frac{4}{\ell} \sin(ky) \sin(ky') \\
&= \sum_{\sigma_a=\pm, k_a \in \Lambda_{\sigma_a}} \sum_{\sigma_b=\pm, k_b \in \Lambda_{\sigma_b}} \sum_{k \in \Lambda_-, k \leq k_R} \phi_{\sigma_a, k_a}^*(x) \phi_{\sigma_b, k_b}(x') e^{i(E(k_a)-E(k_b))t} \\
&\quad \int_0^{\ell/2} dy \sqrt{\frac{4}{\ell}} \phi_{\sigma_a, k_a}(y) \sin(ky) \int_0^{\ell/2} dy' \sqrt{\frac{4}{\ell}} \phi_{\sigma_b, k_b}^*(y') \sin(ky'), \tag{78}
\end{aligned}$$

where, in the third and fourth lines, we have just reorganized the discrete sums and the integrals over y and y' . The same manipulations can be performed for $K_L(x, x', t)$. The overlap integrals over y and y' can be performed explicitly, which gives

$$\begin{aligned}
K_{R/L}(x, x', t) &= \sum_{\sigma_a=\pm, k_a \in \Lambda_{\sigma_a}} \sum_{\sigma_b=\pm, k_b \in \Lambda_{\sigma_b}} \sum_{k \in \Lambda_-, k \leq k_{R/L}} \phi_{\sigma_a, k_a}^*(x) \phi_{\sigma_b, k_b}(x') e^{i(E(k_a)-E(k_b))t} \\
&\quad \times \left(\frac{1}{\sqrt{2}} \delta_{\sigma_a, -\delta_{k, k_a}} \pm \frac{2^{3/2}}{\ell} \frac{k k_a}{(k^2 - k_a^2) \sqrt{g^2 + k_a^2 + \frac{2g}{\ell}}} \delta_{\sigma_a, +} \right) \\
&\quad \times \left(\frac{1}{\sqrt{2}} \delta_{\sigma_b, -\delta_{k, k_b}} \pm \frac{2^{3/2}}{\ell} \frac{k k_b}{(k^2 - k_b^2) \sqrt{g^2 + k_b^2 + \frac{2g}{\ell}}} \delta_{\sigma_b, +} \right), \tag{79}
\end{aligned}$$

where, in the last two factors in brackets, the $+$ sign refers to K_R and the $-$ to K_L . To compute the full kernel we add the two halves and develop the product to get

$$\begin{aligned}
K(x, x', t) &= \underbrace{\left(\sum_{n=1}^{N_R} + \sum_{n=1}^{N_L} \right) \frac{1}{2} \frac{2}{\ell} \sin\left(\frac{2\pi n x}{\ell}\right) \sin\left(\frac{2\pi n x'}{\ell}\right)}_{A=A_R+A_L} \tag{80} \\
&+ \underbrace{\left(\sum_{k \in \Lambda_-, k \leq k_R} + \sum_{k \in \Lambda_-, k \leq k_L} \right) \sum_{k_a \in \Lambda_+, k_b \in \Lambda_+} 2 \left(\frac{2}{\ell}\right)^3 \frac{k_a \cos(k_a x) + g \sin(k_a |x|)}{g^2 + k_a^2 + \frac{2g}{\ell}}}{B=B_R+B_L} \\
&\times \underbrace{\frac{k_b \cos(k_b x') + g \sin(k_b |x'|)}{g^2 + k_b^2 + \frac{2g}{\ell}} \frac{k^2 k_a k_b}{(k_a^2 - k^2)(k_b^2 - k^2)} e^{i(E(k_a)-E(k_b))t}}_{B=B_R+B_L} \\
&+ \underbrace{\sum_{k \in \Lambda_-, k_L < k \leq k_R} \sum_{k_b \in \Lambda_+} \left(\frac{2}{\ell}\right)^2 \sin(kx) \frac{k_b \cos(k_b x') + g \sin(k_b |x'|)}{g^2 + k_b^2 + \frac{2g}{\ell}} \frac{k k_b}{k^2 - k_b^2} e^{i(E(k)-E(k_b))t}}_C \\
&+ \underbrace{\sum_{k \in \Lambda_-, k_L < k \leq k_R} \sum_{k_a \in \Lambda_+} \left(\frac{2}{\ell}\right)^2 \sin(kx') \frac{k_a \cos(k_a x) + g \sin(k_a |x|)}{g^2 + k_a^2 + \frac{2g}{\ell}} \frac{k k_a}{k^2 - k_a^2} e^{i(E(k_a)-E(k))t}}_D,
\end{aligned}$$

which is the sum of four terms denoted $A = A_R + A_L, B = B_R + B_L, C, D$ as indicated in the equation. These terms satisfy the symmetries: $A(x, x')$ is real and symmetric, $B(x, x') = B^*(x', x)$ and $D(x, x') = C^*(x', x)$.

Remarks:

(i) *Symmetries:* Since the initial kernel is unchanged under the simultaneous transformation $(k_L, k_R, x) \rightarrow (k_R, k_L, -x)$ and because of the invariance of \hat{H}_g under parity transformation $x \rightarrow -x$, it follows that $K(x, x', t)$ is also unchanged under $(k_L, k_R, x) \rightarrow (k_R, k_L, -x)$. The density $\rho(x, t)$ has thus the same invariance and the current satisfies $J_{k_L, k_R}(x, t) = -J_{k_R, k_L}(-x, t)$. This property is the finite time analog of the relations valid for the NESS stated in Eq. 20.

(ii) *Contribution to the current:* Since the term A is real, it does not contribute to $J(x, t)$, i.e., $J_A(x, t) = 0$ (see Eq. (15)). It is easy to see that the term B gives only an odd contribution to the current, i.e. $J_B(x, t) = -J_B(-x, t)$. Hence the term B cannot contribute to J_∞ , the current in the NESS, which is uniform. It does however contribute to $\rho_\infty(x)$. The current in the NESS is thus only determined by $C + D$ which gives an even contribution at all time t , i.e., $J_{C+D}(x, t) = J_{C+D}(-x, t)$.

5 Thermodynamic limit $\ell \rightarrow +\infty$

Our first goal is to obtain a formula for the kernel for the infinite system, i.e., $\lim_{\ell \rightarrow +\infty} K(x, x', t)$ for fixed x, x', t , which, for notational convenience, we will also denote by $K(x, x', t)$. Here we consider the case of a repulsive impurity $g > 0$ – the analysis of an attractive impurity $g < 0$ is performed in Appendix C. Let us recall that we take the limit $\ell \rightarrow \infty$ while fixing the left and right initial densities $\frac{2N_{L/R}}{\ell} = \rho_{L/R} = \frac{k_{L/R}}{\pi}$. This is possible thanks to a contour integration trick that we explain below. From the exact expression for the kernel in (80), one can write

$$K(x, x', t) = A_L(x, x') + A_R(x, x') + C(x, x', t) + C^*(x', x, t) + B_L(x, x', t) + B_R(x, x', t), \quad (81)$$

where we have used the relation $D(x, x', t) = C^*(x', x, t)$. We now give the expressions of the limits when $\ell = +\infty$ of the terms $A_{L/R}, B_{L/R}$ and C separately.

The term $A(x, x')$: From (80) we see that it is time independent and, in the large ℓ limit, it is given by the reflected sine-kernel (see e.g. [10, 11])

$$\begin{aligned} A_{L/R}(x, x') &= \lim_{\ell \rightarrow \infty} \frac{1}{\ell} \sum_{n=1}^{N_{L/R}} \sin\left(\frac{2\pi n x}{\ell}\right) \sin\left(\frac{2\pi n x'}{\ell}\right) = \int_0^{k_{L/R}} \frac{dk}{2\pi} \sin(kx) \sin(kx') \\ &= \frac{\rho_{L/R}}{4} \left(\frac{\sin(k_{L/R}(x - x'))}{k_{L/R}(x - x')} - \frac{\sin(k_{L/R}(x + x'))}{k_{L/R}(x + x')} \right). \end{aligned} \quad (82)$$

The term $C(x, x', t)$: From (80) the term C is given by a double sum

$$C = C(x, x', t) = \frac{4}{\ell^2} \sum_{k_b \in \Lambda_+} \sum_{k \in \Lambda_-, k = k_L^+}^{k_R} \frac{h_{x, x', t}(k, k_b)}{k - k_b} \quad (83)$$

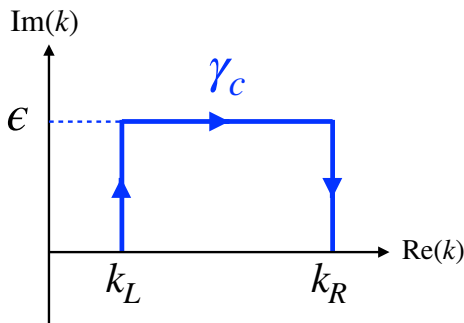


Figure 7: Illustration of the contour γ_c over which the integral over k in the first line of (85) is performed.

with $k_L = 2\pi N_L/\ell$, $k_L^+ = 2\pi(N_L + 1)/\ell$ and $k_R = 2\pi N_R/\ell$ and we recall that the lattices Λ_- and Λ_+ are defined in Eqs. (68) and (71) respectively. We have also defined the function ¹

$$h_{x,x',t}(k, k_b) = \sin(kx) \frac{k_b \cos(k_b x') + g \sin(k_b |x'|)}{g^2 + k_b^2} \frac{k k_b}{k + k_b} e^{\frac{i}{2}(k^2 - k_b^2)t}. \quad (84)$$

Taking the limit $\ell \rightarrow \infty$ of (83) to obtain a double integral is very delicate due to the presence in the sum of a pole $\frac{1}{k - k_b}$ and the fact that the two lattices Λ_- and Λ_+ are intertwined (see Fig. 6). Let us first state the result and give its derivation below. One finds

$$\begin{aligned} \lim_{\ell \rightarrow \infty} C(x, x', t) &= \int_0^{+\infty} \frac{dk_b}{\pi} \left[\left(\int_{k_L}^{k_L + i\epsilon} \frac{dk}{\pi} + \int_{k_L + i\epsilon}^{k_R + i\epsilon} \frac{dk}{\pi} - \int_{k_R}^{k_R + i\epsilon} \frac{dk}{\pi} \right) \frac{h_{x,x',t}(k, k_b)}{k - k_b} \right] \\ &+ \int_{k_L}^{k_R} \frac{dk_b}{\pi} \left(i + \frac{g}{k_b} \right) h_{x,x',t}(k_b, k_b). \end{aligned} \quad (85)$$

The first line of (85) is an integral over a contour that we denote γ_c consisting in straight lines in the complex k -plane, forming a half-rectangle as represented in Fig. 7. Its value does not depend on the parameter $\epsilon > 0$ since $h_{x,x',t}(k, k_b)$ as a function of k does not have poles in the strip $[k_L, k_R] + i\mathbb{R}^+$. In addition to the derivation given below we have carefully checked numerically this formula (85) for a variety of function h which share the same properties.

Let us now give the derivation of this result in Eq. (85). The idea is inspired from [51], although some details are different here. The trick is to replace the discrete sum over k in (83) by a contour integral as follows

$$C(x, x', t) = \frac{4}{\ell^2} \sum_{k_b \in \Lambda_+} \int_{\Gamma_0} \frac{dk}{2\pi} \frac{\ell}{e^{i\ell k} - 1} \frac{h_{x,x',t}(k, k_b)}{k - k_b}, \quad (86)$$

where the contour Γ_0 is a union of very small circles centered around the points $k = \frac{2\pi n}{\ell}$ with $N_L + 1 \leq n \leq N_R$ and oriented counterclockwise (see Fig. 8). The circles should be small enough so that the contour does not enclose any point $k = k_b \in \Lambda_+$. We now deform the contour Γ_0 into the closed counterclockwise contour γ_δ which is the rectangle with the four corners $k_L^+ - \frac{2\pi\delta}{\ell} - i\epsilon$, $k_L^+ - \frac{2\pi\delta}{\ell} + i\epsilon$, $k_R + \frac{2\pi\delta}{\ell} + i\epsilon$, $k_R + \frac{2\pi\delta}{\ell} - i\epsilon$, represented in Fig. 8. The parameter $0 < \delta < 1$ is chosen small enough so that the contour does not contain any point k_b

¹Since we are eventually interested in the large ℓ limit we omitted in (84) the unimportant extra factor $2g/\ell$ in the denominator in (80), which should be restored to obtain finite ℓ formula.

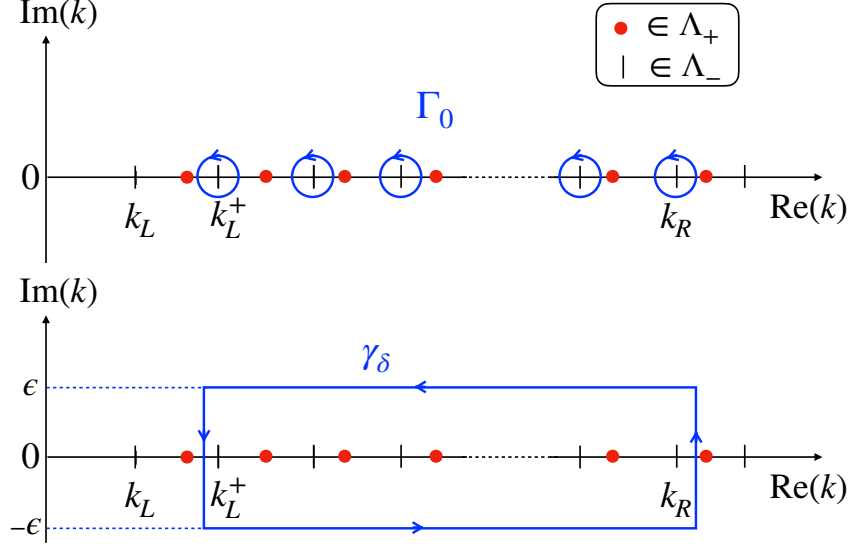


Figure 8: Illustration of the contours Γ_0 (upper panel) and γ_δ (lower panel) used in Eqs. (86) and (87) respectively.

of Λ_+ located to the left of k_L^+ and to the right of k_R . During this deformation one encounters only the poles at $k = k_b \in \Lambda_+ \cap]k_L^+, k_R[$. Taking into account the residues associated to these poles one obtains

$$C(x, x', t) = \frac{4}{\ell^2} \left(\sum_{k_b \in \Lambda_+} \oint_{\gamma_\delta} \frac{dk}{2\pi} \frac{\ell}{e^{i\ell k} - 1} \frac{h_{x, x', t}(k, k_b)}{k - k_b} - 2\pi i \sum_{k_b \in \Lambda_+ \cap]k_L^+, k_R[} \frac{\ell}{2\pi} \frac{1}{e^{i\ell k_b} - 1} h_{x, x', t}(k_b, k_b) \right). \quad (87)$$

Until now this is an exact rewriting of $C(x, x', t)$ in Eq. (83) valid for any ℓ . For any $k_b \in \Lambda_+$, using the second relation in (70), one can evaluate the factor

$$\frac{1}{e^{i\ell k_b} - 1} = -\frac{1}{2} + \frac{i}{2} \frac{g}{k_b}. \quad (88)$$

We now take the large ℓ limit on Eq. (87). The factor $\frac{1}{e^{i\ell k} - 1} \rightarrow 0$ for $\text{Im } k < 0$ and $\frac{1}{e^{i\ell k} - 1} \rightarrow -1$ for $\text{Im } k > 0$. Hence the k integral in (87) over the counterclockwise closed contour γ_δ becomes the k integral over the clockwise half-rectangle in (85).² In addition the sum over k_b becomes an integral in the large ℓ limit. This leads to the result (85).

The term $B(x, x', t)$: We now give the large ℓ limit of $B_L(x, x')$ and $B_R(x, x')$ defined in (80). Each term can be decomposed as the sum of two terms

$$B_{R/L}(x, x', t) = B_{R/L}^{\text{off-diag}}(x, x', t) + B_{R/L}^{\text{diag}}(x, x') \quad (89)$$

where the first term comes from the terms $k_a \neq k_b$ in the triple sum in (80), while the second one comes from the terms $k_a = k_b$ and does not depend on time. As detailed in the Appendix

²Proving the convergence for the vertical parts of the contour γ_c is non-trivial, which is why we did careful numerical checks of (85). This problem does not occur in [51, 63].

A, we obtain the first term in (89) as

$$B_R^{\text{off-diag}}(x, x', t) = \int_0^\infty \int_0^\infty \frac{dk_a}{\pi} \frac{dk_b}{\pi} F_{x, x'}(k_a, k_b) e^{\frac{1}{2}i(k_a^2 - k_b^2)t} \quad (90)$$

$$\times \left[\frac{1}{2\pi} \left(\frac{k_b \log\left(\frac{k_b + k_R}{|k_b - k_R|}\right) - k_a \log\left(\frac{k_a + k_R}{|k_a - k_R|}\right)}{k_a^2 - k_b^2} \right) + \frac{g}{2(k_a^2 - k_b^2)} (\Theta(k_R - k_a) - \Theta(k_R - k_b)) \right],$$

where we have defined the function

$$F_{x, x'}(k_a, k_b) = 2 \frac{k_a \cos(k_a x) + g \sin(k_a |x|)}{g^2 + k_a^2} \frac{k_b \cos(k_b x') + g \sin(k_b |x'|)}{g^2 + k_b^2} k_a k_b. \quad (91)$$

The second term in (89) is obtained in the large ℓ limit as

$$B_R^{\text{diag}}(x, x') = \int_0^{k_R} \frac{dk_a}{2\pi} F_{x, x'}(k_a, k_a) \frac{(g^2 + k_a^2)}{2k_a^2}. \quad (92)$$

The terms $B_L^{\text{off-diag}}(x, x', t)$ and $B_L^{\text{diag}}(x, x')$ are simply obtained from $B_R^{\text{off-diag}}(x, x', t)$ and $B_R^{\text{diag}}(x, x')$ by substituting $k_R \rightarrow k_L$ in Eqs. (90) and (92).

6 Large time limit: stationary state at fixed position x

In the previous section we have obtained the expression of the kernel in the thermodynamic limit $\lim_{\ell \rightarrow +\infty} K(x, x', t)$ in (81) together with (89), as a sum of several terms. Now we can take the limit $t \rightarrow +\infty$ of each term in this expression for fixed positions x and x' to obtain

$$K_\infty(x, x') = \lim_{t \rightarrow +\infty} \lim_{\ell \rightarrow +\infty} K(x, x', t). \quad (93)$$

In (81) and (89) the terms $A_{L/R}(x, x')$ and $B_{R/L}^{\text{diag}}(x, x')$ are independent of time. As shown in Appendix B, the terms $B_{L/R}^{\text{off-diag}}(x, x', t)$ decay to zero at large time as power laws in time. Finally $C(x, x', t)$ goes to a finite limit $C_\infty(x, x')$ where only the last term in (85) (coming from the residues) survives at large time, as discussed in Appendix B where the time decay is studied. From the last term in (85) we obtain

$$C_\infty(x, x') = \frac{1}{2} \int_{k_L}^{k_R} \frac{dk}{\pi} (g + ik) \sin(kx) \frac{k \cos(kx') + g \sin(k|x'|)}{g^2 + k^2}. \quad (94)$$

As a result the kernel at infinite time, i.e., in the NESS, is obtained as the sum

$$K_\infty(x, x') = A_R(x, x') + A_L(x, x') + B_R^{\text{diag}}(x, x') + B_L^{\text{diag}}(x, x') + E(x, x'), \quad (95)$$

where the terms $A_{L/R}(x, x')$ are given in (82),

$$E(x, x') = C_\infty(x, x') + C_\infty(x', x)^*, \quad (96)$$

where $C_\infty(x, x')$ is given in (94), and we recall

$$B_{R/L}^{\text{diag}}(x, x') = \int_0^{k_{R/L}} \frac{dk}{2\pi} \frac{k \cos(kx) + g \sin(k|x|)}{g^2 + k^2} (k \cos(kx') + g \sin(k|x'|)). \quad (97)$$

Stationary density. The stationary density can be obtained from the kernel using the relation $\rho_\infty(x) = K_\infty(x, x)$. It can be written as the sum $\rho_\infty(x) = \rho_A(x) + \rho_B(x) + \rho_E(x)$ of the contributions of the terms in (95) with

$$\rho_A(x) = \frac{\rho_R}{4} \left(1 - \frac{\sin(2k_R x)}{2k_R x} \right) + \frac{\rho_L}{4} \left(1 - \frac{\sin(2k_L x)}{2k_L x} \right) \quad (98)$$

$$\rho_B(x) = \frac{\rho_R}{4} + \frac{\rho_L}{4} + \left(\int_0^{k_R} + \int_0^{k_L} \right) \frac{dk}{4\pi} \frac{(k^2 - g^2) \cos(2kx) + 2gk \sin(2k|x|)}{g^2 + k^2} \quad (99)$$

$$\begin{aligned} \rho_E(x) &= g \int_{k_L}^{k_R} \frac{dk}{\pi} \sin(kx) \frac{k \cos(kx) + g \sin(k|x|)}{g^2 + k^2} \\ &= \int_{k_L}^{k_R} \frac{dk}{2\pi} \frac{g}{g^2 + k^2} (k \sin(2kx) + \operatorname{sgn}(x)g(1 - \cos(2kx))) . \end{aligned} \quad (100)$$

Let us rewrite $\rho_A(x)$ using the identity

$$\frac{\rho_R \sin(2k_R x)}{4 \cdot 2k_R x} = \frac{\sin(2k_R x)}{8\pi x} = \int_0^{k_R} \frac{dk}{4\pi} \cos(2kx) . \quad (101)$$

Summing the different contributions to $\rho_\infty(x)$, one obtains

$$\rho_\infty(x) = \frac{k_R + k_L}{2\pi} + \operatorname{sgn}(x) \int_{k_L}^{k_R} \frac{dk}{2\pi} \frac{g^2}{g^2 + k^2} \quad (102)$$

$$\begin{aligned} &+ \left(\int_0^{k_R} + \int_0^{k_L} \right) \frac{dk}{4\pi} \frac{(-2g^2) \cos(2kx) + 2gk \sin(2k|x|)}{g^2 + k^2} \\ &+ \int_{k_L}^{k_R} \frac{dk}{2\pi} \frac{g}{g^2 + k^2} (k \sin(2kx) - g \operatorname{sgn}(x) \cos(2kx)) . \end{aligned} \quad (103)$$

In that expression the constant parts can be rewritten for $x > 0$ and $x < 0$ respectively as

$$\frac{k_R + k_L}{2\pi} + \int_{k_L}^{k_R} \frac{dk}{2\pi} \frac{g^2}{g^2 + k^2} = \frac{k_R}{\pi} - \int_{k_L}^{k_R} \frac{dk}{2\pi} \frac{k^2}{g^2 + k^2} , \quad (x > 0) \quad (104)$$

$$\frac{k_R + k_L}{2\pi} - \int_{k_L}^{k_R} \frac{dk}{2\pi} \frac{g^2}{g^2 + k^2} = \frac{k_L}{\pi} - \int_{k_R}^{k_L} \frac{dk}{2\pi} \frac{k^2}{g^2 + k^2} , \quad (x < 0) , \quad (105)$$

as in Eq. (21). Next, regrouping the terms proportional to $\cos(2kx)$ and $\sin(2kx)$ in the integrals one can check that it is identical to the expression given in Eq. (21).

Stationary current. For the current, using (15) one obtains in the large time limit

$$J_A(x) = 0 \quad (106)$$

$$J_B(x) = 0 \quad (107)$$

$$J_E(x) = - \int_{k_L}^{k_R} \frac{dk}{2\pi} \frac{k^3}{g^2 + k^2} = \frac{1}{4\pi} (k_L^2 - k_R^2 + \frac{g^2}{2} \ln(\frac{g^2 + k_R^2}{g^2 + k_L^2})) \quad (108)$$

where the first two contributions vanish since A and B are both real, and the third simplifies. The total result for the current in the NESS regime can thus be written as

$$J_\infty(x) = J_\infty = \frac{1}{4\pi} \left(k_L^2 - k_R^2 + \frac{g^2}{2} \ln \left(\frac{g^2 + k_R^2}{g^2 + k_L^2} \right) \right) \quad (109)$$

Using $\mu_{R/L} = \frac{1}{2}k_{R/L}^2$ one can rewrite this result as in (26) in terms of the Fermi energies on both sides.

Stationary kernel. Putting all terms together in (95) and using standard trigonometric relations we find for $x, x' > 0$ the result for $K_\infty(x > 0, x' > 0)$ given in Eq. (29). Note that the first term in (29) is the sine-kernel associated to the right side of the system, namely $\sin(k_R(x - x'))/(\pi(x - x'))$. One can rewrite this result as (we recall that here $g > 0$)

$$\begin{aligned} K_\infty(x > 0, x' > 0) &= \int_0^{k_R} \frac{dk}{\pi} \cos(k(x - x')) - \int_{k_L}^{k_R} \frac{dk}{2\pi} \frac{k^2}{g^2 + k^2} e^{-ik(x-x')} \\ &+ \frac{g}{\pi} e^{g(|x|+|x'|)} \text{Im} E_1((g + ik_R)(|x| + |x'|)) . \end{aligned} \quad (110)$$

Similarly, for $x > 0$ and $x' < 0$ one finds the result for $K_\infty(x > 0, x' < 0)$ given in Eq. (30). Once again, it is equivalent to the following expression

$$\begin{aligned} K_\infty(x > 0, x' < 0) &= \frac{g}{2\pi} e^{g(|x|+|x'|)} (\text{Im} E_1((g + ik_R)(|x| + |x'|)) + \text{Im} E_1((g + ik_L)(|x| + |x'|))) \\ &+ \left(\int_0^{k_R} + \int_0^{k_L} \right) \frac{dk}{2\pi} \cos(k(x - x')) \\ &+ \int_{k_L}^{k_R} \frac{dk}{2\pi} \frac{k}{g^2 + k^2} (g \sin k(x + x') + i(k \sin k(x - x') - 2g \sin(kx) \sin(kx'))) . \end{aligned} \quad (111)$$

Large distance limits. Interestingly this stationary kernel has several non-trivial limits far from the defect. Indeed consider first the expression (29) for $x, x' \rightarrow +\infty$ with $x - x'$ fixed. Let us use the following property. For any smooth function with bounded $f''(k)$, as $u \rightarrow +\infty$ one has

$$\int_0^{k_R} dk f(k) \sin(ku) = \frac{f(0) - f(k_R) \cos k_R u}{u} + o\left(\frac{1}{u}\right) \quad (112)$$

$$\int_0^{k_R} dk f(k) \cos(ku) = \frac{f(k_R) \sin k_R u}{u} + o\left(\frac{1}{u}\right) . \quad (113)$$

This can be shown by performing two successive integrations by parts with respect to k . This shows that the last term in (29)

$$\begin{aligned} &\int_0^{k_R} \frac{dk}{\pi} \frac{gk \sin(k(x + x')) - g^2 \cos(k(x + x'))}{k^2 + g^2} \\ &\simeq \frac{-1}{\pi(x + x')} \frac{g}{k_R^2 + g^2} (k_R \cos(k_R(x + x')) + g \sin(k_R(x + x'))) , \end{aligned} \quad (114)$$

decays to zero at large distance. The asymptotic behavior is thus given by (31).

Another interesting limit is $x \rightarrow +\infty$, $x' \rightarrow -\infty$ with $x + x' = O(1)$ fixed. In that case, by a similar calculation as above, the terms depending on $x - x'$ in (30) decay to zero leading to the asymptotics given in (32).

7 Large time limit with $\xi = x/t, \xi' = x'/t$ fixed

In this section we study the large time limit of the kernel in the regimes of rays, i.e. $x, x', t \rightarrow \infty$ with $\xi = x/t$ and $\xi' = x'/t$ fixed and $O(1)$. We start from the expression (81) for the kernel

$K(x, x', t)$ in the $\ell = +\infty$ limit. It is a sum of terms of type A, C, B which are given in Eq. (82) for A , in Eq. (85) for C and in Eqs. (89), (90) and (92) for B . In these expressions, we will set $x = \xi t + y$ and $x' = \xi t + y'$ and study the large t limit at fixed $\xi, \xi' = O(1)$ and fixed $y, y' = O(1)$. As we show below the terms $A_{L/R}$ and $B_{L/R}^{\text{diag}}$ are simple to analyze. The study of the term C requires a modification of the contour integral trick used for the NESS, as pointed out in [51]. We now examine these terms independently.

The term $A(x, x')$. From (82) this term decays to zero unless $\xi = \pm \xi'$. In the first case one finds

$$A_{L/R}(\xi t + y, \xi t + y') \simeq \frac{\rho_{L/R}}{4} \frac{\sin(k_{L/R}(y - y'))}{k_{L/R}(y - y')}, \quad (115)$$

while in the second case one finds

$$A_{L/R}(\xi t + y, -\xi t + y') \simeq -\frac{\rho_{L/R}}{4} \frac{\sin(k_{L/R}(y + y'))}{k_{L/R}(y + y')}. \quad (116)$$

The term $C(x, x', t)$. Inserting $x = \xi t + y$ and $x' = \xi t + y'$ in (85) we will treat separately the contour integral in the first line and the residue part in the second line of that equation. In the contour integral over k in (85) one must be careful with the factor which comes from the factor containing $\sin(kx)$ in the function $h_{x, x', t}(k, k_b)$ in (84), and which reads schematically

$$\frac{e^{ik(\xi t + y)} - e^{-ik(\xi t + y)}}{2i(k - k_b)} e^{\frac{i}{2}k^2 t}. \quad (117)$$

Previously, for $\xi = 0$, this term was decaying to zero at large t since $\text{Im}(k) > 0$ along the contour. For $\xi \neq 0$ let us rewrite (117) setting $k = \bar{k} + iq$, as

$$\frac{e^{\frac{i}{2}(\bar{k}^2 - q^2)t}}{2i(k - k_b)} \left(e^{-q((\xi + \bar{k})t + y)} e^{i\bar{k}(\xi t + y)} - e^{q((\xi - \bar{k})t + y)} e^{-i\bar{k}(\xi t + y)} \right). \quad (118)$$

Let us recall that on the contour in (85) $q = \text{Im}(k) > 0$ and $\bar{k} \in [k_L, k_R]$. Consider first $\xi > 0$. In that case the first term in (118) can be discarded at large time, and the second term diverges at large time if $\bar{k} = \text{Re}k < \xi$. Since $\bar{k} \geq k_L$, if $\xi < k_L$ we can still discard the contribution of the contour integral at large time. If $\xi > k_L$ we need to deform the contour to be able to handle the large time limit of (85). Consider first the case $k_L < \xi < k_R$. Denoting γ_c the original contour, one writes $\int_{\gamma_c} = \int_{\gamma_{c'}} + \oint_{\gamma_{c''}}$ where the contours are represented in Fig. 9. One has

$$\int_{\gamma_{c'}} dk = - \int_{k_L - i\epsilon}^{k_L} dk + \int_{k_L - i\epsilon}^{\xi + \frac{y}{t} - i\epsilon} dk + \int_{\xi + \frac{y}{t} - i\epsilon}^{\xi + \frac{y}{t} + i\epsilon} dk + \int_{\xi + \frac{y}{t} + i\epsilon}^{k_R + i\epsilon} dk - \int_{k_R}^{k_R + i\epsilon} dk \quad (119)$$

and, as we argue below, the contribution of $\gamma_{c'}$ vanishes at large time. On the other hand, since $\gamma_{c''}$ is a closed contour which surrounds the interval $[k_L, \xi + \frac{y}{t}]$, its total contribution to $C(\xi t + y, \xi' t + y', t)$ is given by a sum of residues at $k = k_b$ and reads (it involves only the second term in (117) since the first term can be discarded for any $\xi > 0$)

$$\int_0^{+\infty} \frac{dk_b}{\pi} \oint_{\gamma_{c''}} \frac{dk}{\pi} \frac{h_{\xi t + y, \xi' t + y', t}(k, k_b)}{k - k_b} = -2i \int_{k_L}^{\xi + \frac{y}{t}} \frac{dk_b - 1}{\pi} \frac{1}{2i} e^{-ik_b(\xi t + y)} \tilde{h}_{\xi' t + y', t}(k_b, k_b), \quad (120)$$

where

$$\tilde{h}_{x', t}(k, k_b) = \frac{k_b \cos(k_b x') + g \sin(k_b |x'|)}{g^2 + k_b^2} \frac{k k_b}{k + k_b} e^{\frac{i}{2}(k^2 - k_b^2)t} \quad (121)$$

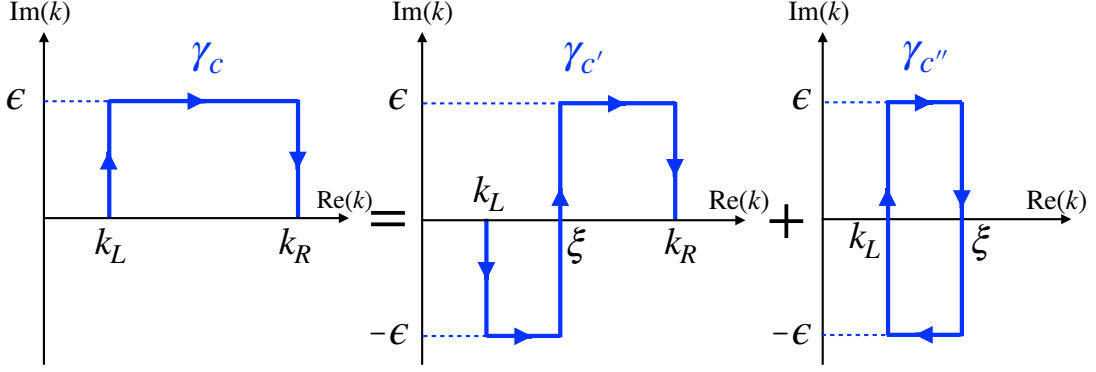


Figure 9: Illustration of the contour γ_c , $\gamma_{c'}$ and $\gamma_{c''}$. To be precise the contour $\gamma_{c'}$ includes the vertical line at $\xi + \frac{y}{t}$ (instead of ξ as indicated in the figure) but this difference is irrelevant in the large t limit.

It thus adds to the residue term on the second line of (85), noting however that in (85) $h_{x,x',t}(k, k_b) = \sin(kx)\tilde{h}_{x',t}(k, k_b)$.

Let us now discuss the contribution of the contour $\gamma_{c'}$ in Fig. (9) denoting $k = \bar{k} + iq$. The general idea is that this new contour has been chosen such that its contribution decays to zero at large time. For the first and last term in (119), it is clear that the large time limit vanishes since $q(\xi - \bar{k}) < 0$ in both cases on the new contour. It is convenient to take again the limit $\epsilon \rightarrow +\infty$ which makes the contributions of the horizontal parts (second and fourth terms in (119)) vanish. Let us analyze the contribution to C of the remaining integral (the third integral in the right hand side of Eq. (119)) along the vertical axis at $\bar{k} = \xi + \frac{y}{t}$, setting $y = y' = 0$ the conclusion remains unchanged for the general case. Writing $q = \xi + iq$, it reads (retaining only the second term in Eq. (118))

$$\frac{-1}{2} \int_0^{+\infty} \frac{dk_b}{\pi} \int_{-\infty}^{+\infty} \frac{dq}{\pi} \frac{k_b \cos(k_b \xi' t) + g \sin(k_b |\xi'| t)}{g^2 + k_b^2} \frac{(\xi + iq)k_b}{(\xi + iq)^2 - k_b^2} e^{-\frac{i}{2}(\xi^2 + q^2 + k_b^2)t}. \quad (122)$$

One can argue that this integral vanishes at large time. By expressing the sine and cosine terms in (122) as the sum of exponentials, the resulting exponential terms have the form $e^{-\frac{i}{2}(q^2 + (k_b \pm \xi')^2 + \xi^2 - (\xi')^2)t}$ which have a saddle point at $q = 0$, $k_b = \pm \xi'$. By expanding around these saddle points $k_b = \pm \xi' + p$ one finds that the integral decays algebraically at large t .

For $\xi < 0$ it is the second term in (118) which vanishes at large time. For the first term in (118) one can perform the same manipulations as above with $\xi \rightarrow |\xi|$ and the right hand side in (120) is changed to

$$\text{sign}(\xi) \int_{k_L}^{|\xi|} \frac{dk_b}{\pi} e^{-\text{sign}(\xi)ik_b(\xi t + y)} \tilde{f}_{\xi' t + y', t}(k_b, k_b), \quad (123)$$

where we have used that the shift by y/t in the bounds of the integral is irrelevant in the following.

Discarding all the terms which vanish at large time, we are left with the sum of (118) and the contribution from the second line in (85) which leads to

$$C(\xi t + y, \xi' t + y') \simeq \left(\text{sign}(\xi) \int_{k_L}^{\max(|\xi|, k_R, k_L)} \frac{dk_b}{\pi} e^{-\text{sign}(\xi)ik_b(\xi t + y)} \right. \quad (124) \\ \left. + \int_{k_L}^{k_R} \frac{dk_b}{\pi} \left(i + \frac{g}{k_b} \right) \sin(k_b(\xi t + y)) \right) \frac{k_b}{2} \frac{k_b \cos(k_b(\xi' t + y')) + g \sin(k_b|\xi'| t + y')}{g^2 + k_b^2}.$$

It vanishes at large time unless $\xi' = \xi$ or $\xi' = -\xi$. For $\xi' = \xi$ we find using standard trigonometric identities

$$C(\xi t + y, \xi t + y') \simeq \text{sign}(\xi) \int_{k_L}^{\max(\min(|\xi|, k_R), k_L)} \frac{dk_b}{4\pi} \frac{k_b(k_b - ig)}{g^2 + k_b^2} e^{-i\text{sign}(\xi)k_b(y-y')} \quad (125)$$

$$+ \int_{k_L}^{k_R} \frac{dk_b}{\pi} \frac{g + ik_b}{4(g^2 + k_b^2)} (k_b \sin(k_b(y - y')) + (\text{sign}(\xi))g \cos(k_b(y - y'))),$$

from which one computes the combination $C(\xi t + y, \xi t + y') + C(\xi t + y', \xi t + y)^*$ which is needed for the kernel (see Eq. (81)). For $\xi' = -\xi$ we find similarly

$$C(\xi t + y, -\xi t + y') \simeq \text{sign}\xi \int_{k_L}^{\max(\min(|\xi|, k_R), k_L)} \frac{dk_b}{4\pi} \frac{k_b(k_b - ig)}{g^2 + k_b^2} e^{-i\text{sign}(\xi)k_b(y+y')} \quad (126)$$

$$+ \int_{k_L}^{k_R} \frac{dk_b}{4\pi} \frac{ik_b + g}{g^2 + k_b^2} (k_b \sin(k_b(y + y')) + g(\text{sign}\xi) \cos(k_b(y + y')))$$

from which one computes the combination $C(\xi t + y, -\xi t + y') + C(-\xi t + y', \xi t + y)^*$ which is needed for the kernel (see Eq. (81)).

The term $B(x, x', t)$. Let us start with $B_R^{\text{diag}}(x, x', t)$. From (92) one has

$$B_R^{\text{diag}}(\xi t + y, \xi t + y') = \int_0^{k_R} \frac{dk_a}{2\pi} \frac{\tilde{F}_{\xi t + y, \xi t + y'}(k_a)}{g^2 + k_a^2} \quad (127)$$

where

$$\tilde{F}_{x, x', t}(k_a) = (k_a \cos(k_a x) + g \sin(k_a |x|))(k_a \cos(k_a x') + g \sin(k_a |x'|)) \quad (128)$$

Using trigonometric identities, one finds that it vanishes at large time except for $\xi' = \pm\xi$. One finds for $\xi' = \xi$

$$B_R^{\text{diag}}(\xi t + y, \xi t + y') = \int_0^{k_R} \frac{dk_a}{4\pi} \cos k_a (y - y') \quad (129)$$

and for $\xi' = -\xi$

$$B_R^{\text{diag}}(\xi t + y, -\xi t + y') = \int_0^{k_R} \frac{dk_a}{4\pi} \cos k_a (y + y'). \quad (130)$$

Finally note that the term $B_{L/R}^{\text{off-diag}}(x, x', t)$, which was shown to vanish in the NESS regime (see previous Section 6), is expected to also vanish in the present ray regime (although we will not study here its decay in detail).

Final result. Adding all the terms computed above we obtain the final result for the kernel $K_\xi^\pm(y, y') = \lim_{t \rightarrow +\infty} K(\xi t + y, \pm \xi t + y')$. For K_ξ^+ we obtain, recalling the identity $\frac{\rho_R}{4} \frac{\sin(k_R x)}{k_R x} = \int_0^{k_R} \frac{dk}{4\pi} \cos(kx)$,

$$K_\xi^+(y, y') = \frac{\rho_L}{2} \frac{\sin(k_L(y - y'))}{k_L(y - y')} + \frac{\rho_R}{2} \frac{\sin(k_R(y - y'))}{k_R(y - y')} \quad (131)$$

$$+ \text{sign}(\xi) \int_{k_L}^{\max(\min(|\xi|, k_R), k_L)} \frac{dk_b}{2\pi} \frac{k_b^2}{g^2 + k_b^2} e^{-i\text{sign}(\xi)k_b(y-y')}$$

$$+ \int_{k_L}^{k_R} \frac{dk_b}{2\pi} \frac{ik_b^2 \sin(k_b(y - y')) + (\text{sign}\xi)g^2 \cos(k_b(y - y'))}{g^2 + k_b^2}.$$

This can be reorganized, leading to the result given in the text in (47). From this formula we obtain the density $\tilde{\rho}(\xi) = K_{\xi}^{+}(y, y)$, which is independent of y , and given in the text in (41). Similarly one obtains the current $\tilde{J}(\xi) = \text{Im}K_{\xi,01}^{+}(y, y)$ leading to the expression (44).

For K_{ξ}^{-} , i.e. $\xi' = -\xi$, we obtain

$$K_{\xi}^{-}(y, y') = -i \text{sign}(\xi) \int_{k_L}^{\max(\min(|\xi|, k_R), k_L)} \frac{dk_b}{2\pi} \frac{k_b g}{g^2 + k_b^2} e^{-i \text{sign}(\xi) k_b (y + y')} + \int_{k_L}^{k_R} \frac{dk_b}{2\pi} \frac{g k_b}{g^2 + k_b^2} (\sin(k_b (y + y')) + i(\text{sign}\xi) \cos(k_b (y + y'))) \quad (132)$$

These two terms can be combined and one obtains the result (48).

8 Wigner function and semi-classical approach

It turns out that the results for the density and current obtained here by an exact computation in the regime of large time and $\xi = x/t$ fixed, agree with the prediction of a semi-classical approach. A similar agreement was observed for the discrete model studied in [51]. Here in addition we show that the agreement extends to the full kernel $K(x, x', t)$ at large time with $x = \xi t + y$, $x' = \xi' t + y'$ obtained here in Section 7 with $\xi' = \xi$ and $y, y' = O(1)$ from an exact computation. However, as we discuss below, this semi-classical approach does not allow to predict the non trivial correlations obtained here for $\xi' = -\xi$. Let us present here this approach.

The many-body Wigner function $W(x, k, t)$ was defined and studied in e.g. [67] in the case of noninteracting fermions (see also [25]). It was shown to be related to the kernel via (we recall that we set here $\hbar = 1$)

$$W(x, k, t) = \int_{-\infty}^{\infty} \frac{dy}{2\pi} e^{iky} K(x + \frac{y}{2}, x - \frac{y}{2}, t), \quad (133)$$

and we recall that the time-dependent mean fermion density is simply

$$\rho(x, t) = \int_{-\infty}^{\infty} dk W(x, k, t). \quad (134)$$

The Wigner function for fermions in an external potential obeys an exact time evolution equation, see e.g. [24]. For smooth potentials one can define a semi-classical limit ($\hbar \rightarrow 0$, large N and fixed $N\hbar$ see e.g. [25]) and this equation simplifies into the Liouville equation $\partial_t W = -k\partial_x W + V'(x)\partial_k W$. For a delta function potential this limit cannot be defined in that way, but one can define instead a semi-classical form for the Wigner function by introducing transmission and reflection coefficients, as was done in [51]. Let us now recall this approach.

Consider first the easier case with no defect. The fermions evolve freely with speed $v(k)$, and in the present model $v(k) = k$. The Liouville equation applies to this free evolution with $V'(x) = 0$ and the Wigner function is simply transported along the classical trajectories. It is thus obtained from the trajectories run backward in time as

$$W(x, k, t) = W_0(x - v(k)t, k) \quad (135)$$

where $W_0(x, k)$ is the Wigner function at time $t = 0$. As described in Section 2.2, here we consider an initial condition which is the product of two independent fermionic ground states, separated by an infinite hard wall at $x = 0$. On each side of the wall one considers the ground

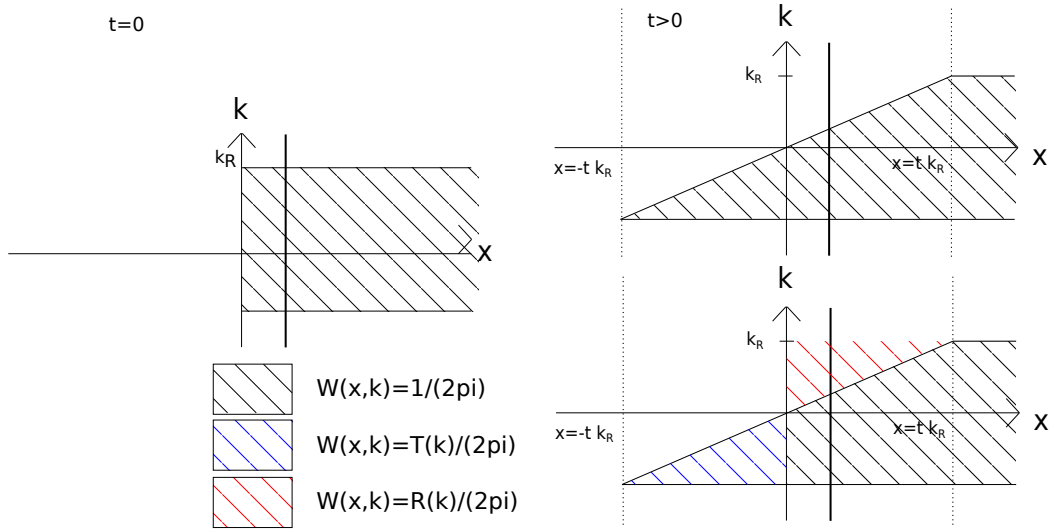


Figure 10: Semi-classical evolution of the Wigner function. On the left panel we have indicated the initial condition for which the Wigner function is equal to $\frac{1}{2\pi}$ in the black hatched area and 0 otherwise. For simplicity we choose $k_L = 0$ and $k_R > 0$. On the right top panel the Wigner function is propagated at time t without reflection at $x = 0$ (this corresponds to $g = 0$ or $T(k) = 1$). On the bottom right panel we show the evolution with $g \neq 0$: the blue hatched area corresponds to transmitted part, while the red hatched area corresponds to the reflected part. Therefore the Wigner function is affected by the corresponding factors $R(k)$ and $T(k)$ (see Eqs. (138) and (139)). Note that to compute the density at a given point x one has to integrate the Wigner function over the vertical line passing through x , as indicated in the figure.

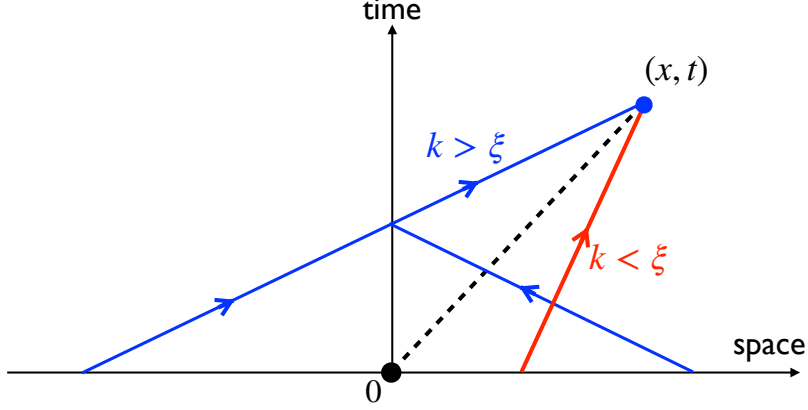


Figure 11: Illustration of some trajectories in the semi-classical method. The defect is at position $x = 0$ (black dot). Consider a fermion which at time t is at position $x = \xi t$ (blue dot) with momentum k . There are several possibilities for its initial position: (i) $k < \xi$ and it was to the right of the defect at time zero, (ii) $k > \xi$ and either it was to the left of the defect and has been transmitted (with probability $T(k)$) or it was to the right of the defect and has been reflected (with probability $R(k) = 1 - T(k)$). The dashed line corresponds to $k = \xi$. Here we assume $T(k) = T(-k)$.

state at Fermi energy $\mu_L = \frac{k_L^2}{2}$ for $x < 0$, respectively $\mu_R = \frac{k_R^2}{2}$ for $x > 0$, of noninteracting fermions in the absence of an external potential, with vanishing wave function at $x = 0$. The corresponding kernel is given in Eqs. (4)-(6). As a consequence

$$W_0(x, k) = W_0^R(x, k)\Theta(x > 0) + W_0^L(x, k)\Theta(x < 0) \quad (136)$$

where the functions $W_0^{L/R}(x, k)$ are obtained from $K_{L/R}(x, x')$ in (5),(6) by the same transformation as in (133). The exact calculation of these functions is performed in Appendix C.1 of [68]. Away from a small layer of width $x = O(1/k_{L/R})$ near the wall, it takes the form predicted by the local density approximation (LDA)

$$W_0(x, k) \simeq \frac{1}{2\pi}\Theta(k_R - |k|)\Theta(x > 0) + \frac{1}{2\pi}\Theta(k_L - |k|)\Theta(x < 0) \quad (137)$$

which is discontinuous at $x = 0$, as represented in Fig. 10 (left panel). We will use this form (137) from now on.

Now we add the defect at $x = 0$. Consider a fermion at position (x, t) with $x > 0$ and with momentum k . If the condition $\xi = \frac{x}{t} > v(k)$ holds, then the fermion has traveled to position x without crossing the defect, as shown by the red solid line in Fig. 11. On the other hand, if the condition $\xi < v(k)$ holds, there are two possibilities (indicated by the blue solid lines in Fig. 11): (i) either the fermion was at $t = 0$ on the half-line $x < 0$ to the left of the defect, and it has been transmitted, or (ii) it was at $t = 0$ on the half-line $x > 0$ to the right of the defect, and it has been reflected, see Fig. 11. The picture is similar for $x < 0$. Setting $v(k) = k$ this leads to the prediction, for $x > 0$

$$W(x, k, t) = \frac{1}{2\pi}((T(k)\Theta(k_L - |k|) + R(k)\Theta(k_R - |k|))\Theta(k > \frac{x}{t}) + \Theta(k_R - |k|)\Theta(k < \frac{x}{t})) \quad (138)$$

and for $x < 0$

$$W(x, k, t) = \frac{1}{2\pi}((T(k)\Theta(k_R - |k|) + R(k)\Theta(k_L - |k|))\Theta(k < \frac{x}{t}) + \Theta(k_L - |k|)\Theta(k > \frac{x}{t})) \quad (139)$$

where $T(k)$ and $R(k) = 1 - T(k)$ are the transmission and reflection coefficients of the defect. We have assumed here for simplicity that $T(k) = T(-k)$. Although this applies to any defect which is symmetric under $x \rightarrow -x$, for the present delta function potential one has

$$R(k) = \frac{g^2}{g^2 + k^2} \quad , \quad T(k) = \frac{k^2}{g^2 + k^2} . \quad (140)$$

Note that the Wigner function is invariant under the symmetry $x \rightarrow -x$ and $k_L \rightarrow k_R$.

It is useful to rewrite the Wigner function using $R(k) = 1 - T(k)$ in the following form, with $\xi = x/t$, for $\xi > 0$

$$W(x, k, t) = \frac{1}{2\pi} \Theta(k_R - |k|) - \frac{T(k)}{2\pi} \Theta(k_L \leq k \leq k_R) \Theta(k > \xi) , \quad (141)$$

and for $\xi < 0$

$$W(x, k, t) = \frac{1}{2\pi} \Theta(k_L - |k|) + \frac{T(k)}{2\pi} \Theta(-k_R \leq k \leq -k_L) \Theta(k < \xi) . \quad (142)$$

The density is then obtained from (134). Using (141) and (142) we obtain, with $\xi = \frac{x}{t}$ fixed

$$\rho(x > 0, t) = \rho_R - \int_{k_L}^{k_R} \frac{dk}{2\pi} T(k) \Theta(k - \xi) \quad (143)$$

$$\rho(x < 0, t) = \rho_L + \int_{k_L}^{k_R} \frac{dk}{2\pi} T(k) \Theta(k - |\xi|) , \quad (144)$$

where in the second equation we have changed $k \rightarrow -k$ and used $T(k) = T(-k)$. One can check upon rearranging and using $R(k) = 1 - T(k)$ that this prediction coincides with the result of the exact calculation obtained in (41).

Let us now extend this prediction to the full kernel using the semi-classical Wigner function. By inverse Fourier transform of (133) one has

$$K(x, x', t) = \int dk e^{-ik(x-x')} W\left(\frac{x+x'}{2}, k, t\right) . \quad (145)$$

Let us consider the large time limit in the ray regime with $x = \xi t + y$ and $x' = \xi t + y'$, where $y, y' = O(1)$. In that case one can approximate (145) as

$$K(\xi t + y, \xi t + y', t) \simeq \int dk e^{-ik(y-y')} W(\xi t, k, t) . \quad (146)$$

Using again (141), for $t \rightarrow +\infty$ and $\xi > 0$ one obtains

$$K(\xi t + y, \xi t + y', t) \simeq \int_0^{k_R} \frac{dk}{\pi} \cos(k(y-y')) - \int_{k_L}^{k_R} \frac{dk}{2\pi} T(k) e^{-ik(y-y')} \Theta(k - \xi) \quad (147)$$

and using (142) for $\xi < 0$

$$K(\xi t + y, \xi t + y', t) \simeq \int_0^{k_L} \frac{dk}{\pi} \cos(k(y-y')) + \int_{k_L}^{k_R} \frac{dk}{2\pi} T(k) e^{ik(y-y')} \Theta(k - |\xi|) , \quad (148)$$

where we have used $k \rightarrow -k$ and the symmetry $T(k) = T(-k)$. Remarkably, this semi-classical prediction coincides with the exact limiting kernel in (47) obtained by explicit calculation for the delta function potential model in the ray regime for any $\xi \neq 0$, including $\xi = 0^+$ and $\xi = 0^-$. It is natural to expect that this semi-classical method will predict the correct behavior for more general potential, although this remains to be explored. However, as discussed in the previous section, the semi-classical approach, in the present form, does not predict the kernel in the NESS regime (except in the limit $x, x' \rightarrow +\infty$ with $x - x' = O(1)$) nor the kernel $K_\xi^-(y, y')$ which is obtained for $\xi' = -\xi$.

9 Conclusion

In summary, we have studied a quantum quench of noninteracting fermions in one dimension in the presence of a delta impurity at the origin whose strength is changed at $t = 0$ from $g = +\infty$ to a finite value g . The initial state consists in two Fermi gases separately at equilibrium on the two half-axis, with different bulk densities and temperatures $T_{L/R}$. We have obtained exact results in the thermodynamic limit (i.e., for an infinite size system) for the correlation kernel, density and current (particle and energy) for any time t after the quench. This allowed us to study analytically the large time limit of these quantities and their relaxation properties. We found that there are two distinct regimes:

(i) For fixed position x and large time, the system relaxes to a non equilibrium steady state (NESS) characterized by a uniform particle transport current J_∞ and energy current J_∞^Q . We have obtained explicit expressions for the kernel, density and J_∞, J_∞^Q in this regime as a function of g . In particular, we showed that the density in the NESS exhibits a non-trivial spatial dependence near the defect, with a jump in the first derivative at $x = 0$, oscillations which extend far from the defect (which are non equilibrium analogs of Friedel oscillations) and different plateau values at $x = \pm\infty$. We obtain the temperature dependence of the currents J_∞ and J_∞^Q . In particular, in the low temperature limit, we find $J_\infty^Q \sim T_L^2 - T_R^2$, with a prefactor that matches with the conformal field theory universal prediction in the small g limit.

(ii) The ray regime $x \sim \xi t$, at fixed ξ , where the density and current reach asymptotic finite values which depend only on ξ . At zero temperature, their dependence on ξ shows slope discontinuities along the two pairs of light cones at $\xi = \pm k_{L/R}$. We also obtain the spatial dependence of the asymptotic kernel, denoted K_ξ^+ , in the vicinity of the ray ξ . We also obtain K_ξ^- , which describes the correlations between two points with two opposite rays ξ and $-\xi$.

It is important to note that these two regimes match smoothly, as we have shown, which indicates the absence of possible intermediate regime. This means that in the ray regime, as $\xi \rightarrow 0^\pm$ one recovers the asymptotic densities $\rho_\infty(\pm\infty)$ of the NESS, as well as the current J_∞ . Finally, in the case (i) we have studied in detail the convergence in time t towards the NESS. We have found that at zero temperature the kernel and the density decay as $t^{-5/2}$ modulated by oscillations, superposed to a t^{-3} non-oscillating part, towards their values in the NESS.

The present study is the analog for the non-equilibrium dynamics of our recent work in [14] where we studied the ground state of noninteracting fermions in the presence of a delta impurity. The form obtained here for the kernel and density in the NESS can be compared with the one obtained at equilibrium in [14]. Although they have some common features (such as the cusp in the density and Friedel-like oscillations) their overall form is different. In the limit $k_R = k_L$ (at zero temperature) they become identical, however only in the case $g > 0$. This can be qualitatively understood since for $g > 0$ the excitations which are present in the initial state can propagate to infinity, while for $g < 0$ there is a bound state which cannot carry propagating excitations.

Our work has close relations to the work of Ljubotina, Sotiriadis and Prosen [51], which has inspired the analytical methods used here. However, in addition to being defined on a lattice, the initial state considered there is completely uncorrelated, while in our case there are the correlations of a Fermi gas with two Fermi momenta k_R and k_L . This leads to a different structure in the ray regime with two distinct pairs of light cones. As pointed out in Ref. [51], the results for the density and the current in the ray regime can be obtained from a semi-classical method. However the density in the NESS (at finite x) cannot be obtained from this method. We have shown that the same properties hold in the present continuum model. In addition we have computed the kernels K_ξ^\pm : while K_ξ^+ can indeed be predicted by the semi-classical method, the kernel K_ξ^- which measures correlations in opposite rays cannot be predicted by

this approach, and requires exact methods.

The present study unveils a number of correlation kernels, which have a non trivial form at the Fermi scale $k_{L/R}$, different from the universal sine kernel (which is recovered here only outside the light cones). At variance with standard kernels of RMT, which also describe trapped fermions at equilibrium, the present ones found here carry currents, hence they are not purely real. It would be interesting to find analog in the context of RMT.

Finally, we obtained here the kernel in the NESS, but it would be interesting to obtain also the full density matrix and compute other observables such as the entanglement entropy. This is left for future studies.

Acknowledgements We thank D. S. Dean for suggesting this calculation and helpful comments. We thank D. Bernard, A. Krajenbrink, S. N. Majumdar and L. Zadnik for useful discussions. We acknowledge support from ANR grant ANR-17-CE30-0027-01 RaMaTraF.

Appendix A: Large ℓ limit, term B

In this appendix we give some more details on the evaluation of the large ℓ limit of the term $B(x, x', t) = B_R(x, x', t) + B_L(x, x', t)$ defined in the text in (80). As discussed in the text [see Eq. (89)] each $B_{L/R}$ is split into two parts, an off-diagonal one with $k_a \neq k_b$ and a diagonal one with $k_a = k_b$. Below, we discuss them separately.

A.1 The off-diagonal part

Let us focus on the off-diagonal term $B_R^{\text{off-diag}}$ from (80) (the term $B_L^{\text{off-diag}}$ is obtained similarly by changing $k_R \rightarrow k_L$)

$$B_R^{\text{off-diag}}(x, x', t) = \left(\frac{2}{\ell}\right)^3 \sum_{k \in \Lambda_-, k \leq k_R} \sum_{\substack{k_a \in \Lambda_+, k_b \in \Lambda_+ \\ k_a \neq k_b}} 2 \frac{k_a \cos(k_a x) + g \sin(k_a |x|)}{g^2 + k_a^2} \\ \times \frac{k_b \cos(k_b x') + g \sin(k_b |x'|)}{g^2 + k_b^2} \frac{k^2 k_a k_b}{(k_a^2 - k^2)(k_b^2 - k^2)} e^{i(E(k_a) - E(k_b))t}, \quad (\text{A1})$$

where the discrete sum has been restricted to $k_a \neq k_b$ (and the term $2g/\ell$ which is subdominant at large ℓ has been removed). As in the text we denote

$$F_{xx'}(k_a, k_b) = 2 \frac{k_a \cos(k_a x) + g \sin(k_a |x|)}{g^2 + k_a^2} \frac{k_b \cos(k_b x') + g \sin(k_b |x'|)}{g^2 + k_b^2} k_a k_b. \quad (\text{A2})$$

The large ℓ analysis is very similar to the one presented in the text for the term C in Section 5. Namely we replace the discrete sum over k in (A1) by a contour integral using the same trick as in (87). The contour γ_δ in Fig. 8 is now a rectangle with k_L replaced by 0, which in the large ℓ limit becomes again a half-rectangle, similar to γ_c in Fig. 7 (with k_L set to zero). In addition to this contour integral there are residues which we need to take into account. Since $k_a \neq k_b$ one sees that there are only simple poles at either $k = k_a$ or $k = k_b$ and their residues must be

summed up. Hence we arrive at the following formula in the large ℓ limit

$$\begin{aligned}
B_R^{\text{off-diag}}(x, x', t) &= \int_0^\infty \int_0^\infty \frac{dk_a}{\pi} \frac{dk_b}{\pi} F_{xx'}(k_a, k_b) e^{i(E(k_a) - E(k_b))t} \\
&+ \left(\int_0^{i\epsilon} \frac{dk}{\pi} + \int_{+i\epsilon}^{k_R+i\epsilon} \frac{dk}{\pi} - \int_{k_R}^{k_R+i\epsilon} \frac{dk}{\pi} \right) \frac{k^2}{(k_a^2 - k^2)(k_b^2 - k^2)} \\
&- 2i \left[\Theta(k_R - k_a) \left(-\frac{1}{2} + \frac{i}{2} \frac{g}{k_a} \right) \text{Res}_{k=k_a} + \Theta(k_R - k_b) \left(-\frac{1}{2} + \frac{i}{2} \frac{g}{k_b} \right) \text{Res}_{k=k_b} \right] \frac{k^2}{(k_a^2 - k^2)(k_b^2 - k^2)}
\end{aligned} \tag{A3}$$

Let us now compute each term separately in (A3). The last line (the residue part) is found to be equal to

$$\frac{1}{2(k_a^2 - k_b^2)} (\Theta(k_R - k_a)(ik_a + g) - \Theta(k_R - k_b)(ik_b + g)). \tag{A4}$$

On the other hand the contour integral can be calculated explicitly, namely

$$\begin{aligned}
&\left(\int_0^{i\epsilon} \frac{dk}{\pi} + \int_{+i\epsilon}^{k_R+i\epsilon} \frac{dk}{\pi} - \int_{k_R}^{k_R+i\epsilon} \frac{dk}{\pi} \right) \frac{k^2}{(k_a^2 - k^2)(k_b^2 - k^2)} \\
&= \frac{1}{\pi(k_a^2 - k_b^2)} \left[\frac{k_b}{2} \left(\log\left(\frac{k_b + k}{|k_b - k|}\right) + i\pi\Theta(k - k_b) \right) - \frac{k_a}{2} \left(\log\left(\frac{k_a + k}{|k_a - k|}\right) + i\pi\Theta(k - k_a) \right) \right]_0^{k_R},
\end{aligned} \tag{A5}$$

which holds for any $\epsilon > 0$. When adding to (A4) we see that the imaginary part cancels and we are left with the result given in the text in (90).

A.2 The diagonal part

We now turn to the diagonal part, i.e., the term with $k_a = k_b$ in (80), focusing on B_R^{diag} (the term B_L^{diag} is obtained similarly by changing $k_R \rightarrow k_L$). It reads

$$B_R^{\text{diag}}(x, x') = \left(\frac{2}{\ell}\right)^3 \sum_{k \in \Lambda_-, k \leq k_R} \sum_{k_a \in \Lambda_+} F_{xx'}(k_a, k_a) \frac{k^2}{(k_a^2 - k^2)^2}, \tag{A6}$$

where $F_{xx'}(k_a, k_b)$ is given in (A2). To take the large ℓ limit, we again use the contour integral trick used above. We convert the discrete sum over k into a contour integral, denoted by $B_R^{\text{diag},1}(x, x')$, plus a residue term, denoted by $B_R^{\text{diag},2}(x, x')$. However, instead of having two simple poles as in the off-diagonal terms, we now have a double pole at $k = k_a$, which changes the result for the residue.

Let us first consider the contour integral term. It has the form, in the large ℓ limit

$$B_R^{\text{diag},1}(x, x') \simeq \left(\frac{2}{\ell}\right)^3 \ell^2 \int_0^{+\infty} \frac{dk_a}{2\pi} F_{xx'}(k_a, k_a) I(k_a, k_R) \tag{A7}$$

where the expression of the integral $I(k_a, k_R)$ is obtained from (A5) by setting $k_b = k_a$. We get

$$\begin{aligned}
I(k_a, k_R) &= \left(\int_0^{i\epsilon} \frac{dk}{\pi} + \int_{+i\epsilon}^{k_R+i\epsilon} \frac{dk}{\pi} - \int_{k_R}^{k_R+i\epsilon} \frac{dk}{\pi} \right) \frac{k^2}{(k_a^2 - k^2)^2} \\
&= \frac{k_R}{2\pi(k_a^2 - k_R^2)} - \frac{1}{4\pi k_a} \log \frac{k_a + k_R}{|k_a - k_R|} - \frac{i}{4k_a} \Theta(k_R - k_a).
\end{aligned} \tag{A8}$$

The remaining integral over k_a is well defined (in the principal value sense around k_R). Hence this term clearly vanishes in the large ℓ limit since it is of order $O(1/\ell)$. This is because the initial *triple* sum in $B_R^{\text{diag},1}(x, x')$ has become a *double* integral, and hence an extra factor $1/\ell$.

Let us now consider the residue term. It can be read off from (A6) as

$$B_R^{\text{diag},2}(x, x') = \left(\frac{2}{\ell}\right)^2 \int_0^{+\infty} \frac{dk_a}{\pi} F_{xx'}(k_a, k_a) \int_{\Gamma_1} \frac{dk}{2\pi} \frac{\ell}{e^{ik\ell} - 1} \frac{v(k, k_a)}{(k - k_a)^2}, \quad v(k, k_a) = \frac{k^2}{(k + k_a)^2}, \quad (\text{A9})$$

where Γ_1 is a contour in the complex k -plane consisting of the union of small circles oriented clockwise centered around $k = k_a$ with $0 < k_a \leq k_R$. We now use the residue formula for a double pole with a counterclockwise contour around $z = 0$, namely

$$\oint \frac{dz}{2i\pi z^2} h(z) = h'(0), \quad (\text{A10})$$

which, applied to the integral over k in Eq. (A9), leads to

$$\begin{aligned} \int_{\Gamma_1} \frac{dk}{2\pi} \frac{\ell}{e^{ik\ell} - 1} \frac{v(k, k_a)}{(k - k_a)^2} &= -i \frac{d}{dk} \left(v(k, k_a) \frac{\ell}{e^{ik\ell} - 1} \right) \Big|_{k=k_a} \\ &= \frac{k_a^2 + g^2}{16k_a^2} \ell^2 + \frac{g + ik_a}{8k_a^2} \ell, \end{aligned} \quad (\text{A11})$$

where, in the last line, we have computed the derivative with respect to k , set $k = k_a$ and used the quantification condition (70) $e^{ik\ell} = -\frac{k_a + ig}{k_a - ig}$. In the large ℓ limit, the first term $\propto \ell^2$ in (A11) dominates and plugging it into (A9), we finally obtain the residue part as

$$B_R^{\text{diag},2}(x, x') \approx \int_0^{k_R} \frac{dk_a}{\pi} F_{xx'}(k_a, k_a) \frac{k_a^2 + g^2}{4k_a^2}. \quad (\text{A12})$$

Since we found that $B_R^{\text{diag},1}(x, x')$ vanishes, we finally obtain the result for the limit $\ell \rightarrow +\infty$ given in the text for $B_R^{\text{diag}}(x, x')$ in (92).

Appendix B: Convergence to the NESS at large time ($x, x' = O(1)$)

In this appendix we extract the leading decay in time of the kernel to its stationary value in the NESS. We start from the result for the kernel at infinite ℓ given as a sum of terms in (81), where the $B_{L/R}$ terms are themselves decomposed in (89). In this sum only the terms $C(x, x', t)$ and $B_{L/R}^{\text{off-diag}}(x, x', t)$ depend on time. Below we study them separately.

B.1 Time decay of the term C

Let us define $\Delta C(x, x', t) = C(x, x', t) - C_\infty(x, x')$. We start from the expression (85) for $C(x, x', t)$. Only the contour integral in the first line depends on time. As discussed above it is independent of $\epsilon > 0$ so we can choose here $\epsilon = +\infty$, in which case the contribution of the second integral in the first line of (85) vanishes (since it contains a factor $e^{-\epsilon pt}$ where $k = i\epsilon + p$ with $p \in [k_L, k_R]$ on this contour). Hence we obtain

$$\Delta C(x, x', t) = \int_0^{+\infty} \frac{dk_b}{\pi} \left[\left(\int_{k_L}^{k_L+i\infty} \frac{dk}{\pi} - \int_{k_R}^{k_R+i\infty} \frac{dk}{\pi} \right) \frac{h_{x,x',t}(k, k_b)}{k - k_b} \right] \quad (\text{B1})$$

where $h_{x,x',t}(k, k_b)$ is defined in (84). We now notice that it is convenient to take the time

derivative of this expression so that the two integrals decouple, leading to

$$\partial_t \Delta C(x, x', t) = \frac{i}{2} G_b(t) (G_L(t) - G_R(t)) \quad (\text{B2})$$

$$G_b(t) = \int_0^{+\infty} \frac{dk_b}{\pi} k_b \frac{k_b \cos(k_b x') + g \sin(k_b |x'|)}{g^2 + k_b^2} e^{-\frac{i}{2} k_b^2 t} \quad (\text{B3})$$

$$G_{L/R}(t) = i \int_0^{+\infty} \frac{dp}{\pi} (k_{L/R} + ip) \sin((k_{L/R} + ip)x) e^{\frac{i}{2} (k_{L/R} + ip)^2 t} \quad (\text{B4})$$

At large t , the integral in $G_b(t)$ is dominated by the vicinity of $k_b = 0$, while the integral in $G_L(t)$ is dominated by the vicinity of $p = 0$. One finds, assuming $g > 0$ and x fixed

$$G_b(t) \simeq \frac{1}{g^2 \sqrt{2\pi}} (1 + g|x'|) \frac{1}{(it)^{3/2}} \quad , \quad G_{L/R}(t) = \frac{i}{\pi t} \sin(k_{L/R} x) e^{\frac{i}{2} k_{L/R}^2 t} \quad (\text{B5})$$

Putting all together and integrating (up to subdominant terms) we obtain the estimate

$$\Delta C(x, x', t) \simeq \frac{e^{-i\frac{\pi}{4}}}{(\pi)^{3/2} g^2 \sqrt{2}} (1 + g|x'|) \frac{1}{t^{5/2}} \left(\frac{1}{k_L^2} e^{\frac{i}{2} k_L^2 t} \sin(k_L x) - \frac{1}{k_R^2} e^{\frac{i}{2} k_R^2 t} \sin(k_R x) \right) \quad (\text{B6})$$

which we have also checked numerically.

Remark. One can also start from the *discrete* double sum expression (83) at finite ℓ for $C(x, x', t)$ and take a time derivative, which leads to a product of two decoupled discrete sums

$$\partial_t C(x, x', t) = \frac{i}{2} H_b(t) H(t) \quad (\text{B7})$$

$$H_b(t) = \frac{2}{\ell} \sum_{k_b \in \Lambda_+} k_b \frac{k_b \cos(k_b x) + g \sin(k_b |x|)}{g^2 + k_b^2} e^{-\frac{i}{2} k_b^2 t} \quad (\text{B8})$$

$$H(t) = \frac{2}{\ell} \sum_{k \in \Lambda_-, k = k_L^+}^{k_R} k \sin(kx) e^{\frac{i}{2} k^2 t} \quad (\text{B9})$$

For each term the large ℓ limit is straightforward, hence here there is no need for the contour integral trick. The formula for $H_b(t)$ gives immediately the formula for $G_b(t)$ in Eq. (B3) in the large ℓ limit. The formula for $H(t)$ becomes, in the large ℓ limit

$$H(t) = \int_{k_L}^{k_R} \frac{dk}{\pi} k \sin(kx) e^{\frac{i}{2} k^2 t} \quad (\text{B10})$$

which can be shown to be equal to $G_L(t) - G_R(t)$ upon changing the contour of integration. Note that using the integration by part method described in (112) one shows that for any smooth function with bounded $h''(k)$

$$\int_0^{k_R} dk k h(k) e^{\frac{i}{2} k^2 t} = \frac{i}{t} (h(0) - h(k_R) e^{\frac{i}{2} k_R^2 t}) + o\left(\frac{1}{t}\right) \quad (\text{B11})$$

from which we can obtain the asymptotics of $H(t)$ from (B10), recovering the result in (B5).

B.2 Time decay of the term B

We start from the expression for $B_R^{\text{off-diag}}(x, x', t)$ in (90) together with the definition of $F_{x, x'}(k_a, k_b)$ in (91). The same analysis can be made for $B_L^{\text{off-diag}}(x, x', t)$. As we show below, the large time limit is dominated by two contributions: one where k_a, k_b in the double integral in (90) are both close to zero, and one where one of these momenta is close to k_R . Before presenting the detailed computation, let us show how the first contribution can be obtained by a simple argument. Upon rescaling $k_a \rightarrow k_a/\sqrt{t}$ and $k_b \rightarrow k_b/\sqrt{t}$, this gives straightforwardly by estimating the behavior of the integrand near $k_a = k_b = 0$,

$$\begin{aligned} B_R^{\text{off-diag}}(x, x', t) &\simeq -\frac{2}{t^3 g^4 \pi k_R} (1 + g|x|)(1 + g|x'|) \int_0^\infty \int_0^\infty \frac{dk_a}{\pi} \frac{dk_b}{\pi} k_a^2 k_b^2 e^{\frac{i}{2}(k_a^2 - k_b^2)} \\ &= -\frac{1}{\pi^2 g^4 k_R} (1 + g|x|)(1 + g|x'|) \frac{1}{t^3}. \end{aligned} \quad (\text{B12})$$

In this calculation the terms in (90) containing the Θ functions do not contribute since they vanish when both $k_a, k_b < k_R$. However the full calculation, to which we now turn, shows that this part does produce an additional contribution.

Let us now again consider the time derivative of $B_R^{\text{off-diag}}(x, x')$ which allows to decouple the two integrals over k_a and k_b . It can be written as a sum of two parts. The first part is

$$\partial_t B_R^{\text{off-diag},1}(x, x') = i(\mathbf{G}_x(t)^* \mathbf{H}_{x'}(t) - \mathbf{G}_{x'}(t) \mathbf{H}_x(t)^*), \quad (\text{B13})$$

where we have defined

$$\mathbf{G}_x(t) = \int_0^{+\infty} \frac{dk_a}{\pi} k_a \frac{k_a \cos(k_a x) + g \sin(k_a |x|)}{g^2 + k_a^2} e^{-\frac{i}{2} k_a^2 t} \quad (\text{B14})$$

$$\mathbf{H}_x(t) = \int_0^{+\infty} \frac{dk_a}{\pi} k_a \frac{k_a \cos(k_a x) + g \sin(k_a |x|)}{g^2 + k_a^2} \frac{1}{2\pi} k_a \log\left(\frac{k_a + k_R}{|k_a - k_R|}\right) e^{-\frac{i}{2} k_a^2 t}. \quad (\text{B15})$$

It is easy to analyze the large time behavior of these functions, and one obtains

$$\mathbf{G}_x(t) \simeq \frac{1}{g^2 \sqrt{2\pi}} (1 + g|x|) \frac{1}{(it)^{3/2}}, \quad \mathbf{H}_x(t) \simeq \frac{3}{\pi k_R \sqrt{2\pi} g^2} (1 + g|x|) \frac{1}{(it)^{5/2}}. \quad (\text{B16})$$

This leads to

$$\partial_t B_R^{\text{off-diag},1}(x, x') = \frac{3}{g^4 k_R \pi^2} (1 + g|x|)(1 + g|x'|) \frac{1}{t^4}, \quad (\text{B17})$$

which agrees with the previous result (B12). The second part reads

$$\partial_t B_R^{\text{off-diag},2}(x, x') = i \frac{g}{2} (\mathbf{G}_x(t)^* \mathbf{G}_{x'}^>(t) - (\mathbf{G}_x^>(t))^* \mathbf{G}_{x'}(t)) \quad (\text{B18})$$

where we have defined

$$\mathbf{G}_x^>(t) = \int_{k_R}^{+\infty} \frac{dk_a}{\pi} k_a \frac{k_a \cos(k_a x) + g \sin(k_a |x|)}{g^2 + k_a^2} e^{-\frac{i}{2} k_a^2 t}. \quad (\text{B19})$$

Using linear combinations of (B11) (and the fact that $h(k) \rightarrow 0$ as $k \rightarrow +\infty$, we obtain at large time

$$\mathbf{G}_x^>(t) \simeq \frac{k_R \cos(k_R x) + g \sin(k_R |x|)}{g^2 + k_R^2} \frac{e^{-\frac{i}{2} k_R^2 t}}{i\pi t}. \quad (\text{B20})$$

This leads to

$$\begin{aligned} \partial_t B_R^{\text{off-diag},2}(x, x') &\simeq \frac{1}{g(2\pi)^{3/2}t^{5/2}} \left((1 + g|x'|) \frac{k_R \cos(k_R x) + g \sin(k_R |x|)}{g^2 + k_R^2} \frac{1}{i^{3/2}} e^{\frac{i}{2}k_R^2 t} \right. \\ &\left. + (1 + g|x|) \frac{k_R \cos(k_R x') + g \sin(k_R |x'|)}{g^2 + k_R^2} \frac{1}{(-i)^{3/2}} e^{-\frac{i}{2}k_R^2 t} \right). \end{aligned}$$

Integrating with respect to time, and putting together the two terms, we finally obtain the large time behavior

$$\begin{aligned} B_R^{\text{off-diag}}(x, x') &\simeq -\frac{1}{\pi^2 g^4 k_R} (1 + g|x|)(1 + g|x'|) \frac{1}{t^3} \\ &- \frac{2}{g(2\pi)^{3/2} k_R^2 t^{5/2}} \left((1 + g|x'|) \frac{k_R \cos(k_R x) + g \sin(k_R |x|)}{g^2 + k_R^2} e^{-i\frac{\pi}{4}} e^{\frac{i}{2}k_R^2 t} \right. \\ &\left. + (1 + g|x|) \frac{k_R \cos(k_R x') + g \sin(k_R |x'|)}{g^2 + k_R^2} e^{i\frac{\pi}{4}} e^{-\frac{i}{2}k_R^2 t} \right), \end{aligned} \quad (\text{B21})$$

which is the sum of $1/t^3$ term and an oscillating $1/t^{5/2}$ term.

B.3 Summary

One can put together the terms computed above and obtain the convergence of the kernel towards its asymptotic value in the NESS. Denoting $\Delta K(x, x', t) = K(x, x', t) - K_\infty(x, x')$ we obtain

$$\Delta K(x, x', t) = \Delta C(x, x', t) + \Delta C(x', x, t)^* + B_R^{\text{off-diag}}(x, x') + B_L^{\text{off-diag}}(x, x') \quad (\text{B22})$$

where ΔC is given in (B6) and $B_R^{\text{off-diag}}(x, x')$ is given in (B21) (with the same formula for $B_L^{\text{off-diag}}(x, x')$ with k_R replaced by k_L). We display here the large time behavior of the density

$$\begin{aligned} \rho(x, t) - \rho_\infty(x) &= -\frac{1}{\pi^2 g^4} (1 + g|x|)^2 \frac{1}{t^3} \left(\frac{1}{k_L} + \frac{1}{k_R} \right) \\ &- \frac{4(1 + g|x|)}{g(2\pi)^{3/2} t^{5/2}} \left(\frac{k_R \cos(k_R x) + g \sin(k_R |x|)}{k_R^2 (g^2 + k_R^2)} \cos\left(\frac{k_R^2 t}{2} - \frac{\pi}{4}\right) \right. \\ &\left. + \frac{k_L \cos(k_L x) + g \sin(k_L |x|)}{k_L^2 (g^2 + k_L^2)} \cos\left(\frac{k_L^2 t}{2} - \frac{\pi}{4}\right) \right) \\ &+ \frac{4(1 + g|x|)}{g^2 (2\pi)^{3/2} t^{5/2}} \left(\frac{\sin(k_L x)}{k_L^2} \cos\left(\frac{k_L^2 t}{2} - \frac{\pi}{4}\right) - \frac{\sin(k_R x)}{k_R^2} \cos\left(\frac{k_R^2 t}{2} - \frac{\pi}{4}\right) \right). \end{aligned} \quad (\text{B23})$$

We note that these formulae are valid for large time at fixed x and for $g > 0$. We expect that this expansion breaks down when x becomes large simultaneously with t . Note also that this formula does not apply to the case $g = 0$. Indeed, consider e.g. the $1/t^3$ in Eq. (B12): this decay was obtained by rescaling $k_a \rightarrow k_a/\sqrt{t}$ and $k_b \rightarrow k_b/\sqrt{t}$, and approximating the denominator $k_a^2 + g^2$ by g^2 . Obviously, this estimate and the $1/t^3$ decay holds only if $t \gg 1/g^2$.

Finally note that the decay of the time dependent current $J(x, t) - J_\infty$ can be obtained from the kernel (B22) using (15). We find that it decays as $t^{-5/2}$ modulated by oscillating terms. It can also be obtained from the conservation equation (16) and (B23).

Appendix C: Details for $g < 0$

If g is negative there is an additional eigenstate of \hat{H}_g , namely $\phi_g(x) \underset{\ell \rightarrow \infty}{\simeq} \sqrt{-g} e^{g|x|}$ of energy $E = -\frac{g^2}{2}$. The kernel then has an additional term which we call δK .

Before we start our computation we recall the overlap of the eigenstate $\phi_{1,k'}$ and $\phi_{-1,k'}$ with the initial state

$$\begin{aligned} R_{k',k}^+ &:= \int_0^{\ell/2} dy \sqrt{\frac{4}{\ell}} \sin(ky) \phi_{+,k'}(y) = \frac{2^{3/2}}{\ell} \frac{kk'}{(k^2 - k'^2) \sqrt{g^2 + k'^2 + \frac{2g}{\ell}}}, \\ L_{k',k}^+ &:= \int_{-\ell/2}^0 dy \sqrt{\frac{4}{\ell}} \sin(ky) \phi_{+,k'}(y) = -R_{k',k}^+, \\ R_{k',k}^- &:= \int_0^{\ell/2} dy \sqrt{\frac{4}{\ell}} \sin(ky) \phi_{-,k'}(y) = \frac{1}{\sqrt{2}} \delta_{k,k'}, \\ L_{k',k}^- &:= \int_{-\ell/2}^0 dy \sqrt{\frac{4}{\ell}} \sin(ky) \phi_{-,k'}(y) = R_{k',k}^-, \end{aligned} \quad (\text{C1})$$

and we also introduce the new overlaps of ϕ_g with the left and right initial states

$$R_{g,k} := \int_0^{\ell/2} dy \sqrt{\frac{4}{\ell}} \sin(ky) \phi_g(y) \underset{\ell \rightarrow \infty}{\simeq} \sqrt{-g} \sqrt{\frac{4}{\ell}} \frac{k}{g^2 + k^2}, \quad (\text{C2})$$

$$L_{g,k} := \int_{-\ell/2}^0 dy \sqrt{\frac{4}{\ell}} \sin(ky) \phi_g(y) = -R_{g,k}. \quad (\text{C3})$$

Let us first consider $K_R(x, x', t)$ which for $g > 0$ is given by (79) and reads

$$\begin{aligned} K_R(x, x', t) &= \sum_{\sigma_a = \pm, k_a \in \Lambda_{\sigma_a}} \sum_{\sigma_b = \pm, k_b \in \Lambda_{\sigma_b}} \sum_{k \in \Lambda_-, k \leq k_R} \phi_{\sigma_a, k_a}^*(x) \phi_{\sigma_b, k_b}(x') e^{i(E(k_a) - E(k_b))t} \\ &\times \left(\delta_{\sigma_a, -} R_{k_a, k}^- + \delta_{\sigma_a, +} R_{k_a, k}^+ \right) \left(\delta_{\sigma_b, -} R_{k_b, k}^- + \delta_{\sigma_b, +} R_{k_b, k}^+ \right). \end{aligned} \quad (\text{C4})$$

For simplicity let us introduce the schematic notation

$$K_R = \sum_{k_a} \sum_{k_b} \dots \quad (\text{C5})$$

Now for $g < 0$, we must add one additional term to the sum over k_a corresponding to the bound state. This means that we substitute $\phi_{\sigma_a, k_a} \rightarrow \phi_g$, $E(k_a) \rightarrow E(g) = -\frac{g^2}{2}$ and the overlap

$$\left(\delta_{\sigma_a, -} R_{k_a, k}^- + \delta_{\sigma_a, +} R_{k_a, k}^+ \right) \rightarrow R_{g, k}. \quad (\text{C6})$$

In our schematic notation (C5) this becomes $\sum_{k_a} \rightarrow (\sum_{k_a} + g)$. The same procedure is applied to the sum over k_b . The product of sums have to be expanded leading to three additional terms

$$K_R^{g < 0} = \left(\sum_{k_a} + g \right) \left(\sum_{k_b} + g \right) = \sum_{k_a} \sum_{k_b} + (g, \sum_{k_b})_R + \left(\sum_{k_a}, g \right)_R + (g, g)_R = K_R + \delta K_R, \quad (\text{C7})$$

with $\delta K_R = (g, \sum_{k_b})_R + (\sum_{k_a}, g)_R + (g, g)_R$ in terms of our schematic notations. Each term is given explicitly below. Similarly, one can obtain δK_L . The full expression of δK is then obtained by summing the right and left contributions, namely $\delta K = \delta K_R + \delta K_L$. Among those

three terms, the only one remaining in the stationary state is (g, g) which is time independent and computed as follows.

$$(g, g)(x, x') = (g, g)_R(x, x') + (g, g)_L(x, x') \quad (\text{C8})$$

$$= \sum_{k_n < k_R} \phi_g^*(x) \phi_g(x') R_{g, k_n}^2 + \sum_{k_n < k_L} \phi_g^*(x) \phi_g(x') L_{g, k_n}^2 \quad (\text{C9})$$

$$= -g e^{g(|x|+|x'|)} \left(\sum_{k_n < k_R} + \sum_{k_n < k_L} \right) R_{g, k_n}^2 \quad (\text{C10})$$

$$= 2g^2 e^{g(|x|+|x'|)} \left(\sum_{k_n < k_R} + \sum_{k_n < k_L} \right) \frac{2}{\ell} \frac{k_n^2}{(g^2 + k_n^2)^2} \quad (\text{C11})$$

$$\underset{\ell \rightarrow \infty}{\simeq} 2g^2 e^{g(|x|+|x'|)} \left(\int_0^{k_R} + \int_0^{k_L} \right) \frac{dk}{\pi} \frac{k^2}{(g^2 + k^2)^2}. \quad (\text{C12})$$

This term corresponds precisely to δK_∞ given in Eq. (33) in the text. Now we show that the other terms do not contribute to the large time limit. For the other term, we have (here implicitly, in all the discrete sums, $k \in \Lambda_-$ and $k_b \in \Lambda_+$)

$$(g, \sum_{k_b})(x, x') = (g, \sum_{k_b})_R(x, x') + (g, \sum_{k_b})_L(x, x') \quad (\text{C13})$$

$$= \sum_{k < k_R, k_b} \phi_g^*(x) \phi_{\sigma_b, k_b}(x') e^{-i \frac{g^2 + k_b^2}{2} t} R_{g, k} (\delta_{\sigma_b, -} R_{k_b, k}^- + \delta_{\sigma_b, +} R_{k_b, k}^+) \quad (\text{C14})$$

$$+ \sum_{k < k_L, k_b} \phi_g^*(x) \phi_{\sigma_b, k_b}(x') e^{-i \frac{g^2 + k_b^2}{2} t} L_{g, k} (\delta_{\sigma_b, -} L_{k_b, k}^- + \delta_{\sigma_b, +} L_{k_b, k}^+)$$

$$= (g, \sum_{k_b})(x, x')_1 + (g, \sum_{k_b})(x, x')_2, \quad (\text{C15})$$

in terms of the quantities

$$(g, \sum_{k_b})(x, x')_1 = \left(\sum_{k < k_R, k_b} + \sum_{k < k_L, k_b} \right) \phi_g^*(x) \phi_{+, k_b}(x') e^{-i \frac{g^2 + k_b^2}{2} t} \frac{R_{g, k}}{\ell} \frac{2^{3/2} k k_b}{(k^2 - k_b^2) \sqrt{g^2 + k_b^2 + \frac{2g}{\ell}}} \quad (\text{C16})$$

$$(g, \sum_{k_b})(x, x')_2 = \frac{1}{\sqrt{2}} \sum_{k_L < k < k_R} \phi_g^*(x) \phi_{-, k}(x') e^{-i \frac{g^2 + k^2}{2} t} R_{g, k}, \quad (\text{C17})$$

where we have used the explicit expressions of the overlaps R_{k_b, k_n}^\pm and L_{k_b, k_n}^\pm in Eq. (C1).

It is easy to take the large ℓ limit of the second piece (C17), which gives

$$(g, \sum_{k_b})(x, x')_2 = -g e^{g|x|} \int_{k_L}^{k_R} \frac{dk}{\pi} \sin(kx') \frac{k}{g^2 + k^2} e^{-i \frac{g^2 + k^2}{2} t}. \quad (\text{C18})$$

At large times, this term decays to zero as $1/t$ modulated by oscillations at k_R and k_L . To take the large ℓ limit of the first piece (C16) requires again to introduce a contour integral because of the pole at $k = k_b$. The contours γ_R and γ_L are defined such that $\int_{\gamma_{R/L}} =$

$\int_0^{i\epsilon} + \int_{i\epsilon}^{i\epsilon+k_{R/L}} + \int_{i\epsilon+k_{R/L}}^{k_{R/L}}$. Let us introduce the notations

$$i_k(x) = \frac{k \cos(kx) + g \sin(k|x|)}{\sqrt{g^2 + k^2}} \quad (\text{C19})$$

$$I(k_b, x') = 2 \left[\int_{\gamma_R} \frac{dk}{\pi} + \int_{\gamma_L} \frac{dk}{\pi} + \left(\frac{g}{k_b} + i \right) (\Theta(k_b < k_R) + \Theta(k_b < k_L)) \text{Res}_{k=k_b} \right] \frac{i_{k_b}(x')}{\sqrt{k_b^2 + g^2}} \frac{k}{g^2 + k^2} \frac{k k_b}{k^2 - k_b^2} \quad (\text{C20})$$

where $I(k_b, x')$ is a continuous function except for $k_b = k_{L/R}$ where it has a logarithmic divergence. Using the usual arguments we obtain

$$(g, \sum_{k_b})(x, x')_1 = -g e^{g|x|} e^{-i \frac{g^2}{2} t} \int_0^\infty \frac{dk_b}{\pi} e^{-i \frac{k_b^2}{2} t} I(k_b, x'), \quad (\text{C21})$$

and one can argue that the large time limit of this term vanishes. Finally the last term can be computed using $(\sum_{k_a}, g)(x, x') = (g, \sum_{k_b})^*(x', x)$ with a similar conclusion.

Appendix D: Details for finite temperature

In this appendix we give some details of the finite temperature calculation. One starts from the initial kernel defined in Section 3.3. The formula (79) for $K_{R/L}(x, x', t)$ becomes

$$K_{R/L}(x, x', t) = \sum_{\sigma_a = \pm, k_a \in \Lambda_{\sigma_a}} \sum_{\sigma_b = \pm, k_b \in \Lambda_{\sigma_b}} \sum_{k \in \Lambda_-} f_{L/R}(k) \phi_{\sigma_a, k_a}^*(x) \phi_{\sigma_b, k_b}(x') e^{i(E(k_a) - E(k_b))t} \\ \times \left(\frac{1}{\sqrt{2}} \delta_{\sigma_a, -} \delta_{k, k_a} \pm \delta_{\sigma_a, +} \frac{2^{3/2}}{\ell} \frac{k k_a}{(k^2 - k_a^2) \sqrt{g^2 + k_a^2 + \frac{2g}{\ell}}} \right) \\ \times \left(\frac{1}{\sqrt{2}} \delta_{\sigma_b, -} \delta_{k, k_b} \pm \delta_{\sigma_b, +} \frac{2^{3/2}}{\ell} \frac{k k_b}{(k^2 - k_b^2) \sqrt{g^2 + k_b^2 + \frac{2g}{\ell}}} \right), \quad (\text{D1})$$

where the only difference with (79) is the introduction of the Fermi factors $f_{L/R}(k)$ and the fact that the sum over k extends over the entire lattice Λ_- . Expanding the terms in parenthesis one finds an expression similar to (80). The obtained expression defines the terms A, B, C, D as in (81).

D.1 Large ℓ limit

The large ℓ limit is easy to perform on the term A and one obtains

$$A_{L/R}(x, x') = \int_0^\infty \frac{dk}{2\pi} f_{L/R}(k) \sin(kx) \sin(kx')$$

which is the finite temperature generalization of (82).

For the term C one needs again to use the contour integral trick. The contour γ_δ in Fig. 8 is now replaced by the semi-infinite rectangular contour $\gamma_{\delta'}$ with horizontal width 2ϵ shown in Fig. D1 (top right panel). A formula analogous to (87) can be written where the integrand

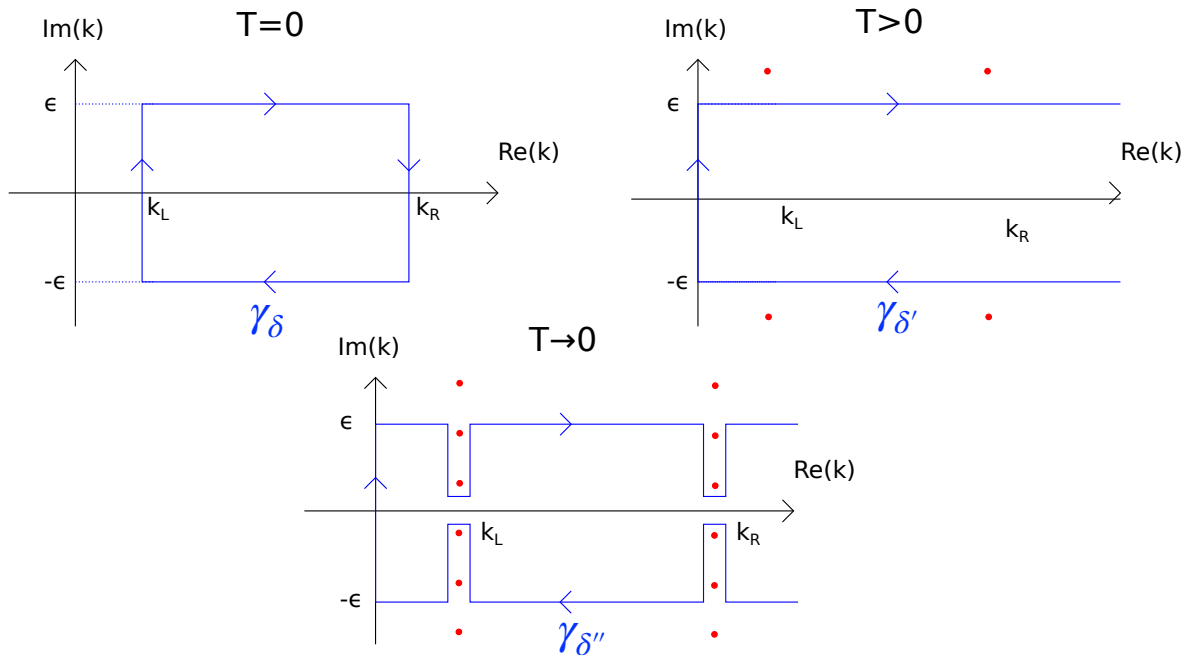


Figure D1: Modification of the contour of integration for nonzero temperature. The top left part shows the zero temperature contour γ_δ , while the top right panel shows the contour $\gamma_{\delta'}$ used at finite temperature. The red dots are the poles of the Fermi functions which, at low temperature, are located approximately along two vertical lines going through k_L and k_R . As explained in the text the residues at these poles can be used to recover the results in the $T \rightarrow 0$ limit, using the contour $\gamma_{\delta''}$ shown on the lower panel.

in the first term now contains the additional factor $f_R(k) - f_L(k)$ while the sum in the second term contains the additional factor $f_R(k_b) - f_L(k_b)$ and k_b is now summed over the whole lattice Λ_+ . This formula is valid however only provided the contour $\gamma_{\delta'}$ does not enclose a pole of the Fermi factors. Recall that the Fermi factor $f_{L/R}(k)$ has poles at $k = \pm k_n$ with

$$k_n^{L/R} = \sqrt{k_{L/R}^2 + 2(2n+1)i\pi T} \quad , \quad n \in \mathbb{Z} . \quad (\text{D2})$$

Hence we need to choose

$$\epsilon < \sqrt{k_{L/R}^2 + 2i\pi T} , \quad (\text{D3})$$

which we will assume from now on. The limit $\ell \rightarrow +\infty$ can now be performed and as before (see Section 5) the contribution of the lower half of γ'_δ (i.e., for $\text{Im}(k) < 0$) vanishes in that limit. This leads to the finite temperature formula for the term C at infinite ℓ

$$\begin{aligned} \lim_{\ell \rightarrow \infty} C(x, x', t) &= \int_0^{+\infty} \frac{dk_b}{\pi} \left[\int_{\eta_\infty} \frac{dk}{\pi} (f_R(k) - f_L(k)) \frac{h_{x,x',t}(k, k_b)}{k - k_b} \right] \\ &+ \int_0^\infty \frac{dk_b}{\pi} (f_R(k_b) - f_L(k_b)) \left(i + \frac{g}{k_b} \right) h_{x,x',t}(k_b, k_b) \end{aligned} \quad (\text{D4})$$

where we denote γ_ϵ the integration contour $\int_{\gamma_\epsilon} = \int_0^{+i\epsilon} + \int_{+i\epsilon}^{\infty+i\epsilon}$, which is the finite temperature analog of (85) and $h_{xx't}$ is defined in (84).

The analysis of the term B proceeds along the same line as in the zero-temperature case (see Section A). The term B is the sum of two parts as in (89). The starting formula for $B_R^{\text{off-diag}}(x, x', t)$ (and similarly for B_L) is (A1) where the sum over k is over the whole lattice Λ_- and the Fermi factor $f_R(k)$ has been inserted. One then uses the contour integral trick with the same modifications of the contour as explained above (see Fig. D1). This leads to the finite temperature analog of the formula (A3) which reads

$$\begin{aligned} B_R^{\text{off-diag}}(x, x', t) &= \int_0^\infty \int_0^\infty \frac{dk_a}{\pi} \frac{dk_b}{\pi} F_{x,x'}(k_a, k_b) e^{i(E(k_a) - E(k_b))t} \\ &+ \left(\int_0^{i\epsilon} \frac{dk}{\pi} + \int_{+i\epsilon}^{+\infty+i\epsilon} \frac{dk}{\pi} \right) f_R(k) \frac{k^2}{(k_a^2 - k^2)(k_b^2 - k^2)} \\ &- 2i \left[\left(-\frac{1}{2} + \frac{i}{2} \frac{g}{k_a} \right) \text{Res}_{k=k_a} + \left(-\frac{1}{2} + \frac{i}{2} \frac{g}{k_b} \right) \text{Res}_{k=k_b} \right] f_R(k) \frac{k^2}{(k_a^2 - k^2)(k_b^2 - k^2)} \end{aligned} \quad (\text{D5})$$

where $F_{x,x'}(k_a, k_b)$ is defined in (91) and $B_L^{\text{off-diag}}(x, x')$ is obtained by changing $f_R \rightarrow f_L$. The starting formula for $B_R^{\text{diag}}(x, x', t)$ is (A6) where the sum over k is over the whole lattice Λ_- and the Fermi factor $f_R(k)$ has been inserted. The same argument shows, as in Appendix A, that the first part $B_R^{\text{diag},1}(x, x', t)$ vanishes at large ℓ . The second part $B_R^{\text{diag},2}(x, x', t)$ is given by formula (A9) where the factor $f_R(k)$ has been inserted in the contour integral which is now over Γ'_1 which is the union of small circles oriented clockwise centered around $k = k_a$ with $0 \leq k_a < +\infty$. When computing the residues of the double pole one must be careful that the Fermi factor has been inserted. Hence Eq. (A11) is replaced by

$$\begin{aligned} \int_{\Gamma'_1} \frac{dk}{2\pi} \frac{\ell}{e^{ik\ell} - 1} \frac{f_R(k)v(k, k_a)}{(k - k_a)^2} &= -i \frac{d}{dk} \left(f_R(k)v(k, k_a) \frac{\ell}{e^{ik\ell} - 1} \right) \Big|_{k=k_a} \\ &= \frac{k_a^2 + g^2}{16k_a^2} f_R(k_a) \ell^2 + O(\ell) \end{aligned} \quad (\text{D6})$$

This finally leads to the large ℓ limit of the B_R^{diag} term as

$$B_R^{\text{diag}}(x, x') = B_R^{\text{diag},2}(x, x') = \int_0^{+\infty} \frac{dk_a}{\pi} f_R(k_a) F_{xx'}(k_a, k_a) \frac{k_a^2 + g^2}{4k_a^2}, \quad (\text{D7})$$

and $B_L^{\text{diag}}(x, x')$ is obtained by changing $f_R \rightarrow f_L$.

To summarize, the infinite ℓ limit of the kernel at finite temperature is equal to the following sum

$$\begin{aligned} K(x, x', t) &= A_L(x, x') + A_R(x, x') + C(x, x', t) + C(x', x, t)^* \\ &+ B_R^{\text{off-diag}}(x, x', t) + B_L^{\text{off-diag}}(x, x', t) + B_R^{\text{diag}}(x, x') + B_L^{\text{diag}}(x, x') \end{aligned} \quad (\text{D8})$$

where $A_{L/R}$ is given in (D2), C is given in (D4), $B_{R/L}^{\text{off-diag}}$ is given in (D5) and $B_{R/L}^{\text{diag}}$ is given in (D7). Note that $A_{L/R}$ and $B_{L/R}^{\text{diag}}$ are time independent.

Remark. In the above formula we have assumed that ϵ satisfies the bound in (D3) such that the contour γ'_δ does not enclose any pole of the Fermi factors. However these poles get closer to the real axis when temperature goes to zero. In other words the bound (D3) becomes $\epsilon < \frac{\pi T}{k_R}$ at low T . So one can ask how is the $T = 0$ recovered. The answer is illustrated in the

Fig. D1. The contour $\gamma_{\delta'}$ can be deformed into the contour $\gamma_{\delta''}$ as shown in the third panel in Fig. D1. Consider for instance the term C . One notes that as $T \rightarrow 0$ the contribution of the part of the contour to the left of k_L and the part of the contour to the right of k_R vanishes. Hence the result is identical in that limit to the one obtained from the previously considered contour γ_{δ} (see first panel in Fig. D1), and to the $T = 0$ result.

D.2 Large time limit: regime of the NESS

In the large time limit (once the infinite ℓ limit has been taken) the terms $B_{R/L}^{\text{off-diag}}(x, x', t)$ in (D8), as well as the contour integral part of $C(x, x', t)$ are found to vanish, by similar arguments as for $T = 0$. One is thus left with

$$K_{\infty}(x, x') = A_L(x, x') + A_R(x, x') + C_{\infty}(x, x') + C_{\infty}(x', x)^* + B_R^{\text{diag}}(x, x') + B_L^{\text{diag}}(x, x') \quad (\text{D9})$$

with

$$C_{\infty}(x, x') = \frac{1}{2} \int_0^{\infty} \frac{dk}{\pi} (f_R(k) - f_L(k)) (g + ik) \sin(kx) \frac{k \cos(kx') + g \sin(k|x'|)}{g^2 + k^2}, \quad (\text{D10})$$

given by the residue part in (D4).

Putting all terms together, using also (D2) and (D7) we obtain the kernel in the NESS at finite temperature for $g > 0$ as

$$\begin{aligned} K_{\infty}(x, x') &= \int_0^{\infty} \frac{dk}{2\pi} (f_R(k) + f_L(k)) \sin(kx) \sin(kx') \quad (\text{D11}) \\ &+ (f_R(k) + f_L(k)) \frac{(k \cos(kx) + g \sin(k|x|))(k \cos(kx') + g \sin(k|x'|))}{g^2 + k^2} \\ &+ (f_R(k) - f_L(k)) (g + ik) \sin(kx) \frac{k \cos(kx') + g \sin(k|x'|)}{g^2 + k^2} \\ &+ (f_R(k) - f_L(k)) (g - ik) \sin(kx') \frac{k \cos(kx) + g \sin(k|x|)}{g^2 + k^2}. \end{aligned}$$

We have checked that, in the limit $T \rightarrow 0$, this formula (D11) coincides with the expression obtained for the zero-temperature kernel in the NESS given in Eqs. (29) and (30). From the kernel (D11), we can recover the result for the density and the current at finite temperature given in (53) and (54).

Large time decay to the NESS. The decay in time to the NESS is different at finite T . We will not present the analysis for the full kernel but only show the decay of the term $C(x, x', t)$. For fixed T let us compute the large time behaviour of $\Delta C = C - C_{\infty}$. One has, from (D4), where the time independent residue part is cancelled,

$$\Delta C(x, x', t) = \int_0^{\infty} \frac{dk_b}{\pi} \int_{\gamma_{\epsilon}} \frac{dk}{\pi} (f_R(k) - f_L(k)) \sin(kx) \frac{k_b \cos(k_b x') + g \sin(k_b |x'|)}{g^2 + k_b^2} \frac{k k_b}{k^2 - k_b^2} e^{i(k^2 - k_b^2) \frac{t}{2}} \quad (\text{D12})$$

Taking the time derivative leads to the following decoupling of integrals

$$\partial_t \Delta C(x, x', t) = \frac{i}{2} G_b(t) G(t) \quad (\text{D13})$$

where $G_b(t)$ is defined in (B3) and

$$G(t) = \int_{\gamma_{\epsilon}} \frac{dk}{\pi} (f_R(k) - f_L(k)) k \sin(kx) e^{\frac{i}{2} k^2 t}. \quad (\text{D14})$$

The large time behavior of $G_b(t)$ was obtained before, and now the behavior of $G(t)$ is dominated by the vicinity of $k = ip = 0$ on the vertical part of the contour, leading to

$$G_b(t) \simeq \frac{1}{g^2 \sqrt{2\pi}} (1 + g|x'|) \frac{1}{(it)^{3/2}} \quad (\text{D15})$$

$$G(t) \simeq -i(f_R(0) - f_L(0)) \frac{x}{t^{3/2}} \int_0^{+\infty} \frac{dp}{\pi} p^2 e^{-\frac{i}{2}p^2} = (-1 + i)(f_R(0) - f_L(0)) \frac{x}{2\sqrt{\pi}t^{3/2}}. \quad (\text{D16})$$

In summary we obtain the decay (provided $\beta_R \mu_R \neq \beta_L \mu_L$)

$$\Delta C(x, x', t) \sim t^{-2}. \quad (\text{D17})$$

It is slower than the result obtained at zero temperature, where we found an oscillating $t^{-5/2}$ decay dominated by $k = k_{L/R}$ (see Eq. (B6)).

It is also interesting to check how to recover the decay in the zero temperature limit. To this aim we first send ϵ to infinity in the contour γ_ϵ . When moving the contour it will cross the poles from the Fermi function (in the upper half-plane) as in Fig. (D1). Taking into account the series of residues at these poles we obtain

$$\begin{aligned} G(t) &= \int_0^{+\infty} \frac{dk}{\pi} (f_R(k) - f_L(k)) k \sin(kx) e^{\frac{i}{2}k^2 t} + \sum_{n=0}^{+\infty} 2iT \sin(k_n^L x) e^{i \frac{(k_n^L)^2}{2} t} \\ &- \sum_{n=0}^{+\infty} 2iT \sin(k_n^R x) e^{i \frac{(k_n^R)^2}{2} t} \end{aligned} \quad (\text{D18})$$

where we recall that $k_n^{L/R}$'s are defined in Eq. (D2). In the zero temperature limit the integral part vanishes since $f_R(k) - f_L(k)$ decays to zero. Using that in that limit $\frac{dk_n}{dn} \simeq \frac{2i\pi T}{k_n}$ the two series converges towards the already known integrals $G_L(t)$ and $G_R(t)$ defined in (B2), leading to

$$\begin{aligned} G(t) &\underset{T \rightarrow 0}{\simeq} \int_{k_L}^{k_L + i\infty} \frac{dk}{\pi} k \sin(kx) e^{i \frac{k^2}{2} t} - \int_{k_R}^{k_R + i\infty} \frac{dk}{\pi} k \sin(kx) e^{i \frac{k^2}{2} t} \\ &= G_L(t) - G_R(t) \end{aligned} \quad (\text{D19})$$

which leads to the zero temperature result $\Delta C(T) \xrightarrow{T \rightarrow 0} \Delta C(T = 0)$ and allows to match the finite temperature decay to the zero temperature decay.

D.3 Large time limit: ray regime at fixed $\xi = \frac{x}{t}$

In the ray regime the Fermi factors do not change the arguments about the contours in Section 7. Hence Eqs.(47) and (48) turn into

$$\begin{aligned} K_\xi^+(y, y') &= \int_0^\infty \frac{dk}{\pi} f_R(k) \cos(k(y - y')) \Theta(\xi) + \int_0^\infty \frac{dk}{\pi} f_L(k) \cos(k(y - y')) \Theta(-\xi) \\ &- \text{sign}(\xi) \int_0^\infty \frac{dk}{2\pi} (f_R(k) - f_L(k)) T(k) e^{-i \text{sign}(\xi) k(y - y')} \Theta(k - |\xi|) \end{aligned} \quad (\text{D20})$$

$$K_\xi^-(y, y') = i \text{sign}(\xi) \int_0^\infty \frac{dk}{2\pi} (f_R(k) - f_L(k)) \frac{gk}{g^2 + k^2} e^{-i \text{sign}(\xi) k(y + y')} \Theta(k - |\xi|). \quad (\text{D21})$$

As a consequence we obtain the expressions for the density (57) and the current (58) in the ray-regime at finite temperature.

Appendix E: Energy current

In this section we give some details about the calculation of the energy current. We recall its definition

$$J_Q^{L/R}(x, t) = \sum_{n=1}^{\infty} f_{L/R}(k_n) \text{Im} \left((\hat{H}_g \psi_{L/R}^n(x, t))^* \partial_x \psi_{L/R}^n(x, t) \right), \quad (\text{E1})$$

where $k_n = \frac{2\pi n}{\ell}$ and \hat{H}_g is the single-particle Hamiltonian with a delta-impurity in Eq. (1). We recall that the evolution of a given state is given by

$$\psi_R^n(x, t) = \int_0^{\ell/2} dy \sum_{\sigma, k \in \Lambda_\sigma} \phi_{\sigma, k}(x) \phi_{\sigma, k}^*(y) e^{-iE(k)t} \psi_n(y, 0), \quad (\text{E2})$$

and similarly for $\psi_L^n(x, t)$. Substituting this expression in Eq. (E1), we get the time evolution of the heat current

$$J_Q^R(x, t) = \text{Im} \left[\sum_{k_n} f_R(k_n) \sum_{\sigma_E, k_E} \sum_{\sigma_j, k_j} \phi_{\sigma_E, k_E}^*(x) E(k_E) \partial_x \phi_{\sigma_j, k_j}(x) e^{i(E(k_E) - E(k_j))t} \right. \\ \left. \times \int_0^{\ell/2} dy \phi_{\sigma_E, k_E}(y) \psi_n(y, 0) \int_0^{\ell/2} dy \phi_{\sigma_j, k_j}^*(y) \psi_n(y, 0) \right]. \quad (\text{E3})$$

where, here and below, $k_n \in \Lambda_-$ and $k_E, k_j \in \Lambda_+$. Injecting the overlaps as in the calculation of the kernel (see Eq. 78) we obtain

$$J_Q^{L/R}(x, t) = \text{Im} \left[\sum_{k_n} f_{L/R}(k_n) \sum_{\sigma_E, k_E} \sum_{\sigma_j, k_j} \phi_{\sigma_E, k_E}^*(x) E(k_E) \partial_x \phi_{\sigma_j, k_j}(x) e^{i(E(k_E) - E(k_j))t} \right. \\ \left. \left(\frac{1}{\sqrt{2}} \delta_{\sigma_E, -1} \delta_{k_E, k_n} \pm \delta_{\sigma_E, 1} \frac{2^{3/2}}{\ell} \frac{k_E k_n}{(k_n^2 - k_E^2) \sqrt{g^2 + k_E^2 + \frac{2g}{\ell}}} \right) \right. \\ \left. \left(\frac{1}{\sqrt{2}} \delta_{\sigma_j, -1} \delta_{k_j, k_n} \pm \delta_{\sigma_j, 1} \frac{2^{3/2}}{\ell} \frac{k_j k_n}{(k_n^2 - k_j^2) \sqrt{g^2 + k_j^2 + \frac{2g}{\ell}}} \right) \right]. \quad (\text{E4})$$

As before for the computation of the kernel, we decompose $J_Q(x, t) = J_Q^L(x, t) + J_Q^R(x, t)$ in four different contributions

$$\begin{aligned}
J_Q(x, t) = & \underbrace{\text{Im}\left[\sum_{k_n} \frac{1}{\ell} (f_R(k_n) + f_L(k_n)) E(k_n) \sin(k_n x) k_n \cos(k_n x)\right]}_{A^Q} \quad (E5) \\
& + \underbrace{\text{Im}\left[2 \sum_{k_n, k_E, k_j} \left(\frac{2}{\ell}\right)^3 (f_R(k_n) + f_L(k_n)) E(k_E) \frac{k_E \cos(k_E x) + g \sin(k_E |x|)}{g^2 + k_E^2 + \frac{2g}{\ell}}\right. \right. \\
& \times \left. \left. k_j \frac{-k_j \sin(k_j x) + g \text{sgn}(x) \cos(k_j x)}{g^2 + k_j^2 + \frac{2g}{\ell}} \frac{k_E k_j k_n^2}{(k_n^2 - k_E^2)(k_n^2 - k_j^2)} e^{i(E(k_E) - E(k_j)t)}\right]}_{B^Q} \\
& + \underbrace{\text{Im}\left[\sum_{k_n, k_j} \left(\frac{2}{\ell}\right)^2 (f_R(k_n) - f_L(k_n)) E(k_n) \sin(k_n x)\right. \right. \\
& \times \left. \left. k_j \frac{-k_j \sin(k_j x) + g \text{sgn}(x) \cos(k_j x)}{g^2 + k_j^2 + \frac{2g}{\ell}} e^{i(E(k_n) - E(k_j)t)} \frac{k_j k_n}{k_n^2 - k_j^2}\right]}_{C^Q} \\
& + \underbrace{\text{Im}\left[\sum_{k_n, k_E} \left(\frac{2}{\ell}\right)^2 (f_R(k_n) - f_L(k_n)) k_n \cos(k_n x)\right. \right. \\
& \times \left. \left. E(k_E) \frac{k_E \cos(k_E x) + g \sin(k_E |x|)}{g^2 + k_E^2 + \frac{2g}{\ell}} e^{i(E(k_E) - E(k_n)t)} \frac{k_E k_n}{k_n^2 - k_E^2}\right]}_{D^Q}.
\end{aligned}$$

The term A_Q is trivially zero since the summand is real. The term B_Q can again be split into off-diagonal and diagonal part. The off-diagonal part vanishes in the large time limit by analogy with the calculation of the kernel (see Section B.2). The diagonal part, i.e. keeping only $k_E = k_j$ in the sum is non zero but becomes zero when taking the imaginary part.

Let us now consider the crossed terms ($C^Q = C_L^Q + C_R^Q$ and $D^Q = D_L^Q + D_R^Q$):

$$\begin{aligned}
C_{R/L}^Q = & \pm \text{Im} \sum_{k_n, k_j} \left(\frac{2}{\ell}\right)^2 f_{R/L}(k_n) k_j E(k_n) \sin(k_n x) \frac{-k_j \sin(k_j x) + g \text{sgn}(x) \cos(k_j x)}{g^2 + k_j^2 + \frac{2g}{\ell}} \quad (E6) \\
& \times e^{i(E(k_n) - E(k_j)t)} \frac{k_j k_n}{k_n^2 - k_j^2}
\end{aligned}$$

$$\begin{aligned}
& \underset{\ell \rightarrow \infty}{\simeq} \pm \text{Im} \left[\int_0^\infty \frac{dk_j}{\pi} \left[\int_{\gamma_\epsilon} \frac{dk_n}{\pi} f_{R/L}(k_n) - 2i \left(-\frac{1}{2} + \frac{i}{2} \frac{g}{k_j}\right) f_{R/L}(k_j) \text{Res}_{k_j=k_n} \right] \right. \\
& \left. k_j E(k_n) \sin(k_n x) \frac{-k_j \sin(k_j x) + g \text{sgn}(x) \cos(k_j x)}{g^2 + k_j^2} e^{i(E(k_n) - E(k_j)t)} \frac{k_j k_n}{k_n^2 - k_j^2} \right] \quad (E7)
\end{aligned}$$

Here γ_ϵ is the contour such that $\int_{\gamma_\epsilon} = \int_0^{i\epsilon} + \int_{i\epsilon}^{+\infty}$. In the large time limit the contour integral vanishes and

$$\lim_{t \rightarrow \infty} C_{R/L}^Q = \pm \int_0^\infty \frac{dk}{2\pi} f_{L/R}(k) k E(k) k \sin(kx) \frac{-k \sin(kx) + g \text{sgn}(x) \cos(kx)}{g^2 + k^2} \quad (E8)$$

A similar method gives $D_{L/R}^Q$.

$$D_{L/R}^Q \underset{\ell \rightarrow \infty}{\simeq} \pm \text{Im} \left[\int_0^\infty \frac{dk_E}{\pi} \left[\int_{\eta_{L/R}} \frac{dk_n}{\pi} f_{L/R}(k_n) + 2i \left(-\frac{1}{2} - \frac{i}{2} \frac{g}{k_E} \right) f_{L/R}(k_E) \text{Res}_{k_E=k_n} \right] \right] \quad (\text{E9})$$

$$E(k_E) \frac{k_E \cos(k_E x) + g \sin(k_E |x|)}{g^2 + k_E^2 + \frac{2g}{\ell}} k_n \cos(k_n x) e^{i(E(k_E) - E(k_n))t} \frac{k_E k_n}{k_n^2 - k_E^2}$$

$$\underset{t \rightarrow \infty}{\simeq} \mp \int_0^\infty \frac{dk}{2\pi} f_{L/R}(k) k E(k) k \cos(kx) \frac{k \cos(kx) + g \sin(k|x|)}{g^2 + k^2} \quad (\text{E10})$$

After summing these contributions, $J_\infty^Q = C_R^Q + C_L^Q + D_R^Q + D_L^Q$ we obtain the result for the asymptotic energy current in the NESS (63).

Appendix F: Low temperature expansions

In this appendix we perform the low temperature expansions for the energy and particle currents.

F.1 Energy current

Let us compute the energy current $J_{Q,\infty}$ as given by formula (63), recalling that here $E(k) = k^2/2$. Using the variable $\epsilon = \frac{k^2}{2}$ it takes the form $J_{Q,\infty} = J_{Q,\infty}^L - J_{Q,\infty}^R$ with

$$J_{Q,\infty}^{L/R} = \int_0^{+\infty} d\epsilon \frac{h(\epsilon)}{1 + e^{\beta_{L/R}(\epsilon - \mu_{L/R})}} \quad (\text{F1})$$

where $h(\epsilon) = \frac{\epsilon^2}{\pi(g^2 + 2\epsilon)}$. At low temperature one can use the Sommerfeld expansion

$$\int_0^{+\infty} d\epsilon \frac{h(\epsilon)}{1 + e^{\beta(\epsilon - \mu)}} \underset{\beta \rightarrow \infty}{\simeq} \int_0^\mu d\epsilon h(\epsilon) + \frac{\pi^2 h'(\mu)}{6\beta^2} + \frac{7\pi^4}{360\beta^4} h'''(\mu) + O(\beta^6) \quad (\text{F2})$$

and one obtains

$$J_{Q,\infty} = - \int_{\mu_L}^{\mu_R} d\epsilon \frac{\epsilon^2}{\pi(g^2 + 2\epsilon)} + \frac{\pi}{6} \left(T_L^2 \frac{2\mu_L(g^2 + \mu_L)}{(g^2 + 2\mu_L)^2} - T_R^2 \frac{2\mu_R(g^2 + \mu_R)}{(g^2 + 2\mu_R)^2} \right) + O(T_R^4, T_L^4). \quad (\text{F3})$$

In the case $\mu_L = \mu_R = \frac{k_F^2}{2}$ it simplifies (using (F2) up to order β^{-4}) into the formula (64) given in the text. In the absence of impurity, for $g = 0$, one has $h(\epsilon) = \frac{\epsilon}{2\pi}$ and all terms beyond $O(\beta^{-2})$ in the Sommerfeld expansion vanish. To obtain the subleading terms which are exponential in β one uses the low temperature expansion

$$\int_0^{+\infty} d\epsilon \frac{\epsilon}{2\pi(1 + e^{\beta(\epsilon - \mu)})} = -\frac{1}{2\pi\beta^2} \text{Li}_2(-e^{\beta\mu}) = \frac{\mu^2}{4\pi} + \frac{\pi}{12\beta^2} - \frac{1}{2\pi\beta^2} e^{-\beta\mu} + O(e^{-2\beta\mu}), \quad (\text{F4})$$

where $\text{Li}_2(z) = \sum_{k \geq 1} z^k/k^2$ is the di-logarithm function. This expansion (F7) leads to the formula (67) in the text.

F.2 Particle current

For the particle current one has $J_\infty = J_\infty^L - J_\infty^R$ with

$$J_\infty^{L/R} = \int_0^{+\infty} d\epsilon \frac{\tilde{h}(\epsilon)}{1 + e^{\beta_{L/R}(\epsilon - \mu_{L/R})}} \quad (\text{F5})$$

where $\tilde{h}(\epsilon) = \frac{\epsilon}{\pi(g^2+2\epsilon)}$. Using the Sommerfeld expansion one obtains

$$J_\infty = - \int_{\mu_L}^{\mu_R} d\epsilon \frac{\epsilon}{\pi(g^2+2\epsilon)} + \frac{\pi}{6} \left(T_L^2 \frac{g^2}{(g^2+2\mu_L)^2} - T_R^2 \frac{g^2}{(g^2+2\mu_R)^2} \right) + O(T_R^4, T_L^4) \quad (\text{F6})$$

In the case $\mu_L = \mu_R = \frac{k_F^2}{2}$ it simplifies (using (F2) up to order β^{-4}) into the formula (55) given in the text.

In the absence of impurity, for $g = 0$, one uses

$$\int_0^{+\infty} d\epsilon \frac{1}{2\pi(1+e^{\beta(\epsilon-\mu)})} = \frac{1}{2\pi\beta} \log(1+e^{\beta\mu}) = \frac{\mu}{2\pi} + \frac{1}{2\pi\beta} e^{-\beta\mu} + O(e^{-2\beta\mu}), \quad (\text{F7})$$

which leads to the formula (56) given in the text.

Appendix G: Remarks on NESS and GGE

For non-interacting fermions the prediction from the GGE takes the form for the density matrix

$$\hat{D}_{\text{GGE}} = \frac{1}{Z_{\text{GGE}}} e^{\sum_\ell f_\ell c_\ell^\dagger c_\ell}, \quad (\text{F8})$$

where here ℓ labels the eigenstates $|\varphi_\ell\rangle$ of the single particle post-quench Hamiltonian \hat{H}_g and the c_ℓ^\dagger are the corresponding creation operators. Since it has a Gaussian form it leads to the kernel

$$K_{\text{GGE}} = \sum_\ell \langle c_\ell^\dagger c_\ell \rangle_{\text{GGE}} |\varphi_\ell\rangle \langle \varphi_\ell|, \quad \langle c_\ell^\dagger c_\ell \rangle_{\text{GGE}} = \nu_\ell = \frac{1}{1+e^{-f_\ell}}. \quad (\text{F9})$$

In the GGE the coefficients f_ℓ (which should not be confused with the Fermi factors $f_{L/R}$) are determined so that the occupation numbers ν_ℓ are equal to those in the initial state (which has density matrix \hat{D}_0). Hence one has

$$\langle c_\ell^\dagger c_\ell \rangle_{\text{GGE}} = \langle c_\ell^\dagger c_\ell \rangle_{t=0} = \langle \varphi_\ell | \hat{D}_0 | \varphi_\ell \rangle. \quad (\text{F10})$$

In the present problem, for any finite size ℓ (i.e. before taking the thermodynamic limit), the post-quench eigenstates are denoted $|\varphi_\ell\rangle = |\phi_{\sigma_a, k_a}\rangle$, where $\sigma_a = \pm 1$ for respectively even and odd eigenstates given explicitly in (69) and (68), and where k_a belongs to either the even or odd lattices respectively, $k_a \in \Lambda^\pm$, see (71) and (68) respectively. The initial density matrix reads

$$\hat{D}_0 = \sum_{k_n} [f_L(k_n) |\phi_n^L\rangle \langle \phi_n^L| + f_R(k_n) |\phi_n^R\rangle \langle \phi_n^R|], \quad (\text{F11})$$

where the $|\phi_n^{L/R}\rangle$ are defined in (2) and $f_{L/R}$ are the Fermi factors for the left and right sides of the system. Hence the GGE prediction (for any ℓ) takes the form

$$\begin{aligned} K_{\text{GGE}}(x, x') &= \sum_{\sigma_a = \pm 1, k_a \in \Lambda_{\sigma_a}} \sum_{k_n} \left(f_L(k_n) \langle \phi_{\sigma_a, k_a}^L | \phi_n^L \rangle \langle \phi_n^L | \phi_{\sigma_a, k_a}^L \rangle \right. \\ &\quad \left. + f_R(k_n) \langle \phi_{\sigma_a, k_a}^R | \phi_n^R \rangle \langle \phi_n^R | \phi_{\sigma_a, k_a}^R \rangle \right) \phi_{\sigma_a, k_a}^*(x) \phi_{\sigma_a, k_a}(x'). \end{aligned} \quad (\text{F12})$$

We can now compare (F12) to the exact formula for $K(x, x', t) = K_R(x, x', t) + K_L(x, x', t)$ at finite ℓ given in (78) in the particular case of an initial condition at zero temperature. Clearly $K_{\text{GGE}}(x, x')$ is obtained by retaining only the terms $k_a = k_b$ and $\sigma_a = \sigma_b$ in the double sum

over post-quench eigenstates. This is also called the *diagonal approximation* and sometimes denoted K_d (the fact that the two coincide quite generally for a finite size system or for trapped fermions was discussed in [24]). In the expression (80) it corresponds to keeping only the terms $A(x, x')$ (which correspond to $\sigma_a = \sigma_b = -1$) and the term denoted $B^{\text{diag}}(x, x')$ in (89) (which correspond to $k_a = k_b$ in the sum $\sigma_a = \sigma_b = 1$). Hence one has, for any ℓ ,

$$K_{\text{GGE}}(x, x') = A(x, x') + B^{\text{diag}}(x, x') , \quad (\text{F13})$$

which is time independent by construction. This has a well defined $\ell = +\infty$ limit, which is studied in this paper.

The important remark is that the GGE prediction (F13) in the $\ell = +\infty$ limit is different from the result that we obtained for the NESS, i.e. $K_{\text{GGE}}(x, x') \neq K_{\infty}(x, x')$. Indeed one has

$$K_{\infty}(x, x') = K_{\text{GGE}}(x, x') + C(x, x', t = +\infty) + C(x', x, t = +\infty)^* . \quad (\text{F14})$$

While $K_{\text{GGE}}(x, x')$ is real and does not carry any current, the additional terms C lead to a non zero current in the NESS. Although they are not strictly diagonal for finite ℓ they contain "almost diagonal" oscillating terms of the form $e^{it(E(k)-E(k_a))}$ where k and k_a do not belong to the same lattice. Since $E(k) - E(k_a)$ can be of order $1/\ell^2$ at large ℓ (for some couples (k, k_a)) they do lead to a finite contribution in the NESS where one takes $\ell \rightarrow +\infty$ first.

The above result also implies that $\hat{D}_{\text{NESS}} \neq \hat{D}_{\text{GGE}}$. One can in principle obtain \hat{D}_{NESS} from our result for the kernel $K_{\infty}(x, x')$. Let us just indicate it in the simpler case $g = 0$. In that case one has from (D11)

$$K_{\infty}(x, x') = \int_{-\infty}^{+\infty} \frac{dk}{2\pi} (f_L(k)\theta(k) + f_R(k)\theta(-k)) e^{-ik(x-x')} . \quad (\text{F15})$$

Using that $c_x^\dagger c_{x'} = \int \frac{dk}{2\pi} c_k^\dagger c_k e^{-ik(x-x')}$ we obtain

$$\hat{D}_{\text{NESS}} = \frac{1}{Z_{\text{NESS}}} e^{\int_{-\infty}^{+\infty} \frac{dk}{2\pi} h_k c_k^\dagger c_k} , \quad \frac{1}{1 + e^{-h_k}} = f_R(k)\theta(-k) + f_L(k)\theta(k) . \quad (\text{F16})$$

Hence $h_k = \beta_L(\frac{k^2}{2} - \mu_L)\theta(k) + \beta_R(\frac{k^2}{2} - \mu_R)\theta(-k)$, i.e. the fermions with positive momentum as those coming from the left and reciprocally.

References

- [1] D. S. Dean, P. Le Doussal, S. N. Majumdar, and G. Schehr, *Noninteracting fermions in a trap and random matrix theory*, J. Phys. A: Math. Theor. **52**, 144006 (2019)
- [2] D. S. Dean, P. Le Doussal, S. N. Majumdar, and G. Schehr, *Noninteracting fermions at finite temperature in a d-dimensional trap: universal correlations*, Phys. Rev. A **94**, 063622 (2016)
- [3] N. R. Smith, P. Le Doussal, S. N. Majumdar and G. Schehr, *Counting statistics for noninteracting fermions in a d-dimensional potential*, Phys. Rev. E **103**, 030105 (2021)
- [4] A. Borodin, *Determinantal point processes*, in *The Oxford Handbook of Random Matrix Theory*, G. Akemann, J. Baik, P. Di Francesco (Eds.), Oxford University Press, Oxford (2011)
- [5] K. Johansson, *Random matrices and determinantal processes*, arXiv preprint: math-ph/0510038, (2005)

- [6] J. Dubail, J.-M. Stéphan, J. Viti, and P. Calabrese, *Conformal Field Theory for Inhomogeneous One-dimensional Quantum Systems: the Example of noninteracting Fermi Gases*, SciPost Phys. **2**, 002 (2017)
- [7] M. L. Mehta, *Random matrices*, Elsevier (2004)
- [8] P. J. Forrester, *Log-Gases and Random Matrices*, (London Mathematical Society monographs, Princeton University Press, Princeton, NJ, 2010)
- [9] P. Calabrese, M. Mintchev, and E. Vicari, *Entanglement entropy of one-dimensional gases*, Phys. Rev. Lett. **107**, 020601 (2011)
- [10] B. Lacroix-A-Chez-Toine, P. Le Doussal, S. N. Majumdar, and G. Schehr, *Statistics of fermions in a d-dimensional box near a hard wall*, EPL **120**, 10006 (2017)
- [11] B. Lacroix-A-Chez-Toine, P. Le Doussal, S. N. Majumdar, and G. Schehr, *Noninteracting fermions in hard-edge potentials*, J. Stat. Mech. 123103 (2018)
- [12] F. D. Cunden, F. Mezzadri, and N. , *Free fermions and the classical compact groups*, J. Stat. Phys. **171**, 768 (2018)
- [13] D. S. Dean, P. Le Doussal, S. N. Majumdar, G. Schehr, and N. R. Smith, *Kernels for non-interacting fermions via a Green's function approach with applications to step potentials*, J. Phys. A: Math. Theor. **54**, 084001 (2021)
- [14] D. S. Dean, P. Le Doussal, S. N. Majumdar, and G. Schehr, *Impurities in systems of noninteracting trapped fermions*, SciPost Phys. **10**, 082 (2021)
- [15] J. Friedel, *XIV. The distribution of electrons round impurities in monovalent metals*, Phil. Mag. **43**, 153 (1952)
- [16] A. Recati, J. N. Fuchs, C. S. Peca, and W. Zwerger, *Casimir forces between defects in one-dimensional quantum liquids*, Phys. Rev. A **72**, 023616 (2005)
- [17] J. N. Fuchs, A. Recati, and W. Zwerger, *Oscillating Casimir force between impurities in one-dimensional Fermi liquids*, Phys. Rev. A **75**, 043615 (2007)
- [18] W. Kohn and L. J. Sham, *Quantum Density Oscillations in an Inhomogeneous Electron Gas*, Phys. Rev. **135**, A1697 (1964)
- [19] P. Le Doussal, S. N. Majumdar, G. Schehr, *Periodic Airy process and equilibrium dynamics of edge fermions in a trap*, Ann. Phys. **383**, 312 (2017)
- [20] M. Adler, and P. van Moerbeke, *PDEs for the joint distributions of the Dyson, Airy and Sine processes*, Ann. Probab. **33**, 1326 (2004)
- [21] A. Minguzzi, and D. M. Gangardt, *Exact coherent states of a harmonically confined Tonks-Girardeau gas*, Phys. Rev. Lett. **94**, 240404 (2005)
- [22] V. Gritsev, P. Barmettler, and E. Demler, *Scaling approach to quantum non-equilibrium dynamics of many-body systems*, New J. Phys. **12**, 113005 (2010)
- [23] P. Ruggiero, Y. Brun, and J. Dubail, *Conformal field theory on top of a breathing one-dimensional gas of hard core bosons*, SciPost Phys. **6**, 051 (2019)

- [24] D. S. Dean, P. Le Doussal, S. N. Majumdar, and G. Schehr, *Nonequilibrium dynamics of noninteracting fermions in a trap*, EPL (Europhys. Lett.) **126**, 20006 (2019)
- [25] M. Kulkarni, M. Gautam, and M. Takeshi, *Quantum quench and thermalization of one-dimensional Fermi gas via phase-space hydrodynamics*, Phys. Rev. A **98**, 043610 (2018)
- [26] P. Ruggiero, P. Calabrese, B. Doyon, and J. Dubail, *Quantum generalized hydrodynamics of the Tonks-Girardeau gas: density fluctuations and entanglement entropy*, J. Phys. A: Math. Theor. **55**, 024003 (2021)
- [27] F. H. Essler, and M. Fagotti, *Quench dynamics and relaxation in isolated integrable quantum spin chains*, J. Stat. Mech. Theory 064002 (2016)
- [28] Y. M. Blanter, M. Büttiker, *Shot noise in mesoscopic conductors*, Phys. Rep. **336**, 1 (2000)
- [29] H. D. Cornean, A. Jensen, and V. Moldoveanu, J. Math. Phys. **46**, 042106 (2005)
- [30] C. L. Kane, and M. P. A. Fisher, *Transport in a one-channel Luttinger liquid*, Phys. Rev. Lett. **68**, 1220 (1992)
- [31] P. Fendley, and H. Saleur, *Nonequilibrium dc noise in a Luttinger liquid with an impurity*, Phys. Rev. B **54**, 10845 (1996)
- [32] D. Bernard, B. Doyon, and J. Viti, *Non-equilibrium conformal field theories with impurities*, J. Phys. A: Math. Theor. **48**, 05FT01 (2015)
- [33] A. Biella, A. De Luca, J. Viti, D. Rossini, L. Mazza, and R. Fazio, *Energy transport between two integrable spin chains*, Phys. Rev. B **93**, 205121 (2016)
- [34] P. Ruggiero, L. Foini, and T. Giamarchi *Large-scale thermalization, prethermalization, and impact of temperature in the quench dynamics of two unequal Luttinger liquids*, Phys. Rev. Res. **3**, 013048 (2021).
- [35] P. Ruggiero, P. Calabrese, L. Foini, and T. Giamarchi, *Quenches in initially coupled Tomonaga-Luttinger Liquids: a conformal field theory approach*, SciPost Phys. **11**, 055 (2021)
- [36] S. Sotiriadis and J. Cardy, *Inhomogeneous quantum quenches*, J. Stat. Mech. 11003 (2008)
- [37] D. Bernard and B. Doyon, *Energy flow in non-equilibrium conformal field theory*, J. Phys. A: Math. Theor. **45**, 362001 (2012)
- [38] A. De Luca, J. Viti, D. Bernard, and B. Doyon, *Nonequilibrium thermal transport in the quantum Ising chain*, Phys. Rev. B **88**, 134301 (2013)
- [39] O. A. Castro-Alvaredo, B. Doyon and T. Yoshimura, *Emergent Hydrodynamics in Integrable Quantum Systems Out of Equilibrium*, Phys. Rev. X **6**, 041065 (2016)
- [40] B. Bertini, M. Collura, J. De Nardis, and M. Fagotti, *Transport in Out-of-Equilibrium XXZ Chains: Exact Profiles of Charges and Currents*, Phys. Rev. Lett. **117**, 207201 (2016)
- [41] T. Antal, Z. Rácz, A. Rákos, and G. M. Schütz, *Transport in the XX chain at zero temperature: Emergence of flat magnetization profiles*, Phys. Rev. E **59**, 4912 (1999)

- [42] T. Antal, P. L. Krapivsky, and A. Rákos, *Logarithmic current fluctuations in nonequilibrium quantum spin chains*, Phys. Rev. E **78**, 061115 (2008)
- [43] J. Viti, J.-M. Stéphan, J. Dubail, and M. Haque, *Inhomogeneous quenches in a free fermionic chain: Exact results*, EPL **115**, 40011 (2016)
- [44] V. Eisler, and Z. Rácz, *Full Counting Statistics in a Propagating Quantum Front and Random Matrix Spectra*, Phys. Rev. Lett. **110**, 060602 (2013)
- [45] V. Eisler, F. Maislinger, and H. G. Evertz, *Universal front propagation in the quantum Ising chain with domain-wall initial states*, SciPost Phys. **1**, 014 (2016)
- [46] G. Perfetto, and A. Gambassi, *Ballistic front dynamics after joining two semi-infinite quantum Ising chains*, Phys. Rev. E **96**, 012138 (2017)
- [47] M. Kormos, *Inhomogeneous quenches in the transverse field Ising chain: scaling and front dynamics*, SciPost Phys. **3**, 020 (2017)
- [48] H. Moriya, R. Nagao and T. Sasamoto, *Exact large deviation function of spin current for the one dimensional XX spin chain with domain wall initial condition*, J. Stat. Mech., 063105 (2019),
- [49] M. Collura, S. Sotiriadis, and P. Calabrese, *Equilibration of a Tonks-Girardeau gas following a trap release*, Phys. Rev. Lett. **110**, 245301 (2013)
- [50] M. Collura, and D. Karevski, *Quantum quench from a thermal tensor state: Boundary effects and generalized Gibbs ensemble*, Phys. Rev. B **89**, 214308 (2014)
- [51] M. Ljubotina, S. Sotiriadis, and T. Prosen, *Non-equilibrium quantum transport in presence of a defect: the non-interacting case*, SciPost Phys. **6**, 004 (2019)
- [52] T. Jin, T. Gautié, A. Krajenbrink, P. Ruggiero and T. Yoshimura, *Interplay between transport and quantum coherences in free fermionic systems*, J. Phys. A **54**, 404001 (2021)
- [53] V. Eisler, and I. Peschel, *On entanglement evolution across defects in critical chains*, EPL **99**, 20001 (2012)
- [54] M. Gruber, and V. Eisler, *Time evolution of entanglement negativity across a defect*, J. Phys. A: Math. Theor. **53**, 205301 (2020)
- [55] O. Gamayun, O. Lychkovskiy, J.S. Caux, *Fredholm determinants, full counting statistics and Loschmidt echo for domain wall profiles in one-dimensional free fermionic chains*, SciPost Physics, 8(3), 036 (2020)
- [56] S. Scopa, A. Krajenbrink, P. Calabrese, and J. Dubail, *Exact entanglement growth of a one-dimensional hard-core quantum gas during a free expansion*, J. Phys. A: Math. Theor. **54**, 404002 (2021)
- [57] G. Del Vecchio Del Vecchio, A. De Luca, and A. Bastianello, *Transport through interacting defects and lack of thermalisation*, SciPost Phys. **12**, 060 (2022)
- [58] B. Bertini, and M. Fagotti, *Determination of the nonequilibrium steady state emerging from a defect*, Phys. Rev. Lett. **117**, 130402 (2016)
- [59] O. Gamayun, A. Slobodeniuk, J.S. Caux, O. Lychkovskiy, *Nonequilibrium phase transition in transport through a driven quantum point contact*, Phys. Rev. B, 103(4), L041405 (2021)

- [60] A. Bastianello, A. De Luca, *Nonequilibrium steady state generated by a moving defect: the supersonic threshold*, Phys. Rev. Lett. **120**, 060602 (2018)
- [61] M. Collura, A. De Luca, P. Calabrese, J. Dubail, *Domain wall melting in the spin-1 2 XXZ spin chain: Emergent Luttinger liquid with a fractal quasiparticle charge*, Phys. Rev. B, 102(18), 180409 (2020).
- [62] A. De Luca, A. Bastianello, *Entanglement front generated by an impurity traveling in an isolated many-body quantum system*, Phys. Rev. B, 101(8), 085139 (2020).
- [63] P. Calabrese, F. H. Essler, and M. Fagotti, *Quantum quench in the transverse field Ising chain: I. Time evolution of order parameter correlators*, J. Stat. Mech., 07016 (2012)
- [64] S. Sotiriadis, *Non-Equilibrium Steady State of the Lieb-Liniger model: exact treatment of the Tonks Girardeau limit*, preprint arXiv:2007.12683 (2020)
- [65] L. Rossi, F. Dolcini, F. Cavaliere, N. T. Ziani, M. Sasseti, and F. Rossi, *Signature of Generalized Gibbs Ensemble Deviation from Equilibrium: Negative Absorption Induced by a Local Quench*, Entropy **23**, 220 (2021)
- [66] W. N. Mathews, *Energy Density and Current in Quantum Theory*, Am. J. Phys. **42**, 214 (1974).
- [67] D. S. Dean, P. Le Doussal, S. N. Majumdar, and G. Schehr, *Wigner function of noninteracting trapped fermions*, Phys. Rev. A **97**, 063614 (2018)
- [68] B. De Bruyne, D. S. Dean, P. Le Doussal, S. N. Majumdar, G. Schehr, *Wigner function for noninteracting fermions in hard wall potentials*, Phys. Rev. A **104**, 013314 (2021)